HETEROGENEOUS WIRELESS NETWORKS: TRAFFIC OFFLOADING, RESOURCE ALLOCATION AND COVERAGE ANALYSIS

A Dissertation

by

ALI RIZA EKTI

Submitted to the Office of Graduate and Professional Studies of
Texas A&M University
in partial fulfillment of the requirements for the degree of

DOCTOR OF PHILOSOPHY

Chair of Committee,	Erchin Serpedin
Co-Chair of Committee,	Khalid A. Qaraqe
Committee Members,	Aydin I. Karsilayan
	Radu Stoleru
Head of Department,	Miroslav M. Begovic

August 2015

Major Subject: Electrical Engineering

ABSTRACT

Unlike 2G systems where the radius of macro base station (MBS) could reach several kilometers, the cell radius of LTE-Advanced and next generation wireless networks (NGWNs) such as 5G networks would be random and up to a few hundred meters in order to overcome the radio signal propagation impairments. Heterogeneous wireless networks (HetNets) are becoming an integral part of the NGWNs especially 5G networks, where small cell base stations (SBSs), wireless-fidelity (WiFi) access points (APs), cellular BSs and device-to-device (D2D) enabled links coexist together. HetNets represent novel approaches for the mobile data offloading, resource allocation and coverage probability problems that help to optimize the network traffic. However, heterogeneity and interworking among different radio access technologies bring new challenges such as bandwidth resource allocation, user/cell association, traffic offloading based on the user activity and coverage probability in HetNets. This dissertation attempts to address three key research areas: traffic offloading, bandwidth resource allocation and coverage probability problems in HetNets.

In the first part of this dissertation, we derive the mathematical framework to calculate the required active user population factor (AUPF) of small cells based on the probabilistic traffic models. The number of total mobile users and number of active mobile users have different probabilistic distributions such as different combinations of Binomial and Poisson distributions. Furthermore, AUPF is utilized to investigate the downlink BS and backhaul power consumption of HetNets.

In the second part, we investigate two different traffic offloading (TO) schemes (a) Path loss (PL) and (b) Signal-to-Interference ratio (SIR) based strategies. In this

context, a comparative study on two techniques to offload the traffic from macrocell to small cell is studied. Additionally, the AUPF, small cell access scheme and traffic-type are included into a PL based TO strategy to minimize the congested macrocell traffic.

In the third part, the joint user assignment and bandwidth resource allocation problem is formulated as a mixed integer non-linear programming (MINLP). Due to its intractability and computational complexity, the MINLP problem is transformed into a convex optimization problem via a binary variable relaxation approach. Based on the mathematical analysis of the problem, a heuristic algorithm for joint user assignment and bandwidth allocation is presented. The proposed solution achieves a near optimal user assignment and bandwidth allocation at reduced computational complexity.

Lastly, we investigate the transition between traditional hexagonal BS deployment to random BS placement in HetNets. Independent Poisson Point Processes (PPPs) are used to model the random locations of BSs. Lloyds algorithm is investigated for analyzing the coverage probability in a network which functions as a bridge between random and structural BS deployments. The link distance distribution is obtained by using the Expectation-Maximization (EM) algorithm which is further utilized for calculating the coverage probability.

DEDICATION

To my beloved wife, Lindsey Marie,

my lovely daughter, Ela Nisa,

my dear sister, Burcu Ceren

my dear parents, Ayşe and Hacı,

whom I love and admire...

ACKNOWLEDGEMENTS

The experience and life lessons I learned during my Ph.D. journey was not only wonderful and unforgettable but also overwhelming. This thesis would only have been a dream without the support and encouragement of many great people.

First, I would like to express my gratitude to Dr. Erchin Serpedin and Dr. Khalid A. Qaraqe. It was a privilege to be their PhD student. I appreciate the freedom they gave me to pursue different research areas. Their influence in shaping my career will be everlasting.

I would also like to thank my committee members Dr. Aydin I. Karsilayan and Dr. Radu Stoleru for their invaluable time, comments and suggestions. I would also like to express my appreciation to Dr. Jose Silva-Martinez for serving as a replacement during my Ph.D. Oral Preliminary examination and his valuable time and suggestions. I would also like to thank Dr. Muhammad Z. Shakir and Dr. Muhammad Ismail for their collaborations during my PhD program.

I would also like to thank Dr. Krishna Narayanan, Dr. Aydın Sunol, Dr. Devrim Eren, Dr. Hazem Nounou, Dr. Arthur David Snider, Dr. Deepa Kundur and Ms. Tammy Carda for their help during my journey in the United States. I am also thankful to Dr. Martin Haenggi for his suggestions regarding the coverage probability analysis.

I specifically grateful and lucky to have such great friends during my graduate programs such as Dr. Sabit Ekin, Mr. Xu Wang, Mr. Bilal Wajid, Mr. Celal Bilgi, Mr. Mustafa Alshawaqfeh, Dr. Nariman Rahimian, Dr. Engin Tunali, Mr. Celal Erbay, Mr. Abdulkadir Bostanci, Dr. Necati Kaya, Dr. Gülnur Efe-Sanden, Mr. Steve Sanden, Mr. Sinan Yiğit and many others. I would like to thank Mr. Ali

Canpolat, Mr. Cihan Canpolat, Mr. Hüseyin Özdem, Mr. Zafer Emirhan and Mr. Taner Alioğlu for their friendship and help during my first arrival in Pittsburgh, PA where I first started my journey in United States.

I am also grateful to have the possibility to interact with Mr. Tevfik Yalçınkaya, Mr. Kıvanç Sahici, Mr. Serkan Göçer, Mr. Fırat İsmailoğlu and many other friends from childhood.

I especially thank Mr. Ali Emre Erçelebi and Dr. Ali Görçin with whom I have begun this graduate study together and share many memories.

I also would like to thank to my undergraduate advisors Dr. Hüseyin Canbolat and Dr. Caner Özdemir for their suggestions and guidance during my undergraduate and graduate student life.

Last but not least, I thank the Turkey Ministry of Education and Qatar National Research Fund (an initiative of Qatar Foundation) for funding the research work during my graduate degrees.

Finally, I thank my wife, my daughter, my parents and my sister for sharing their love all these years. I owe all my success to their blessings and encouragement.

NOMENCLATURE

2D Two–Dimensional

3GPP 3rd Generation Partnership Project

AP Access Point

ARPU Average Revenue per User

AUPF Active User Population Factor

BARON Branch–and–Reduce Optimization Navigator

BS Base Station

CapEx Capital Expenditures

CBR Constant Bit Rate

CDMA Code Division Multiple Access

CVT Centroidal Voronoi Tessellation

D2D Device-to-Device

DSL Digital Subscriber Line

DAS Distributed Antenna Systems

EM Expectation-Maximization

GAMS General Algebraic Modeling System

GPP Ginibre Point Process

HD High–Definition

HSPA High Speed Packet Access

HetNet Heterogeneous Wireless Network

IoT Internet of Things

KKT Karush–Kuhn–Tucker

L-BGFS Limited Broyden-Fletcher-Goldfarb-Shanno

LOS Line–of–Sight

LTE Long Term Evolution

M2M Machine-to-Machine

MBS Macro Base Station

MISR Mean Interference-to-Signal Ratio

MCTCP Multiple–Connection Transmission Control Protocol

MINLP Mixed Integer Non–Linear Program

MT Mobile Terminal

NGWN Next Generation Wireless Network

NP Non–Deterministic Polynomial–Time

OpEx Operational Expenditure

P2P Peer–to–Peer

P2P Point–to–Point

PDF Probability Density Function

PGFL Probability Generating Functional

PL Path Loss

PPP Poisson Point Process

PUSCH Physical Uplink Shared Channel

QoS Quality of Service

RF Radio Frequency

SBS Small Cell Base Station

SINR Signal-to-Interference-Noise Ratio

SIPTO Selected IP Traffic Offloading

SIR Signal-to-Interference Ratio

SON Self Organized Networks

TCO Total Cost of Ownership

TO Traffic Offloading

UMTS Universal Mobile Telecommunications System

VBR Variable Bit Rate

WiFi Wireless Fidelity

WiGig Wireless Gigabit Alliance

WLAN Wireless Local Area Network

TABLE OF CONTENTS

Page

LIST OF FIGURES

FIGURE Page

LIST OF TABLES

TABLE Page

1. INTRODUCTION*

1.1 Heterogeneous Wireless Networks

We are currently witnessing a wireless communications revolution and the wireless network structures are adapting themselves to cope with the increased volume of data transmissions. Earlier wireless communications systems relied on high-power cellular towers called macro base stations (MBSs). The deployment of MBSs was based on the hexagonal traditional grid to provide seamless voice and data connection to all mobile users. Cellular phones were used initially only for voice transmissions along with limited text messaging applications. However, contemporary cellular phones are capable of transmitting high–definition (HD) multimedia, online gaming and video conferencing. From the network architecture perspective it is obvious that adding more MBSs to meet the user demands is not feasible due to the lack of available locations and expensive costs. For instance, in the traditional macrocell network, the placement of a new cellular tower in a highly dense location, i.e., downtown, can be very challenging. Additionally, the main issue that networks operators are facing is the capacity not the coverage due to the ever increasing number of applications and demands in the wireless communications industry.

Moreover, next generation wireless networks are supposed to interwork efficiently

---

*Section 1.3 Reprinted with permission from "Downlink Power Consumption of HetNets Based on the Probabilistic Traffic Model of Mobile Users," by Ali Rıza Ekti, Muhammad Z. Shakir, Khalid A. Qaraqe and Erchin Serpedin, IEEE 24th International Symposium on Personal, Indoor and Mobile Radio Communications (PIMRC), Copyright 2013 by IEEE.

Section 1.3 Reprinted with permission from "End–to–End Downlink Power Consumption of Heterogeneous Small Cell Networks Based on the Probabilistic Traffic Model," by Ali Rıza Ekti, Muhammad Z. Shakir, Khalid A. Qaraqe and Erchin Serpedin, IEEE Wireless Communications and Networking Conference (WCNC), Copyright 2014 by IEEE.

and seamlessly with other radio technologies; This characteristic is referred to as multi-homing. For example, a typical smart phone can establish connections via several different radio technologies such as High Speed Packet Access (HSPA), Long Term Evolution (LTE)-Advanced and wireless–fidelity (WiFi) (e.g., 802.11g, n, c) where each of these connections employ non-overlapping frequencies. Therefore, the agile evolution of wireless communications systems has led to the emergence of new concepts in term of quality of service (QoS) and system efficiency in the next generation wireless networks (NGWNs). In order to support the inevitable dynamic changes in NGWNs such as 4G and 5G networks, heterogeneous wireless networks (HetNets) have become an integral part of NGWNs. Several wireless technologies can co–exist such as WiFi, 3rd Generation Partnership Project (3GPP) systems of the Universal Mobile Telecommunications System (UMTS) and LTE-Advanced in HetNets as illustrated in Fig. 1.1, where several cellular base stations (BSs), WiFi access points (APs) and device-to-device (D2D) enabled links cooperate to improve energy consumption, network capacity, data rate and coverage [1, 9, 33]. This new paradigm shift in cellular network structure deployment assumes MBSs and a combination of low cost, low powered and easy to deploy small cell base stations (SBSs), distributed antenna systems (DAS), D2D links and WiFi APs. HetNets increase spectrum utilization and reduce energy consumption by using shorter propagation distances and by employing higher frequency bands to enable higher data rates. HetNets also offer solutions to network operators to lower the cost per bit and increase the revenue per bit by utilizing multiple access technologies at the same time. Some key elements of HetNets are femtocells (home eNBs), picocells, distributed antenna systems and existing WiFi APs. They are differentiated by their coverage areas, backhaul connections, propagation characteristics and transmit powers. In order to provide a better understanding of the differences between traditional MBS and HetNet deployments, TABLE 1.1

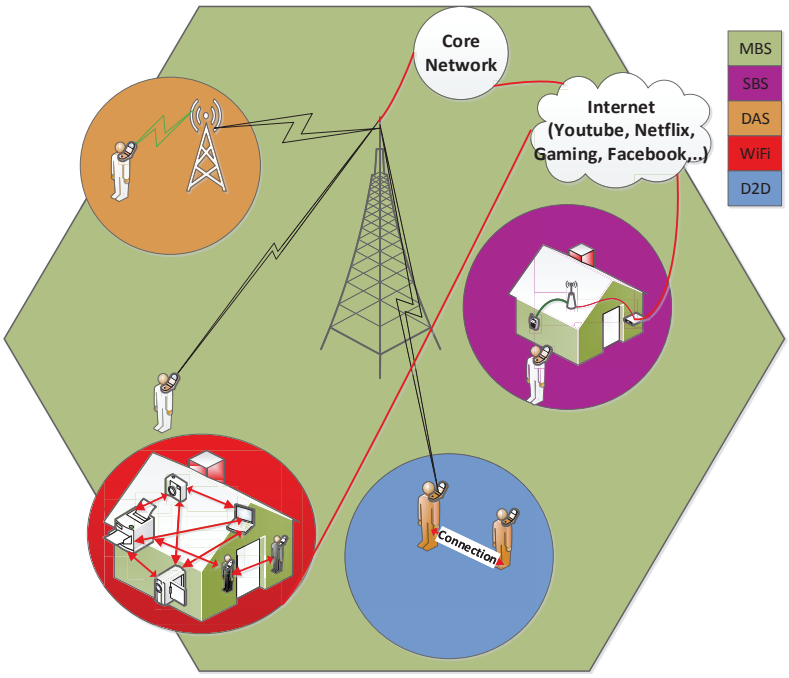

Figure 1.1: A Heterogeneous Wireless Network: Combination of MBS, SBS, WiFi AP, DAS and D2D links.

is constructed [1, 3, 16, 18, 33, 49, 77]. As seen in TABLE 1.1, HetNets emploit the macrocell infrastructure as a backbone, and additionaly utilize the smaller BSs and other radio access technologies at the same time.

1.1.1 Elements of Heterogeneous Wireless Networks

1.1.1.1 Macrocells

Macrocells provide wide area coverage for HetNets and act as a backbone for all the other networks. Macrocells exhibit a coverage range greater than 500m. One of the most important feature of macrocells is that they support high mobility users and minimize the handover.

Table 1.1: Why do we need HetNets?

	HetNet	**Traditional Macro Base Station**
Cell Association	Connect to BS with highest data rate.	Connect to BS with strongest received signal.
Deployment	MBS as backbone. Random and overlapped coverage	Hexagonal grid, MBSs with definite boundaries.
Backhaul Transfer	mmWave band, Fiber, DSL.	DSL and Fiber.
Resource Management	Utilize multiple radio access technologies.	Utilize single type radio access technology.
Coverage Probability	Analytically and numerically available.	Numerically available.

1.1.1.2 Small Cells

Small cells can be divided into two categories: (a) Picocells provide coverage mostly in the hotspot areas such as airports, stadiums, malls and concert areas, and (b) Femtocells present coverage in the residential areas such homes and apartments. Even though, we separated them into two components, the distances between mobile users and SBSs are being short enable high data rates to be achieved via low power transmissions. Also, small cells enable users to enjoy higher data rates while utilizing already existing backhaul infrastructure.

1.1.1.3 Distributed Antenna Systems

DASs create virtual cells among the MBSs and each antenna presents a line–of–sight (LOS) to the mobile user. Thus, DASs provide better coverage and link reliability. DASs utilize the fiber connection as backhaul.

1.1.1.4 Wireless-Fidelity Access Points

WiFi APs use the unlicensed radio frequency (RF) spectrum to offload traffic from macro-cells. WiFi APs are similar to small cells but utilize the unlicensed bands. They can be controlled by mobile users and network operators.

1.1.1.5 Device to Device Links

D2D links are the shortest range communications among all the aforementioned technologies. D2D links provide flexibility and improved coverage. Users may employ common data packages with the neighboring users to reduce the over the air signaling via Bluetooth or WiFi Direct.

The combination of the previously mentioned technologies brings the beauty of the different worlds onto a single plate. Therefore, HetNets represent a promising solution for NGWNs, where many low power, low cost small cells (e.g., femtocells), WiFi APs and D2D links are employed to support the existing macrocell networks to reduce the over the air signaling and uplink power consumption, and to increase capacity. Thus, HetNets enhance the spectral efficiency compared to the MBSs based networks.

However, the increasing complexity of HetNets due to the random deployment of small cells brings into the importance of how to model and analyze the HetNets. Additionally, this new network paradigm also raises new challanges such as the problems of bandwidth resource allocation, user/cell association, traffic offloading based on the user activity and coverage probability regarding the feasibility of current wireless networks.

1.1.2 Research Challenges

Even though offloading traffic to smaller cells will reduce the over the air signaling and increase the capacity, each small cell traffic is limited on the backhaul capacity. Therefore, the overall performance of the small cells is highly dependent on the backhaul connection. Current backhaul technologies are microwave radios, digital subscriber lines (DSLs) and optical fiber links [81]. Moreover, the impact of the wireless network traffic such as user activity, traffic type and dynamic nature of wireless environment on the small cell selection, traffic offloading and power consumption require further investigation [77, 91]. Interference among neighboring cells is highly important due to closer proximity of access points. Furthermore, the resource allocation and scheduling algorithms should be optimized effectively by considering joint bandwidth and user assignments due to the interworking among different radio access technologies. One prominent example is multi–homing where mobile users can utilize WiFi and cellular networks simultaneously. Maximum throughput, mix traffic types, queue stabilization, delay and energy efficiency are the main parameters to consider while formulating each resource allocation problem [43, 44, 86, 91]. Additionally, a key metric in the downlink cellular networks is the probability of coverage which is the received signal strength of the randomly chosen user. Traditional MBS deployment assumes the hexagonal structure, however, it lacks mathematical tractability. Unfortunately, these results cannot be employed in the randomly deployed HetNets. Therefore, the complexity of the HetNets motivates new research investigations to utilize different models such as modeling BS locations via Poisson point process (PPP) [2, 23, 58].

Therefore, an investigation on the bandwidth resource allocation, user/cell association, traffic offloading based on the user activity and coverage probability is a

must for the NGWNs. Some of these challenges, which will be addressed in this dissertation, are:

- Calculation of the number of required SBSs deployment based on the user activity.
- Investigation of the total power consumption with the deployment of SBSs.
- Comparison of Path loss and signal–to–interference ratio (SIR) based traffic offloading strategies and radio access technologies.
- Assignment of the mobile users and their allocated bandwidth.
- The coverage probability transition from the traditional hexagonal MBS deployment to the random deployment scenario.

1.2 Overview of Traffic Offloading

HetNets represent a novel approach to resolve the problem of mobile data offloading and help to optimize the network traffic [33]. HetNets consist of a combination of different size small cells with reduced radius in the range [10–100]m such as picocells and femtocells with WiFi APs and WiFi Direct D2D enabled links as seen in Fig. 1.2a, and are deployed within the existing macrocell. Fig. 1.2a displays WiFi and D2D supported HetNets. HetNets are envisioned to increase the spectral efficiency and enhance the overall network performance by offloading network traffic from the MBS to small cells [73]. Since small cells operate within a smaller distance compared to MBSs and are attached to the macrocell core network via wireless/wired IP backhaul connections, they are expected to provide higher data rates and dedicated capacity to residential areas and hot spots, and to reduce traffic congestion. SBSs have the capability to utilize the unlicensed RF spectrum where WiFi is currently

operating along with the licensed RF spectrum. Such a feature will provide dual mode functionality for SBSs. Therefore, SBSs may provide uninterrupted voice call and text services. At the same time, WiFi satisfies the user's higher demand for multimedia applications such as watching/downloading HD videos and online gaming by employing selected IP traffic offloading (SIPTO).

Fig. 1.2b illustrates the anticipated SIPTO traffic offloading (TO) scenarios for WiFi APs. SIPTO refers to the decision whether the mobile user employs SBS or WiFi APs based on the type or content of the traffic–type. WiFi Direct protocol on IEEE 802.11 may also serve as a good alternative and as it utilizes the unlicensed bands on D2D connections where two closely located devices get connected without routing the traffic through the access network [40]. WiFi Direct is a connection protocol similar to Bluetooth but it utilizes the WiFi interface. Since some users may present common packets within the vicinity of the same receivers, D2D enabled devices can utilize shorter radio links from the neighboring devices. This will increase the overall performance of the small cells and reduce the traffic congestion. The recent advances in mmWave communications at 60 GHz spectrum usage for WiFi are expected to bring a new dimension on the coalition between LTE small cells and WiFi APs such as free spectrum usage, less interference, high data rate and reliable low–range transmission [68]. Collaboration between SBSs, WiFi APs/Wireless Gigabit Alliance (WiGig) and D2D enabled devices will significantly reduce the traffic load in the traditional macrocell networks. According to [19], it is expected that the total percentage of TO from MBSs to small cells will increase by 60% by 2020. Reference [19] describes the TO profiles of countries that began deployment of small cells. Countries where LTE–advanced and WiFi APs communication technologies have already been implemented present higher TO percentages. Therefore, deployment of WiFi supported small cells represents an extremely important task for the network

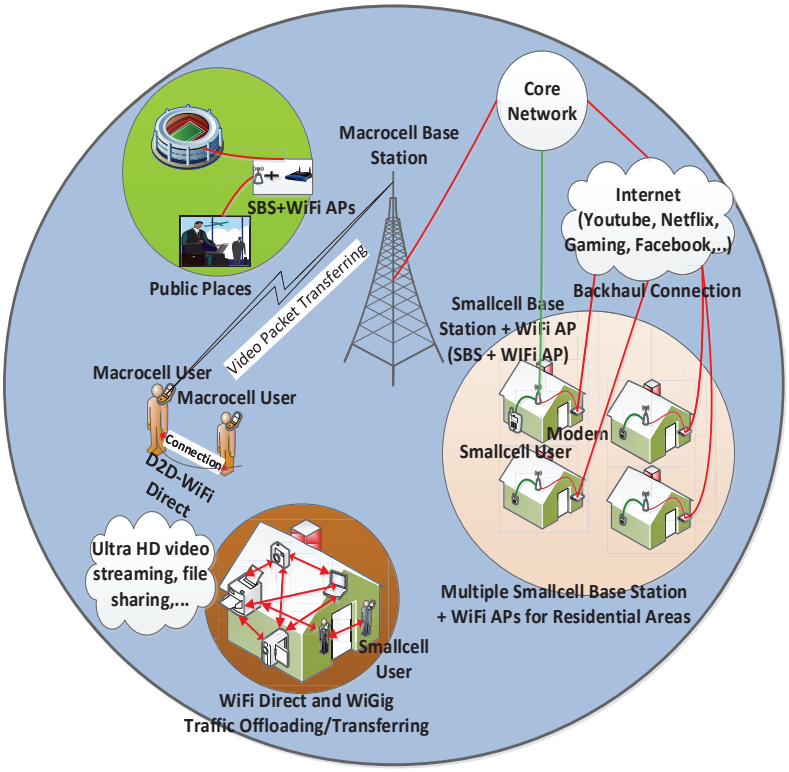

(a) Small cell and WiFi possible connection types.

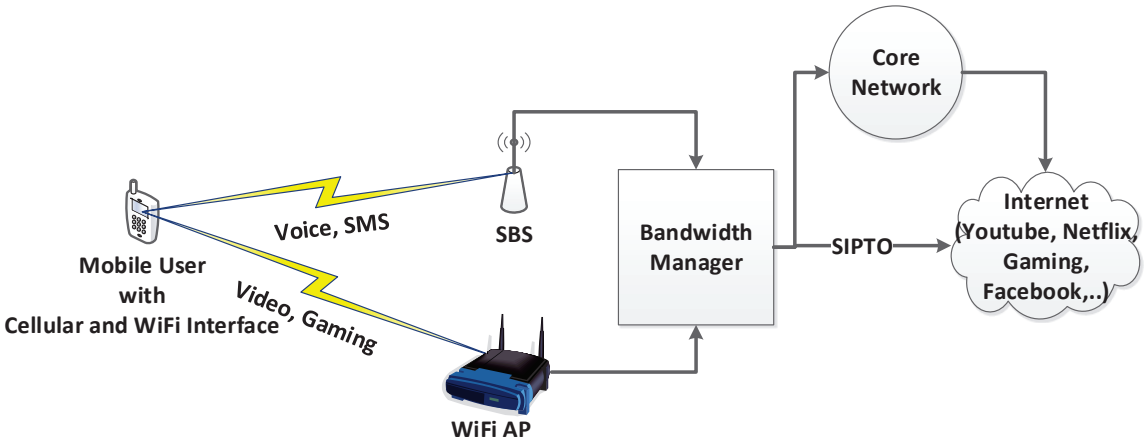

(b) Selective offloading.

Figure 1.2: Graphical illustration of WiFi and Small cell coalition and selective offloading.

operators.

1.2.1 Contributions in Traffic Offloading

We investigate two different traffic offloading schemes (a) path loss (PL) based traffic offloading (TO) strategy and (b) SIR based traffic offloading. In this context, a comparative study of the two techniques to offload the traffic from macrocell to small cell is studied. Additionally, the active user population factor (AUPF), small cell access scheme and traffic-type are included into a PL based TO strategy to minimize congestion of macrocell traffic [27].

1.3 Overview of Power Consumption

Currently, information and communication technology (ICT) industry consumes 0.5% of the total global energy [32]. HetNets are expected to tackle these demands and to improve the overall power consumption by placing numerous low power, low cost small cells (e.g., femtocells) BSs over macrocell networks.

Power consumption of a network can be divided into two subcategories: (F.I) uplink power consumption, and (F.II) downlink power consumption. Highly escalating number of mobile subscribers which was 4.5 billions in 2012 and anticipated to reach 7.6 billions by 2020 and massive mobile data traffic volume which was 45 million tera–byte (TB)/year in 2012 and expected to attain 623 million TB/year till 2020 [24], are the main factors that affect the uplink power consumption. Reference [79] revealed that mobile users with adaptive transmit power schemes reduce the uplink power consumption by using link adaptation, and thus enable greener networks.

1.3.1 Related Work on Power Consumption

In contrast to (F.I), (F.II) can be divided into two subcategories: (i) BS downlink power consumption, and (ii) BS backhaul downlink power consumption. Most of the downlink power is consumed by the BSs. Currently, the number of BSs reached

4 millions and each BS consumes an average of 25 mega–Watt Hour (MWH) per year [38]. To meet the escalating demands of mobile users, cellular operators are placing small cells to complement the macro network which also will reduce the operational expenditure (OpEx) and capital expenditures (CapEx) expenditures of the network. It is estimated that the number of small cells will reach 100 millions with 500 million mobile users in 2020 [24]. At present, a typical small cell consumes about 6–10 W, and it can be predicted that the power consumption of a small cell will still be approximately 5 W in 2020. Hence, 4.4 TWH will be consumed by the 100 million small cells in 2020 which is an extra 5% on top of the power consumption of current BS infrastructure. In order to resolve this issue, numerous avenues are being considered such as [31, 38, 84] (i) developing new power amplifier technologies to design energy efficient BSs; (ii) utilizing power saving protocols where BSs are in sleeping mode under low traffic load; (iii) benefiting from renewable energy sources, e.g., solar and wind energy in place of diesel generators to lower the power consumption of BSs, specifically, the ones at off–grid sites; (iv) modifying cell size intelligently in accordance with the traffic load conditions and the received interference from neighboring cells; and (v) exploiting the amplify–and–forward relays to enrich the power reduction with reduced complexity, even though at an increased cost for infrastructure deployment.

Thus, it is incumbent upon network operators to impose the aforementioned techniques in HetNets so that different radio access technologies are deployed on a large scale. In [55], the impact of reducing the number of active cells during the access portion is underutilized for different network configurations such as hexagonal, crossroads and Manhattan types. In [88], the relationship between traffic load changes and energy savings through dynamic and fixed power ratio for only macro BS (MBS) networks has been illustrated. In [4], HetNets composed of pico BSs (PBSs) and MBS

are examined. The sleeping strategy performs well in order to reduce the total downlink power consumption. The total downlink power consumption has been reduced significantly using the sleeping strategy across various times of the day and different locations of PBSs. In [5], country wide downlink power consumption over different traffic loads for the MBS and micro BSs (mBS) deployment is studied. Also, [57, 82] focused on the impact of backhaul power consumption on different backhaul technologies, e.g., fiber, microwave, along with BS downlink power consumption.

1.3.2 Contributions in Power Consumption

We propose that the population of small cells depends on the traffic load due to the active mobile users, which is modeled as a random-variable, and assumed to be time-varying. It is necessary to assess the number of active small cells based on the AUPF. AUPF defines the ratio of the number of active mobile users to the number of total mobile users, and it also describes the daily user traffic profile. We derive the mathematical framework to calculate the required population of small cells based on the probabilistic traffic models where the number of total mobile users and number of active mobile users have different probabilistic distributions such as different combinations of Binomial and Poisson distributions. Additionally, the large scale deployment of many lightly loaded small cells is expected to increase the downlink and backhaul power consumption of the HetNets. The proposed AUPF model helps to calculate the number of active small cells and to evaluate the power consumption of HetNets [28, 29].

1.4 Overview of Resource Allocation

New radio resource allocation mechanisms should be investigated to provide an efficient usage of all available networks in HetNets. Cooperation among different wireless technologies enable them to complement each other and to provide seamless

data services and connections. The radio resource allocation problem in a HetNet can be categorized into two types: (a) Single network access-allocation where mobile terminals (MTs) can access only the required bandwidth from a single network, and this single network is the best available network at the user location, and (b) Multi–homing network-allocation where MTs can simultaneously utilize all the available networks and aggregate the offered bandwidth from these networks to improve the achieved data rate [89]. Specifically, each MT is covered by a set of overlapped networks which consist of a combination of cellular BSs and wireless local area network (WLAN) APs [41–43]. MT manufacturers, like Apple, LG, Blackberry and Samsung, provide standard built-in WiFi and cellular technologies. For instance, Apple's iPhone operating system (iOS) 7 supports the multiple–connection transmission control protocol (MCTCP) which allows users to utilize both LTE and WiFi connections simultaneously [8]. Another example of "multi–homing" is the concept of "Open Garden" app which enables all devices to find the best available network combination [10].

Currently, MTs are equipped with multiple radio interfaces such as cellular and WiFi in order to efficiently use all the available networks. Additionally, a MT can maintain simultaneous connections from different access networks using its cellular and WiFi interfaces to provide an increased aggregated bandwidth with multi-homing capability to support applications that require higher data rates. Furthermore, due to the fact that at least one radio interface is active, it will provide seamless mobility support and reduce the call blocking rate [15]. Therefore, "multi–homing" has gained significant attention recently.

1.4.1 Related Work on Resource Allocation

There are many studies dedicated to the radio resource allocation problem in HetNets. Existing studies can be divided into two categories single-network resource allocation and multi–homing network-allocation, respectively. In what concerns the first category, the bandwidth resource allocation methods are studied in [12,66,75,80]. Bandwidth allocation and call admission control algorithms are proposed for different classes of services in [75]. The work in [12] develops a distributed resource allocation method based on a convex optimization mechanism in order to find the optimal bandwidth for a minimum required data rate. However, the authors of [12] consider only a single network connection. The authors in [66] introduce a utility function based resource allocation scheme which exploits a convex optimization mechanism for code division multiple access (CDMA) and WLAN networks. The authors in [80] utilize a stochastic programming method to handle the probabilistic nature of demand uncertainty in HetNets. The major drawback of considering a single network connection is that it causes call dropping if there are no other networks such as WLAN and/or cellular networks in the area due to the fact a MT cannot be satisfied with the required bandwidth.

The bandwidth resource allocation methods belonging to the second category are studied in [41–43,47,51,53,60–62] where novel algorithms are proposed to allocate the radio bandwidth resource to different traffic types based on a specific utility of the service supported over all the available networks. Utility fairness is considered in [53] to accomodate the bandwidth for different traffic types such as variable bit rate (VBR) and constant bit rate (CBR). The authors in [60] and [62] use non-cooperative game theory to allocate the bandwidth in a HetNet where the requested bandwidth is collected from all the available networks. The works in [61] and [47] propose a

cooperative game theoretic approach to create an alliance among different types of networks. In [43], the authors consider different traffic types and user types to maximize the utility function while maintaining QoS. The utility maximization problem is solved optimally via a convex optimization method for radio resource allocation in a distributed manner. The work in [51] proposes an opportunistic user association for HetNets to address a resource allocation problem for machine-to-machine (M2M) traffic under a cooperative Nash bargaining solution method. In [41], optimal centralized and suboptimal decentralized resource allocation algorithms are proposed to account for both single network and multi-homing service and their performance is compared. In [42], a decentralized resource allocation algorithm is proposed to reduce the resource allocation complexity in the HetNet while considering the arrivals of new calls and service requests. Therefore, MTs with multi-homing capabilities can further optimize the utilization of the resources of the HetNets [44].

1.4.2 Contributions in Resource Allocation

Unlike the existing research, in order to account for the MT's limited number of radio interfaces and the abundant wireless network options, the joint user assignment and bandwidth allocation problem is formulated to select the optimal subset of networks for each user and allocate the optimal bandwidth share from this subset to maximize the HetNet total utility. The problem is formulated as a mixed integer non–linear program (MINLP) and due to its intractability and computational complexity, we transform the problem into a convex optimization problem via a binary variable relaxation approach. Based on the mathematical analysis of the problem, we present a heuristic algorithm for joint user assignment and bandwidth allocation. The proposed solution achieves a near optimal user assignment and bandwidth allocation at reduced computational complexity [30].

1.5 Overview of Coverage Probability

Rapidly accumulating device diversity, user demands, and need for better coverage make network planning more complicated and introduce randomness in the deployment of BSs in HetNets. In the scenarios where the locations of BSs do not follow a deterministic structure, modeling the performance of the network precisely becomes a challenging task.

1.5.1 Related Work on Coverage Probability

One of the proposed approaches is to model BS deployment as an independent PPP, a methodology which provides analytical tractability for interference and coverage probability analyses [2,39]. However, the independent PPP assumption ignores the correlation among the BSs. Field measurements show that the coverage probability lies in practice between the traditional hexagonal model and the independent PPP approach. This is mainly due to the fact that network operators have still control on BS deployment in a deterministic way [35, 87], which creates intentional repulsion between BSs. Therefore, more realistic ways should be incorporated while still maintaining the tractability of PPP for interference analysis. The authors in [23, 58] apply a α-Ginibre point process (GPP) and a β-GPP to model the correlation between BSs. The GPP is a deterministic point process and takes into account the repulsion between BSs.

1.5.2 Contributions in Coverage Probability

However, PPP allows BSs to be deployed very close to each other and gives pessimistic results compared to the field measurements. In order to address this issue, Lloyd's algorithm, which functions as a bridge between random and structural BS deployments, is investigated for analyzing coverage probability in a network. The

link distance distribution is modeled as a mixture of Weibull distributions and its parameters are obtained by using the expectation-maximization (EM) algorithm for each iteration of Lloyd's algorithm. The link distance distribution is further utilized for calculating the coverage probability approximately by exploiting the tractability of PPP [25].

1.6 Outline

This dissertation attempts to address common problems such as traffic offloading, power consumption, resource allocation and coverage probability in HetNets. The outline of this dissertation is as follows:

1. In Chapter 2, the probabilistic mobile user distribution is analyzed along with its impact on downlink power consumption of HetNets. The daily traffic profile and activity are also considered in the derivations [28, 29].

2. In Chapter 3, we investigate the traffic offloading scenarios in HetNets by considering the benefits of WiFi, D2D and MBS cooperation [27].

3. In Chapter 4, the mobile user assignment and bandwidth resource allocation mechanism is investigated [26, 30].

4. In Chapter 5, the coverage probability analysis for the transition from the traditional hexagonal cellular structure to the randomly deployed HetNets is discussed [25].

2. PROBABILISTIC TRAFFIC MODEL OF MOBILE USERS IN HETEROGENEOUS WIRELESS NETWORKS AND ITS IMPACT ON DOWNLINK POWER CONSUMPTION*

2.1 Introduction

We studied the impact of the probabilistic distributions of the total number of active mobile users and the total number of mobile users on the downlink base station and backhaul power consumption, and the number of active small cells. Herein chapter, we will provide answers to the following questions:

- How to calculate the small cell population based on the variable traffic profile?
- What is the impact of AUPF on the downlink base station and downlink backhaul power consumption of HetNets?
- Which backhaul option consumes the least amount of power, the digital subscriber line (DSL) or fiber?

2.1.1 Organization

The rest of the chapter is organized as follows. In Section 2.2, the system model is presented. Probabilistic distribution analysis of small cells and the downlink power

*Reprinted with permission from "Downlink Power Consumption of HetNets Based on the Probabilistic Traffic Model of Mobile Users," by Ali Rıza Ekti, Muhammad Z. Shakir, Khalid A. Qaraqe and Erchin Serpedin, IEEE 24th International Symposium on Personal, Indoor and Mobile Radio Communications (PIMRC), Copyright 2013 by IEEE.

Reprinted with permission from "End–to–End Downlink Power Consumption of Heterogeneous Small Cell Networks Based on the Probabilistic Traffic Model," by Ali Rıza Ekti, Muhammad Z. Shakir, Khalid A. Qaraqe and Erchin Serpedin, IEEE Wireless Communications and Networking Conference (WCNC), Copyright 2014 by IEEE.

consumption of the system model are provided in Section 2.2.1 and Section 2.3, respectively. Simulation results and discussions are presented in Section 2.4. Finally, concluding remarks are drawn in Section 2.5.

2.2 System Model

A HetNet scenario is assumed where the SBSs are distributed within the macrocell network homogeneously and each SBS can serve up to ten users simultaneously. A typical illustration of the set up considered in this chapter is depicted in Fig. 2.1 where N, D, F, S and O represent the total number of modems and optical network units (ONU), digital subscriber line access multiplexers (DSLAMs) which convert the electrical signals into the data traffic, femto gateways (FGs) which authenticates each femtocell with the core macrocell network and controls the signaling, passive splitters and optical line terminals (OLTs), respectively. ONUs convert optical signals via appropriate electronics to provide provide fiber internet connection, splitters are the passive devices with many input and outputs and OLTs are responsible for coordinating the multiplexing between splitter and gateway. In Fig. 2.1, it is shown that MBS presents fiber backhaul connection to core network, while SBSs are capable of connecting to the core network via DSL or fiber.

A circular macrocell of radius r_m [m] with a BS, B_m, is considered and it is deployed at the center of macrocell with a fiber backhaul connection. HetNets contain N circular small cells of radius r_n [m] with low power, low cost user deployed BS, B_n, which is located at the center of each small cell and with a wired backhaul connection. The number of small cells per macrocell can be computed as follows [28]:

$$N = \gamma \frac{A_m}{A_n} = \frac{m_a}{m_t} \frac{\pi {r_m}^2}{\pi {r_n}^2}, \quad 0 \leq \gamma \leq 1 \tag{2.1}$$

where N denotes the number of active SBSs; γ is a random variable denoting the

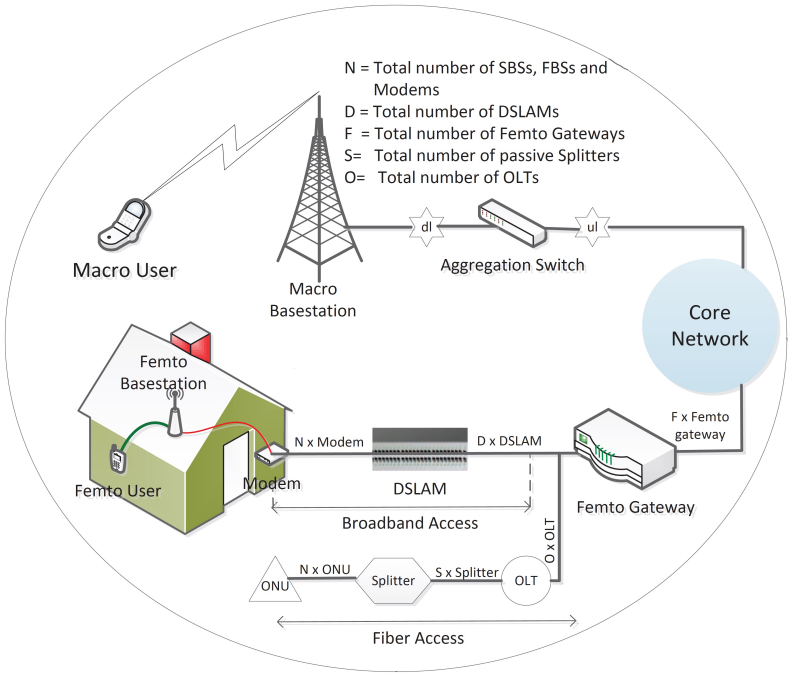

Figure 2.1: End–to–end downlink power consumption of macrocell and small cell networks in HetNet.

population of active mobile users per macrocell. The factor γ is the ratio of the number of active mobile users m_a and the number of total mobile users m_t, and it is referred to as the active user population factor (AUPF)[†]; A_m and A_n stand for the areas of macrocell and small cell, respectively. Moreover, it is assumed that the SBS is active or inactive based on the probability that a mobile user is active in the vicinity of the SBS. Thereby, the population of the SBSs is controlled by the percentile of the active mobile users in a daily traffic profile.

[†] m_a depends on m_t.

2.2.1 Probabilistic Distribution Analysis

We suppress the notations as much as possible, and use m_a, m_t to refer to a random variable, and its values. So for instance the notation $f_{m_a}(m_a)$ becomes $f(m_a)$.

If we are given $f(m_a|m_t)$, the conditional distribution of m_a given m_t, and $f(m_t)$, the distribution of m_t, then the joint distribution of m_a and m_t, $f(m_a, m_t) = f(m_a|m_t)f(m_t)$ and the marginal probability mass function (PMF) can be calculated as:

$$f(m_a) = \sum_{m_t} f(m_a, m_t) = \sum_{m_t} f(m_a|m_t)f(m_t). \tag{2.2}$$

When we are interested in the distribution of $\gamma = \frac{m_a}{m_t}$, then we have:

$$\begin{aligned} \gamma &= \sum_{\gamma=\frac{m_a}{m_t}} f(m_a, m_t), \\ &= \sum_{m_t} \sum_{m_a=\gamma m_t} f(m_a, m_t), \\ &= \sum_{m_t} f(\gamma m_t|m_t)f(m_t). \end{aligned} \tag{2.3}$$

In this study, we consider that the total number of mobile users, m_t and the total number of active mobile users, m_a, are distributed as a mixture of Binomial and Poisson distributions. [‡]

[‡] $B(\cdot,\cdot)$ and $P(\cdot,\cdot)$ denote Binomial and Poisson distributed random variables, respectively.

2.2.1.1 $m_a|m_t$–Discrete Binomal and m_t–Constant

Let's assume $m_{T_{max}}$ is the maximum possible number of the mobile users such that [§] $m_t = m_{T_{max}} = 6250$ as a constant, therefore, $f(m_t) = 1$. Variable m_a is a random variable with $m_a|m_t \sim B(\cdot, \cdot)$.

Let us consider that $f(m_a|m_t)$ is Binomial distributed such that $m_t > 0$ and $0 \leq p \leq 1$, and whose PDF is given by:

$$f(m_a|m_t) = \binom{m_t}{m_a} p^{m_a}(1-p)^{m_t - m_a}, \tag{2.4}$$

where p is the probability of having an active mobile user. Therefore, by substituting $f(m_t)$ and (2.4) into (2.2), one can calculate $f(m_a)$ as follows:

$$f(m_a) = \binom{m_t}{m_a} p^{m_a}(1-p)^{m_t - m_a}, \quad m_a = 0, ..., m_t. \tag{2.5}$$

Using (2.5), one can express the small cell populations factor, γ, as follows:[¶]

$$\gamma = \delta_{I_{m_t}}(\gamma m_t) \binom{m_t}{\gamma m_t} p^{\gamma m_t}(1-p)^{m_t - \gamma m_t}. \tag{2.6}$$

By substituting (2.6) into (3.1) we can obtain the expression to calculate the small cell population, N, under this case as follows:

$$N = \frac{A_m}{A_n} \delta_{I_{m_t}}(\gamma m_t) \binom{m_t}{\gamma m_t} p^{\gamma m_t}(1-p)^{m_t - \gamma m_t}. \tag{2.7}$$

[§] $m_{T_{max}} = \frac{A_m}{A_n} \times 10$ where 10 is the maximum number of mobile users that can be associated with a single SBS as explained in the Section 2.2. Therefore, $m_{T_{max}}$ is equal to 6250. When $m_t = 0$ then $\gamma = \infty$, therefore, $1 \leq m_t \leq m_{T_{max}}$.

[¶] Let A be a set. Define the delta function of A, $\delta_A(.)$ as $\delta_A(x) = 1$ if m_a is in A and 0 otherwise. Example: Let $\mathbb{U}$ denote the set of non–negative integers, then $\delta_{\mathbb{U}}(x) = 1$ if x is a non–negative integer and is zero otherwise.

2.2.1.2 $m_a|m_t$–Discrete Poisson and m_t–Discrete Binomial

In the following case, m_a is a random variable where $m_a|m_t \sim P(\cdot,\cdot)$ and $m_t \sim B(\cdot,\cdot)$. In order to find the total number of active mobile users, we should first calculate the total number of mobile users as:

$$f(m_t) = \binom{m_{T_{max}}}{m_t} q^{m_t}(1-q)^{m_{T_{max}}-m_t}, \tag{2.8}$$

where q is the probability of having a mobile user served by a single small cell whether it is active or inactive, and $0 < q \leq 1$. PDF $f(m_a|m_t)$ is Poisson distributed and given by:

$$f(m_a|m_t) = e^{-\lambda_{m_t}} \frac{{\lambda_{m_t}}^{m_a}}{m_a!}, \tag{2.9}$$

where λ_{m_t} stands for the Poisson arrival rate of active mobile users where the positive parameter λ_{m_t} depends on m_t and p. By substituting (2.8) and (2.9) into (2.2), we can express (2.2) as:

$$f(m_a) = \sum_{m_t=1}^{m_{T_{max}}} \binom{m_{T_{max}}}{m_t} q^{m_t}(1-q)^{m_{T_{max}}-m_t} e^{-\lambda_{m_t}} \frac{{\lambda_{m_t}}^{m_a}}{m_a!}. \tag{2.10}$$

Using (2.10), we can express (2.3) as follows:

$$\gamma = \sum_{m_t=1}^{m_{T_{max}}} \binom{m_{T_{max}}}{m_t} q^{m_t}(1-q)^{m_{T_{max}}-m_t} \delta_{I_{m_t}}(\gamma m_t) e^{-\lambda_{m_t}} \frac{{\lambda_{m_t}}^{\gamma m_t}}{(\gamma m_t)!}. \tag{2.11}$$

By plugging (2.11) into (3.1) we can obtain the expression to calculate N under this case as follows:

$$N = \frac{A_m}{A_n} \sum_{m_t=1}^{m_{T_{max}}} \binom{m_{T_{max}}}{m_t} q^{m_t} (1-q)^{m_{T_{max}} - m_t} \delta_{I_{m_t}}(\gamma m_t) e^{-\lambda_{m_t}} \frac{{\lambda_{m_t}}^{\gamma m_t}}{(\gamma m_t)!}. \tag{2.12}$$

2.2.1.3 $m_a|m_t$–Discrete Poisson and m_t–Discrete Poisson

In the following case, m_a is a random variable where $m_a|m_t \sim P(\cdot,\cdot)$ and $m_t \sim P(\cdot,\cdot)$. $f(m_a|m_t)$ is equal to (2.9) and $f(m_t)$ is given by:

$$f(m_t) = e^{-\mu} \frac{\mu^{m_t}}{m_t!}, \tag{2.13}$$

where μ stands for the Poisson arrival rate of the total number of mobile users and depends on $m_{T_{max}}$ and q. By substituting (2.9) and (2.13) into (2.2), we can express (2.2) as:

$$f(m_a) = \sum_{m_t=1}^{m_{T_{max}}} e^{-\mu} \frac{\mu^{m_t}}{m_t!} e^{-\lambda_{m_t}} \frac{{\lambda_{m_t}}^{m_a}}{m_a!}. \tag{2.14}$$

Using (2.14), we can express (2.3) as follows:

$$\gamma = \sum_{m_t=1}^{m_{T_{max}}} e^{-\mu} \frac{\mu^{m_t}}{m_t!} \delta_{I_{m_t}}(\gamma m_t) e^{-\lambda_{m_t}} \frac{{\lambda_{m_t}}^{\gamma m_t}}{(\gamma m_t)!}. \tag{2.15}$$

By substituting (2.15) into (3.1), N takes the expression:

$$N = \frac{A_m}{A_n} \sum_{m_t=1}^{m_{T_{max}}} e^{-\mu} \frac{\mu^{m_t}}{m_t!} \delta_{I_{m_t}}(\gamma m_t) e^{-\lambda_{m_t}} \frac{{\lambda_{m_t}}^{\gamma m_t}}{(\gamma m_t)!}. \tag{2.16}$$

2.2.1.4 $m_a|m_t$–Discrete Binomial and m_t–Discrete Poisson

In the following case, m_a is a random variable where $m_a|m_t \sim B(\cdot,\cdot)$ and $m_t \sim P(\cdot,\cdot)$. Variable m_t has the same distribution as in (2.13), and it presents $m_{T_{max}}$ and

q dependent parameters. PDF $f(m_a|m_t)$ is equal to (2.4).

By substituting (2.4) and (2.13) into (2.2), we can express (2.2) as:

$$f(m_a) = \sum_{m_t=1}^{m_{T_{max}}} e^{-\mu} \frac{\mu^{m_t}}{m_t!} \binom{m_t}{m_a} p^{m_a} (1-p)^{m_t - m_a}. \tag{2.17}$$

Using (2.17), we can express (2.3) as follows:

$$\gamma = \sum_{m_t=1}^{m_{T_{max}}} e^{-\mu} \frac{\mu^{m_t}}{m_t!} \delta_{I_{m_t}}(\gamma m_t) \binom{m_t}{\gamma m_t} p^{\gamma m_t} (1-p)^{m_t - \gamma m_t}. \tag{2.18}$$

By substituting (2.18) into (3.1), N can be evaluated as:

$$\frac{A_m}{A_n} \sum_{m_t=1}^{m_{T_{max}}} e^{-\mu} \frac{\mu^{m_t}}{m_t!} \delta_{I_{m_t}}(\gamma m_t) \binom{n_{m_t}}{\gamma m_t} p^{\gamma m_t} (1-p)^{m_t - \gamma m_t}. \tag{2.19}$$

2.2.1.5 $m_a|m_t$–Discrete Binomial and m_t–Discrete Binomial

In this case, m_a is a random variable where $m_a|m_t \sim B(\cdot,\cdot)$ and $m_t \sim B(\cdot,\cdot)$. $f(m_a|m_t)$ and $f(m_t)$ are equal to (2.4) and (2.8), respectively. Therefore, we can obtain $f(m_a)$ by substituting (2.4) and (2.8) into (2.2):

$$f(m_a) = \sum_{m_t=1}^{m_{T_{max}}} \binom{m_{T_{max}}}{m_t} q^{m_t} (1-q)^{m_{T_{max}} - m_t} \binom{m_t}{m_a} p^{m_a} (1-p)^{m_t - m_a}. \tag{2.20}$$

Using (2.20), we can express (2.3) as follows:

$$\gamma = \sum_{m_t=1}^{m_{T_{max}}} \binom{m_{T_{max}}}{m_t} q^{m_t} (1-q)^{m_{T_{max}} - m_t} \delta_{I_{m_t}}(\gamma m_t) \binom{m_t}{\gamma m_t} p^{\gamma m_t} (1-p)^{m_t - \gamma m_t}. \tag{2.21}$$

By plugging (2.21) into (3.1), N can be rewritten as:

$$N = \frac{A_m}{A_n} \sum_{m_t=1}^{m_{T_{max}}} \binom{m_{T_{max}}}{m_t} q^{m_t}(1-q)^{m_{T_{max}}-m_t} \delta_{I_{m_t}}(\gamma m_t) \binom{m_t}{\gamma m_t} p^{\gamma m_t}(1-p)^{m_t-\gamma m_t}. \tag{2.22}$$

2.3 Downlink Power Consumption

The downlink power consumption of HetNets is composed of two components: (i) macrocell network downlink power consumption, and (ii) small cell network downlink power consumption [6, 70]. The total downlink power consumption can be expressed as follows:

$$P_{tc} = \underbrace{P_M + P_{bh}^M}_{\text{MBS}} + \underbrace{P_n + P_{bh}^n}_{\text{SBS}} , \tag{2.23}$$

where P_{tc} is the total power consumption; P_M and P_n stand for the power consumption of MBS and SBS, respectively.

2.3.1 Base Station Power Consumption

MBS and SBS power consumption can be calculated respectively as [82] [‖] :

$$P_M = k_m P_m + j_m \tag{2.24}$$

and

$$P_n = N(k_s P_s + j_s), \tag{2.25}$$

where P_m and P_s denote the maxium RF output power of MBS and SBS, respectively; k_m and k_s are the slopes of the load dependent power consumption of MBS

[‖]The power amplifier efficiency is omitted in (2.24), (2.25) [45].

and SBS, respectively; j_m and j_s denote the signal processing and site cooling power consumption of MBS and SBS, respectively; and N denotes the traffic load dependent SBS population which is strictly depending on AUPF. Total downlink power consumption per macrocell based on the traffic load dependent population of small cells can be easily calculated by plugging N into (2.25) for each case in Section 2.2.1, i.e., using (2.7), (2.12), (2.16), (2.19) and (2.22).

2.3.2 Backhaul Power Consumption

In (2.23), P_{bh}^{M} denotes the traffic load dependent backhaul power consumption of MBS and it is given by** [82]:

$$P_{bh}^{M} = \gamma \left(\left\lceil \frac{1}{a_{port}} \right\rceil P_{sw} + P_{dl} + P_{ul} \right), \tag{2.26}$$

where a_{port} denotes the number of ports required for the aggregation switch; P_{sw} stands for the maximum power consumption of the aggregation switch; P_{dl} is the power consumed by one downlink interface in the aggregation switch used to collect the backhaul traffic; and P_{ul} denotes the power consumption of an uplink interface††. Note that the backhaul power consumption of macrocell network is now dependent on the traffic load to be backhauled to the core network such that γ can be calculated by (2.6).

In (2.23), P_{bh}^{n} stands for the traffic load dependent backhaul power consumption of the small cell network which depends on the type of the medium to backhaul

**$\lceil \cdot \rceil$ denotes the ceiling function.

††Uplink interface is a part of the downlink which collects the traffic from the aggregation switch and transfer it to the MBS core network.

Table 2.1: Downlink Power Consumption Parameters.

Base station type	$P_{(\cdot)}$[W]	$k_{(\cdot)}$	$j_{(\cdot)}$[W]	P_{mod}	D_{port}	a_{port}	fg_{port}	P_d	P_{fg}	P_{sw}	P_{ul}	P_{dl}	P_{onu}	P_{olt}	s_{port}	o_{port}	P_s
Macro	40	21.45	354.44	N/A	N/A	32	N/A	N/A	N/A	1000	2	1	N/A	N/A	N/A	N/A	N/A
Small cell	0.05	7.5	4.8	2	72	N/A	100	60	100	N/A	N/A	N/A	2	20	48	48	0

the traffic from access to the core network. In this study, the power consumptions of DSL and fiber based backhaul networks are compared and calculated based on the similar principle in (2.26). It is assumed that the total power consumed by the DSL and fiber based backhaul networks is denoted by $P_{bh}^{n_d}$ and $P_{bh}^{n_f}$, respectively. The backhaul power consumption over DSL, $P_{bh}^{n_d}$, can be represented as in (2.12), which is shown at the top of the next page. In (2.12), P_{mod} and P_{mod}^{t} are the power consumption of one modem and N modems, respectively; d_{port} denotes the number of ports required for the DSLAM; P_d and P_d^t represent the power consumption of one DSLAM and D DSLAMs, respectively; fg_{port} denotes the number of ports required for the femto gateway; P_{fg} and P_{fg}^t represent the power consumption of one femto gateway and F femto gateways, respectively.

Similarly, the backhaul power consumption of the small cell network over the fiber connection, $P_{bh}^{n_f}$, can be calculated as in (2.13), shown at the top of the next page. In (2.13), s_{port} and o_{port} stand for the number of ports required for the passive splitter and OLT, respectively; P_{onu}, P_s and P_{olt} are the powers consumed by a ONU, passive splitter and OLT, respectively; P_{onu}^t, P_s^t and P_{olt}^t denote the total power consumption of the N ONUs, S passive splitters and O OLT, respectively. Downlink power consumption parameters are described in TABLE 2.1.

$$P_{bh}^{n_d} = \underbrace{\left(\underbrace{\left(\gamma \frac{A_m}{A_n}\right)}_{N} P_{mod} \right)}_{P_{mod}^t} + \underbrace{\left(\underbrace{\left\lceil \frac{1}{d_{port}} \left(\gamma \frac{A_m}{A_n}\right) \right\rceil}_{D} P_d \right)}_{P_d^t} + \underbrace{\left(\underbrace{\left\lceil \frac{1}{fg_{port}} \left\lceil \frac{1}{d_{port}} \left(\gamma \frac{A_m}{A_n}\right) \right\rceil \right\rceil}_{F} P_{fg} \right)}_{P_{fg}^t} \tag{2.12}$$

$$P_{bh}^{n_f} = \underbrace{\left(\underbrace{\left(\gamma \frac{A_m}{A_n}\right)}_{N} P_{onu} \right)}_{P_{onu}^t} + \underbrace{\left(\underbrace{\left\lceil \frac{1}{s_{port}} \left(\gamma \frac{A_m}{A_n}\right) \right\rceil}_{S} P_s \right)}_{P_s^t} + \underbrace{\left(\underbrace{\left\lceil \frac{1}{o_{port}} \left\lceil \frac{1}{s_{port}} \left(\gamma \frac{A_m}{A_n}\right) \right\rceil \right\rceil}_{O} P_{olt} \right)}_{P_{olt}^t}$$
$$+ \underbrace{\left(\underbrace{\left\lceil \frac{1}{fg_{port}} \left\lceil \frac{1}{o_{port}} \left\lceil \frac{1}{s_{port}} \left(\gamma \frac{A_m}{A_n}\right) \right\rceil \right\rceil \right\rceil}_{F} P_{fg} \right)}_{P_{fg}^t} \tag{2.13}$$

2.4 Simulation Results and Discussions

In this section, numerical and simulation results are presented to confirm the analytical results and investigate the impact of various probabilistic traffic load profiles in HetNets in terms of SBS population and downlink power consumption. Low traffic load presents the probability value of $p = 0.035$, medium traffic load considers $p = \{0.1, 0.15\}$ and high traffic load assumes $p = \{0.3, 0.35\}$. In order to the evaluate performance of each case in Section 2.2.1, we have used the following parameters in the simulations, $r_m = 500$m, $r_n = 20$m, $m_{T_{max}} = C_{Max} = 6250$ along with the parameters in TABLE 2.1.

The effect of the daily traffic profile, Hours, against $m_a|m_t\%$ is shown in Fig. 2.2. It demonstrates that the daily user traffic and $m_a|m_t\%$ are directly related to each other, as expected. With the activity of the users increasing during the 24 hour period, γ and $m_a|m_t\%$ are taking greater values. For example, when $m_a|m_t\%$ is equal to 4.91, γ becomes 0.0491. During late night hours, most users are sleeping which is directly affecting the γ.

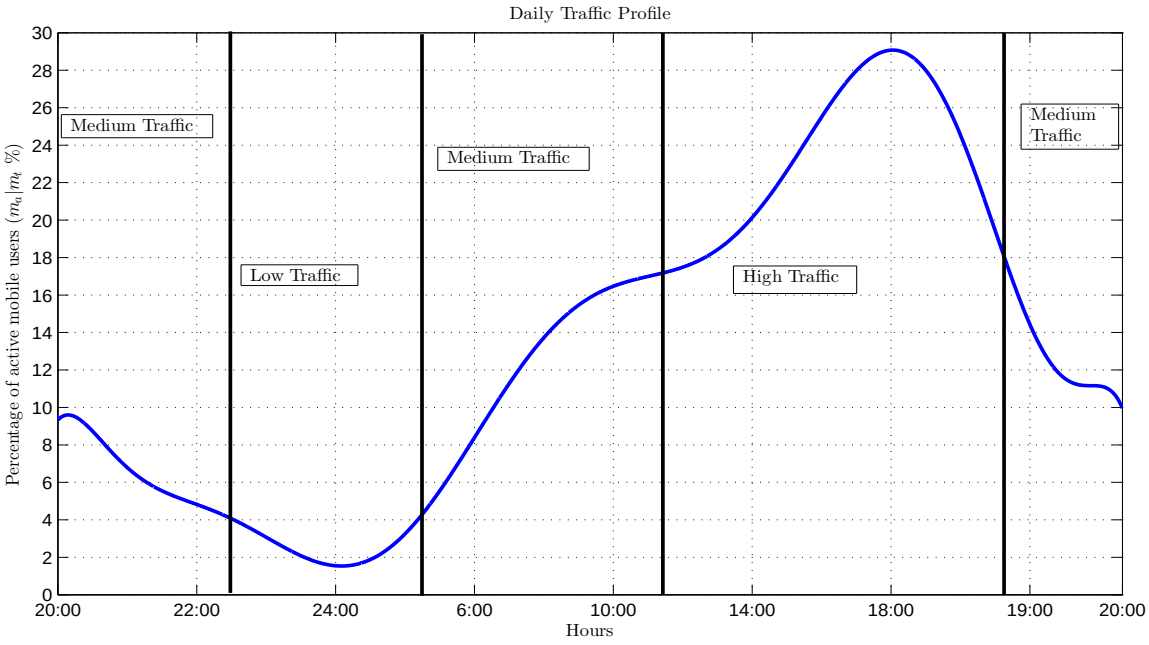

Figure 2.2: Daily traffic profile vs active user percentage.

Fig. 2.3 is plotted to show the impact of γ on N. As expected, when the AUPF increases then N is increasing which means higher traffic load. One can easily relate this relationship to a daily traffic profile for current cellular communications. Under low traffic load, e.g., during night time, less small cells become active. In case of the high traffic, e.g., during day time, the numerical value of N increases with the increase in γ. For instance, under low γ values, the numerical values of N varies in

the interval $(0, 25)$. Under medium and high γ values, N will take values in these intervals $(25, 100)$ and $(100, 188)$, respectively.

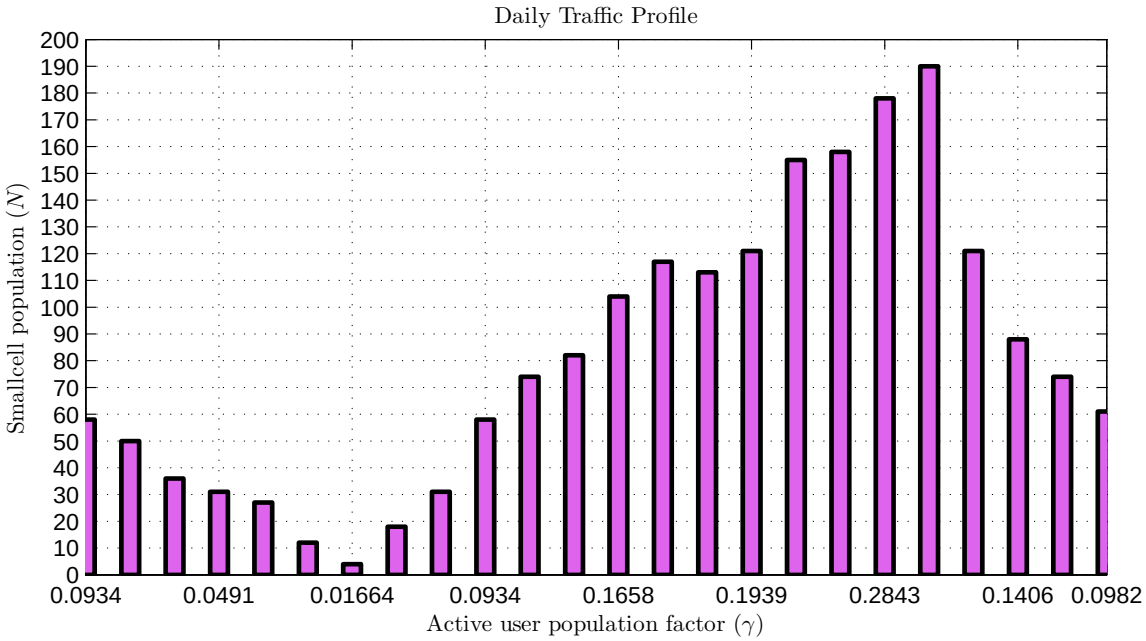

Figure 2.3: Active user population factor (AUPF) vs number of active small cells.

Fig. 2.4 illustrates the downlink power consumption for different traffic loads for the small cell network based on the BS power consumption and DSL backhaul power consumption. When γ increases then the values of power consumption are becoming larger due to an increase in the number of active SBS. As an example, under low traffic values backhaul, SBS and total small cell power consumptions take values in these intervals $(0, 180)$ W, $(0, 200)$ W, and $(0, 380)$ W, respectively.

In order to compare the power consumption between fiber and DSL backhaul cases, Fig. 2.5 illustrates the dependency between AUPF and small cell power consumption over the fiber backhaul. The same pattern is also seen in the fiber backhaul power consumption, but interestingly, fiber backhaul power consumption is less than

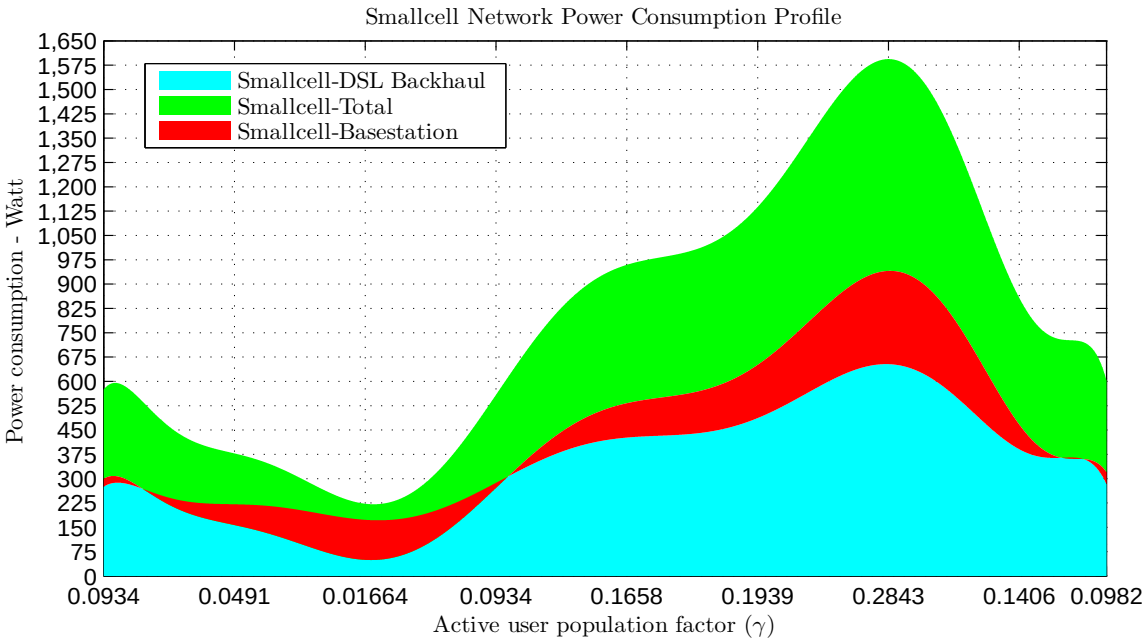

Figure 2.4: Active user population factor (AUPF) vs small cell power consumption over DSL backhaul.

DSL backhaul power consumption due to the less power consumption by fiber interfaces. As an example, the splitter can be considered as a passive interface in fiber based backhaul network and thereby does not consume any power to carry traffic from ONU to OLT, i.e., $P_s = 0$. Under the highest traffic load, the fiber backhaul power consumption is 175 W less than DSL backhaul power consumption.

The downlink power consumption of macrocell network MBS with respect to γ is depicted in Fig. 2.6. Since the MBS is single and active all the times, MBS downlink power consumption is constant with a numerical value of 1212.5 W. On the other hand, the backhaul power consumption varies in the interval $(0, 291)$ W due to the variable traffic loads. The numerical range of total power consumption is the interval $(1212.5, 1503.5)$ W.

A common observation for this section is that N, $P_{bh}^{n_d}$, $P_{bh}^{n_f}$, P_{bh}^{M}, P_n and P_{tc}

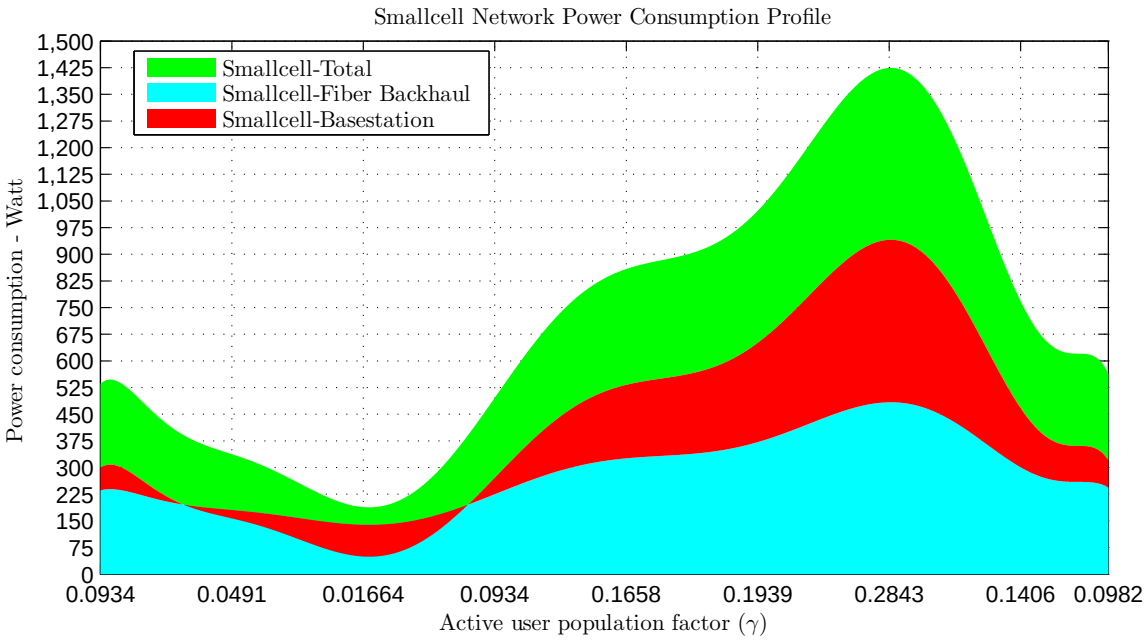

Figure 2.5: Active user population factor (AUPF) vs small cell power consumption over fiber backhaul.

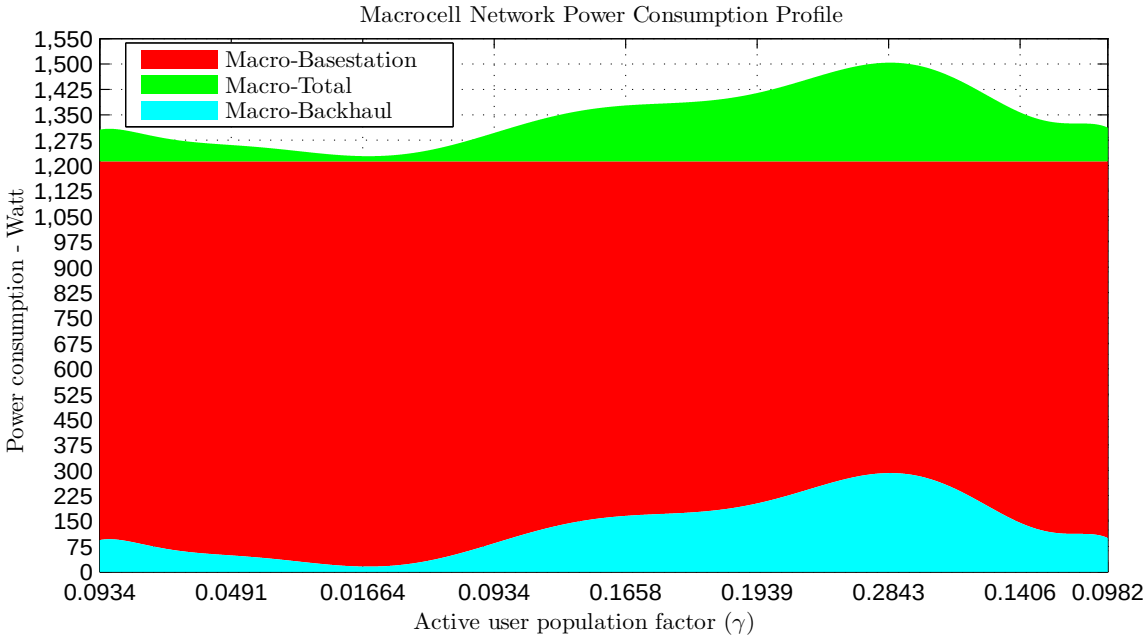

Figure 2.6: Active user population factor (AUPF) vs macrocell power consumption.

are random variables and strictly dependent on the values of γ, which is highly dependent on the population of active mobile users. Numerical values of γ, N and P_{tc} increase as the traffic load increases. Also, distribution of the number of mobile users and active mobile users play a crucial role for the number of active SBS and their downlink power consumption. When p increases, the distinction becomes clear. Moreover, the type of backhaul technology is playing a crucial role in the downlink power consumption analysis.

2.5 Summary

In this study, we proposed a probabilistic traffic model in order to calculate the number of active SBS and thereby control the downlink power consumption of HetNets. It is shown that changes in traffic load profiles lead to changes on the downlink power consumption and the number of active small cells, as expected. The number of active users is calculated by the proposed probabilistic traffic model which assures that downlink power consumption in HetNets will be reduced by switching–off the SBSs intelligently under low and medium traffic load conditions. Furthermore, it turns out that if the traffic load is not extremely large, small cell deployment will reduce the power consumption significantly. Another interesting observation is that fiber based backhaul is consuming less power than DSL based backhaul.

3. ON THE TRAFFIC OFFLOADING IN WIFI SUPPORTED HETEROGENEOUS WIRELESS NETWORKS

3.1 Introduction

In this chapter, an active user dependent PL based TO strategy for HetNets is proposed and analyzed to overcome the aforementioned problems in Section 1.2. The main objective of the PL based strategy is to show the significant difference between SIR based offloading and PL based offloading while considering the AUPF, which is calculated in Section 2.2.1, and traffic–type, where hybrid small cells are distributed homogeneously along the macrocell. PL strategy increases the offloading percentage and ensures that more users will transfer to SBS and experience better data throughput and coverage. Further, the offloaded user traffic gets distributed onto SBS, WiFi and D2D enabled links based on the content of the application.

Factors such as population density, access scheme and distribution of small cells across the macrocell area represent challenging issues that can impact the TO directly. In addition to these factors, the daily traffic profile, active user population and traffic–type should also be investigated to optimize the network deployment and QoS. Therefore, the AUPF of mobile users on the traffic offload has also been studied. Due to the aforementioned reasons, answers to the following questions will be addressed herein chapter:

- What is the impact of hybrid small cell and macrocell radius on the percentage of TO?
- How does the percentage of TO change with respect to the AUPF (γ) and the probability of having an open/closed access hybrid small cell?

- How much of the offloaded traffic will go through SBS, WiFi AP and D2D enabled links?

3.1.1 Organization

The remainder of this chapter is structured as follows. SBS and WiFi APs coalition benefits are discussed in Section 3.3. A layout of the HetNets along with the evaluation of the population factor with respect to the number of active small cells and access schemes are depicted in Section 3.4. PL and SIR TO based strategies are discussed in Section 3.5, respectively. The TO analysis is presented in Section 3.6. Section 3.7 presents economics of TO. Simulation results and discussions are included where required to provide a comparative performance analysis. Finally, the concluding remarks are drawn in Section 3.8.

3.2 Device–to–Device, Small Cell Base Station and Wireless-Fidelity Based Traffic Offloading

In D2D enabled networks direct transmission through each device is considered. For instance, some devices may utilize the SBSs or WiFi APs for downloading a multimedia file while other close–proximity devices can utilize the shorter direct link to fetch data from its D2D peers like a peer–to–peer (P2P) connection with WiFi Direct or WiGig. This will distribute the traffic load onto D2D enabled devices and reduce the total traffic load. A good example of this situation is that of watching ultra HD videos from TV by directly transmitting through a laptop or camera or blu-ray player. However, D2D enabled devices are battery powered equipment, and therefore, the energy consumption will increase and drain the battery of the mobile devices based on the content of the file that is being downloaded or uploaded. This concern can be eliminated by providing higher data rates for the D2D enabled devices. D2D communication does also present reliability concerns due to the rapid RF

environment changes. Almost 38% of the total mobile data traffic is offloaded onto WiFi APs and hotspots in US [20] and it is expected to be higher with the implementation of 5G NGWNs. Since WiFi APs are already deployed at homes, campuses and businesses, it is more convenient for the network operators to utilize the WiFi as the data offloading docking stations. Most of the current cellular phones have the capability of connecting to either WiFi or cellular base stations in order to download multimedia and delay tolerant applications and contents. Mobile devices usually pick the WiFi APs if there is one in the vicinity due to the fact that it will provide higher data rates and reduce the cellular plan cost by utilizing the unlicensed RF spectrum. Especially with the introduction of the WiGig technology which employs the 60 GHz unlicensed and price–free spectrum, it will definitely bring WiFi one step further as the carrier offloading strategy [69]. WiGig operates on a very wide bandwidth which makes the spectrum very attractive for multimedia and delay tolerant applications such as streaming ultra HD from a dvd-player or laptop to a TV set. Especially for backhaul, it creates an opportunity for outdoor point–to–point (P2P) connections to provide Internet access to neighboring buildings to prolong the access of fiber networks. WiGig presents several advantages such as (i) intelligent beam control techniques; (ii) energy efficient transmission, i.e., 30% less energy consumption than LTE small cells; (iii) shorter range and easy interference management; (iv) 7 GHz of free and unlicensed spectrum with Gbps transmission rates; (v) instant wireless synchronization. Lastly, SBSs are a natural extension of the macrocell network. SBSs provide also a better QoS for voice and delay tolerant applications with no disruption. SBSs utilize the licensed spectrum which enable them to avoid easily unwanted radios and penetrate through buildings. On the other hand, licensed spectrum is limited so WiFi will most of the time provide higher data rates. This points out the importance of the multi–homing [43]. Currently, mobile devices are capable of

handling higher bandwidth consuming applications along with basic voice and text applications via WiFi and cellular interfaces. Such type of communication presents multi–homing features. Multi–homing associates each radio interface with the available overlapped mobile networks which can be cellular base stations or WiFi APs. Therefore, multi–homing has gained significant interest within the past years. Most of the smartphones have the capability of multi–homing which enables each device to connect to any available network as shown in Fig. 1.2b. Therefore, after carefully examining these three approaches, one can infer that a combination of these technologies will generate higher data rates, better coverage and less power consumption, a research topic which is currently being investigated in the upcoming WiFi supported 5G NGWNs [9]. Next, the potential benefits of the coalition between SBSs and WiFi will be discussed.

3.3 Small Cell Base Station and WiFi Access Points Coalition Benefits

The capacity of SBS depends directly on the limited availability of the spectrum which can also be dissipated by the interference from the highly dense SBS deployment. To handle such problems, researchers and network operators started to investigate the usage of WiFi to support the SBSs. Possible integration scenarios can be seen in Fig. 1.2a. Integration of these two technologies will bring many benefits.

Radio Frequency Spectrum Utilization: RF spectrum is critical for the wireless communications systems because of its limited availability. Due to the ever increasing demand for it, researchers have sought to find more efficient ways to utilize the RF spectrum. Depending on the design, communication systems use the RF spectrum in different ways. However, one of the most important design features is the fact that wireless systems should optimize the use of resources by employing a set of functionalities. Due to the limited nature of current RF spectrum, the mmWave

communication band 60 GHz will bring new degrees of freedoms in terms of TO such as higher data rates with interference immunity, better security and re–use of the frequency bands.

60 GHz mmWave Communication: Electromagnetic waves can be absorbed by oxygen molecules while traveling through air. The absorption level is higher at 60 Ghz, therefore, the propagation distance diminishes at such high frequencies. With the great absorption rates in the 60 GHz mmWave communication, e.g., WiGig can be used in shorter range communications to provide very high data rates with no interference to neighboring WiGig devices because of the aforementioned oxygen absorption issue. Moreover, this portion of spectrum is unlicensed so far and represents an attractive option for the operators. However, one interesting point that needs to be addressed is the effect of the rain on the deployment of the outdoor 60 GHz technologies. Rain might dominate the mmWave penetration distance more than the oxygen absorption rate.

Smart Traffic Offloading: The combination of WiFi and SBSs will allow network operators to provide voice and text services through the carrier core network while transferring the Internet traffic through WiFi APs and its backhaul as depicted in Fig. 1.2b. This offloading scenario will give the opportunity to use the best of both WiFi and SBSs for the mobile users.

WiFi Backhaul: Small cells typically utilize either the DSL, fiber or cable as backhaul connection technology. Small cell owners are not concerned with the type of technology used for backhaul, however, the network operators are concerned by the technology used for backhaul [81]. Stemming from the limited backhaul capabilities, the volume of offloaded traffic from macrocell can be reduced if the small cell backhaul reaches a certain threshold. Therefore, the backhaul constraint can be integrated with the biased user association technique [33]. The biased user as-

sociation technique refers to the allocation of the mobile user to the available small cells. If the wired backhaul reaches its limits, then WiFi integrated SBSs also enable network operators to use WiFi as a very good candidate for the backhaul transfer. WiFi APs in many SBSs can construct a mesh network for a high quality and dependable wireless backhaul especially with the new WiGig concept which can easily provide fiber optical data transfer rates. Moreover, WiFi can also be used to offload the Machine-type traffic that is envisioned to explode in volume due to the advent of Internet of Things (IoT).

Cost Efficiency: Network operators have a big craving for successful WiFi and SBS integration in order to eliminate extra OpEx and CapEx costs for separate installation/planning of the WiFi APs and SBSs. Therefore, dual mode or hybrid small cells which combine the small cell and WiFi on the same hardware will lower the cost of the ownership and increase the usage of shared resources such as backhaul, site rental, spectrum cost and additional equipment. In the earlier years of the small cell deployments, WiFi was considered as a competitor but now it can be easily seen that SBS and WiFi are the two sides of the same coin that can complement each other well. Mutualism of these two technologies in the same box will guarantee the usage of the right technology all the times without contemplation over the radio access technology.

Handover: Seamless handover is a must for the integrated SBS and WiFi technologies due to excessive traffic and interference. It will assure the uninterrupted service quality for the mobile user regardless of the radio interface technology. In these cases, successful offloading which is a part of handover becomes an important issue. One of the easiest ways of incorporating the impact of environment into the handover analysis is to use a simple PL model with different PL exponents corresponding to different environments and cell types.

3.4 Heterogeneous Small Cell Network Layout

In this section, a HetNets scenario is considered where the small cells are distributed within the macrocell network homogeneously. In terms of the ease of practical implementation, it is assumed that each macrocell is surrounded by six macrocells that generate interference to the corresponding mobile users. Moreover, each small cell is encircled by six small cells in order to provide a fair comparison with macrocells.

A circular macrocell of radius r_m [m] is assigned with a BS, B_m, which is deployed at the center of macrocell. HetNets contain N circular small cells of radius r_n [m] with low power, low cost user deployed BSs, B_n, which are assumed to be located at the center of each small cell and equipped with a wired/wireless backhaul connection. The number of small cells per macrocell can be expressed as in Section 2.2.1 * [28]:

$$N = \underbrace{\gamma \frac{A_m}{A_n} \alpha}_{\text{Open Access}} + \underbrace{\gamma \frac{A_m}{A_n} (1-\alpha)}_{\text{Closed Access}}, \quad 0 \leq \gamma \leq 1 \ , \ 0 \leq \alpha \leq 1, \tag{3.1}$$

where N denotes the number of active small cells, and γ stands for the AUPF parameter which represents a random variable that controls the small cell population per macrocell and daily traffic profile. The AUPF, γ, is the ratio of the number of active mobile users, m_a, and the number of total mobile users, m_t †. Variable α stands for the probability of having an open access small cell. Variables $A_m = \pi r_m^2$ and $A_n = \pi r_n^2$ denote the areas of macrocell and small cell, respectively. Moreover,

*The intuition behind this approach is to associate the active user distribution, daily traffic profile and small cell access schemes together.

†To calculate the AUPF, it is assumed that two types of mobile users exist in the network: (a) active mobile users and (b) inactive mobile users. The number of total mobile users is equal to the total number of active and inactive mobile users, m_t.

it is assumed that the small cell is active or inactive based on the probability that a mobile user is active in the vicinity of the small cell. Thereby, the population of the small cells is controlled by the percentile of the active mobile users in a daily traffic profile and access schemes of the small cells.

3.4.1 Small Cell Access Schemes

Based on the privileges and permissions allocated to customers, small cell access schemes can be classified into:

3.4.1.1 Closed Access

Self deployed small cells have a key limitation in a "closed access" scheme since the customers would opt for limiting the access to themselves and their preferred users. As expected, closed access small cells do not enhance the coverage for all customers. Therefore, operators search for better access schemes such as "open access" small cells in order to reduce the OpEx and increase the coverage [21].

3.4.1.2 Open Access

Any random nearby cellular user can utilize the small cells which are in "open access" mode. This will allow the network operator to expand the coverage and network performance but will create additional interference problems. A small cell owner would still favor a closed access scheme in order to employ small cell backhaul and enhance the capacity for particular users [21].

Fig. 3.1 illustrates[‡] the relationship between γ and α with respect to N and N_o. Variables N_o and N_c denote the number of active open access small cells and active

[‡]In Fig. 3.1 x–axis values are taking decreasing and increasing values in order to show the impact of daily traffic profile. In a 24–hour period, the activity of the mobile users is not monotonically increasing and decreasing.

closed access small cells, respectively. The number of mobile users is assumed to be adaptive in the coverage area. The following parameters are used $r_m = 400$m and $r_n = 20$m to calculate the total number of small cells per macrocell. Low traffic load presents the probability value $p = 0.03$, medium traffic load exhibits $p = 0.15$ and high traffic load assumes $p = 0.3$, where p is the probability of having an active user. Fig. 3.1 demonstrates the impact of variable traffic load profiles on N for different α and γ. When the traffic load increases, then N takes greater values as expected. For instance, the numerical range of N under low traffic load is the interval (0, 16). In case of medium traffic load, the numerical range of N is within the interval (16, 56). Also, under high traffic load, N varies in the interval (56, 114). As a common observation for Fig. 3.1, α represents the scaling factor for the daily traffic profile of N and N_o, where the total number of small cells remains the same while N_o takes different values. Another crucial point, a significant role on the number of active small cells is played by AUPF, which is a function of the active mobile users. Therefore, AUPF directly affects N and N_o and their values fluctuate with the variable traffic load.

Deployment of many small size, low cost and low power SBSs and WiFi APs in the existing macrocell network brings into analysis the important function played by TO. When the congested traffic unloads onto the small cells, MBS will experience less congested traffic and perform better. Small cells reduce the transmission distance and increase the data rate and coverage but such a setup will create a disadvantage in terms of SIR for the offloaded users. Users offloaded to smaller cells receive dissipated SIR due to the strongest interference power received. If SIR based offloading takes place, then most of the users will remain in the MBS coverage and receive low data rates and unsatisfactory QoS. Therefore, in this study, the PL based TO is investigated stemming from the fact that the offloaded users onto small cells

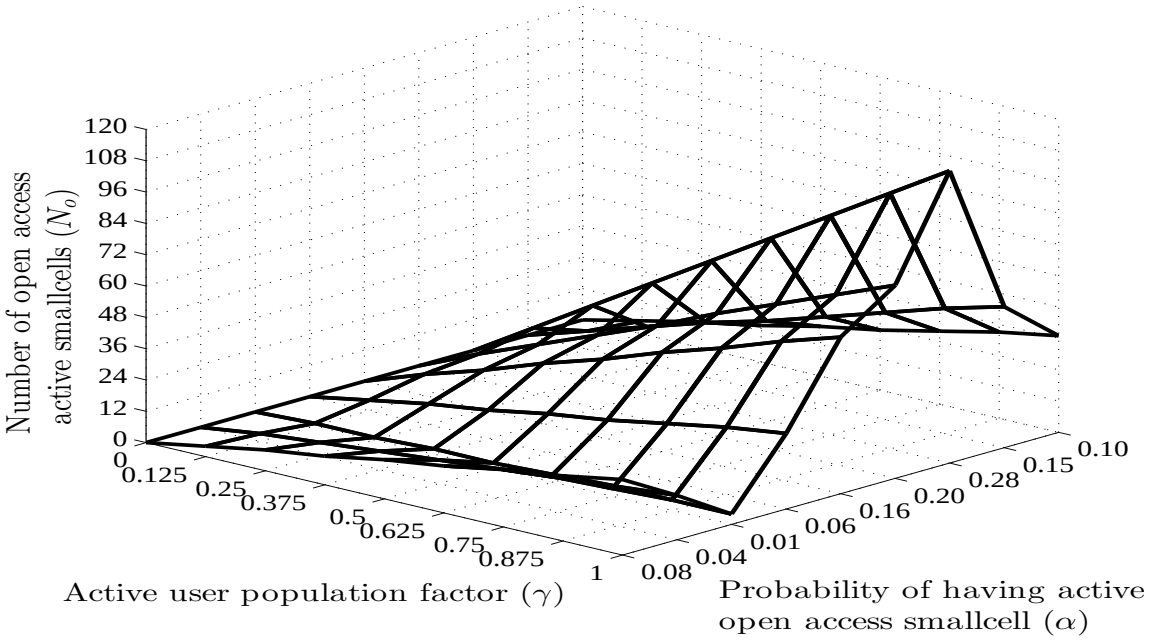

Figure 3.1: Number of small cells per macrocell as a function of active user population factor and probability of having open access small cell for daily traffic profile.

experience better received power from the closer BSs. This will increase the overall offloading percentage and improve the overall system performance and spectral efficiency. Furthermore, offloaded user traffic is divided between WiFi, D2D and SBSs in order to reduce the traffic congestion of SBSs.

3.5 Traffic Offloading Methods: Path loss and Signal–to–Interference Ratio

3.5.1 Path Loss Based Traffic Offloading

The power of the signal propagating through the environment is considered to carry the distance information between transmitter and receiver. This parameter requires knowledge of several wireless propagation characteristics such as PL and shadowing to obtain an estimate about the distance considered. It is known that wireless propagations in different propagation environments differ from each other. The main reason behind this observation lies in the topographical characteristics of

the physical propagation environment. To model the PL in HetNets where multiple small cells complement the macrocell, several empirical models were proposed in [76, Chapter 12]. However, the measurements indicate that a simple power law PL model cannot be used to fit the measurements with good accuracy especially when the distance between the transmitter and receiver is short [71, 73, 76]. Therefore, this study considers a two slope (commonly known as dual slope) PL model for HetNets [71, 73, 76]: (a) PL $= K/(d^{\zeta_1})$ for $d \leq g$, and (b) PL $= K/((d/g)^{\zeta_2} g^{\zeta_1})$ for $d > g$. Two separate PL exponents, ζ_1 and ζ_2, which are referred to as basic and additional PL exponents, respectively, are used to characterize two different propagation regions, together with a breakpoint distance g between them where the propagation changes from one regime to the other. The breakpoint of the PL curve is defined as the point after which the strength of the signal attenuates such that the basic PL exponent ζ_1 represents the slope before breakpoint and the additional PL exponent ζ_2 represents the slope after breakpoint. This can be considered as two regions: for $d \leq g$, i.e., short distances, while for $d > g$, i.e., large distances, where $g = (4h_{rx}h_{tx})/(\lambda_c)$ [m] is the breakpoint of a PL curve which depends on the MBS and SBS (receiver in uplink) antenna height h_{rx} [m], antenna height of the mobile user (transmitter in uplink) h_{tx} [m] and wavelength of the carrier frequency λ_c. Parameter K denotes the PL constant.

To avoid the sharp transition between the two regions of a two slope PL model, a generalized propagation model for both macrocell and smallcell networks is considered in [67, 71]:

$$\text{PL} = \frac{K}{d^{\zeta_1}(1 + d/g)^{\beta}}, \quad \beta = \zeta_2 - \zeta_1. \tag{3.2}$$

In order to decide if a user connects to a small cell or remains with a MBS, the

following strategy is assumed. The active mobile user transfers to the small cell if [§] $\mathrm{PL}_n > \mathrm{PL}_m$. Otherwise, it remains connected to MBS.

3.5.2 Signal–to–Interference Ratio Based Traffic Offloading

Based on the two slope PL model (3.2), the received signal power at MBS or SBS from the active mobile user is given by:

$$P^{rx} = \frac{K}{d^{\zeta_1}(1 + d/g)^{\beta}} P^{tx} \psi, \tag{3.3}$$

where

- P^{rx}[W] denotes the average received signal power at the reference MBS or SBS from the desired mobile user, located at a distance d from the same reference BS;
- ψ is the composite shadowing and fading component over the link between the mobile user and respective MBS or SBS;
- P^{tx} [W] defines the mobile user transmit power for the physical uplink shared channel (PUSCH) such that each mobile user in the macrocell network transmits with the maximum power $P_{\max}$.

SIR is also an important parameter to evaluate the system performance in wireless communications and it is used in many performance metrics such as TO, handover, power control and channel assignment. The general definition of the SIR is the ratio between the average desired received signal power at the reference macrocell or small cell, and the total interference power received from the surrounding MBSs or small cells, $P^{rx}/\sum_{i=1}^{6} P_i^{rx}$. P^{rx}[W] stands for the average desired received signal power at

[§]Subscripts m and n are associated with MBS and SBS, respectively.

the reference macrocell or smallcell, and $\sum_{i=1}^{6} P_i^{rx}$[W] denotes the total interference power received from surrounding MBSs or SBSs. The PL strategy discussed in Section 3.5.1 can also be applied to SIR based offloading. For instance, if $\text{SIR}_n > \text{SIR}_m$, then users transfer to SBS. Otherwise, they will continue using MBS.

3.6 Traffic Offloading Analysis

In order to provide more insightful results, the percentage of TO for PL and SIR based strategies is investigated in three different set–ups[¶]:

3.6.1 Cell Size Dependent Traffic Offloading

In order to point out the impact of cell size on the offloaded traffic, Fig. 3.2 shows the summary of the radius dependent TO for variable small cell and MBS sizes. It is assumed that γ and α are equal to 1, which means that the macrocell is fully loaded with active mobile users and all the small cells are open access. The active mobile users in the macrocell network receive better SIR than those in the small cell network due to fact that the instantaneous SIR is lower in small cells. On the other hand, since the radius of the small cell is relatively smaller than that of macrocell, it will provide a better PL. Therefore, the significant difference between PL and SIR can be seen in Fig. 3.2. The impact of TO with respect to the macrocell radius and different values of r_n is illustrated in Fig. 3.2a. With the increase in r_m, SIR gets better for the macrocell network due to the reduced interference from the surrounding MBSs. Therefore, the percentage of SIR based offloading decreases in Fig. 3.2a. Then again, the PL for the small cell will often be higher and provide at least 78% TO due to the fact that the radius and the PL exponents are smaller than the values corresponding

[¶]In this study, the simulation results exclusively provide the numbers for MBS to small cell TOs.

Table 3.1: Numerical Values of the Number of Traffic Offloadings (TOs), Number of Open–Access small cells and Number of Closed–Access small cells for Low, Medium and High Traffic.

	Low Traffic - $p = 0.03$				Medium Traffic - $p = 0.15$				High Traffic - $p = 0.30$			
α	N_o	N_c	SIR	PL	N_o	N_c	SIR	PL	N_o	N_c	SIR	PL
0	0	12	0	0	0	60	0	0	0	122	0	0
0.25	3	9	1	4	15	45	7	19	31	91	13	38
0.5	6	6	3	8	30	30	10	38	61	61	24	76
0.75	9	3	4	12	45	15	25	57	91	31	39	114
1	12	0	5	15	60	0	21	75	122	0	45	151

to the macrocell. For instance, when r_m takes values in the interval (200, 1000), the percentage of PL based offloading is always greater than 78% even though r_n is increasing from 20m to 200m. This proves that shorter separation leads to a better offloading in terms of PL. As long as there is a drastic ratio between r_m and r_n, PL based offloading will lead to the best performance in terms of TO. Another interesting observation is that SIR_n is getting better when r_n takes greater values since the interference from neighboring small cells is decreasing. Fig. 3.2b depicts the PL, SIR and dual mode cognitive based offloading for different r_n and r_m values. SIR based offloading is increasing as expected due to the fact that r_n takes greater values, a factor which reduces the received interference from surrounding small cells. Compared to PL based offloading, the SIR based method provides less TO than the PL based offloading. SIR and PL based offloading strategies take values in these intervals (24%, 57%) and (78%,100%), respectively, indicating that the radii of MBS and small cell are the main factors that affect the TO. For a clearer view of this impact, TABLE 3.1 depicts a summary of N, N_o, TO for low, medium and high traffic loads for different α values, when $r_n = 20$m and $r_m = 400$m.

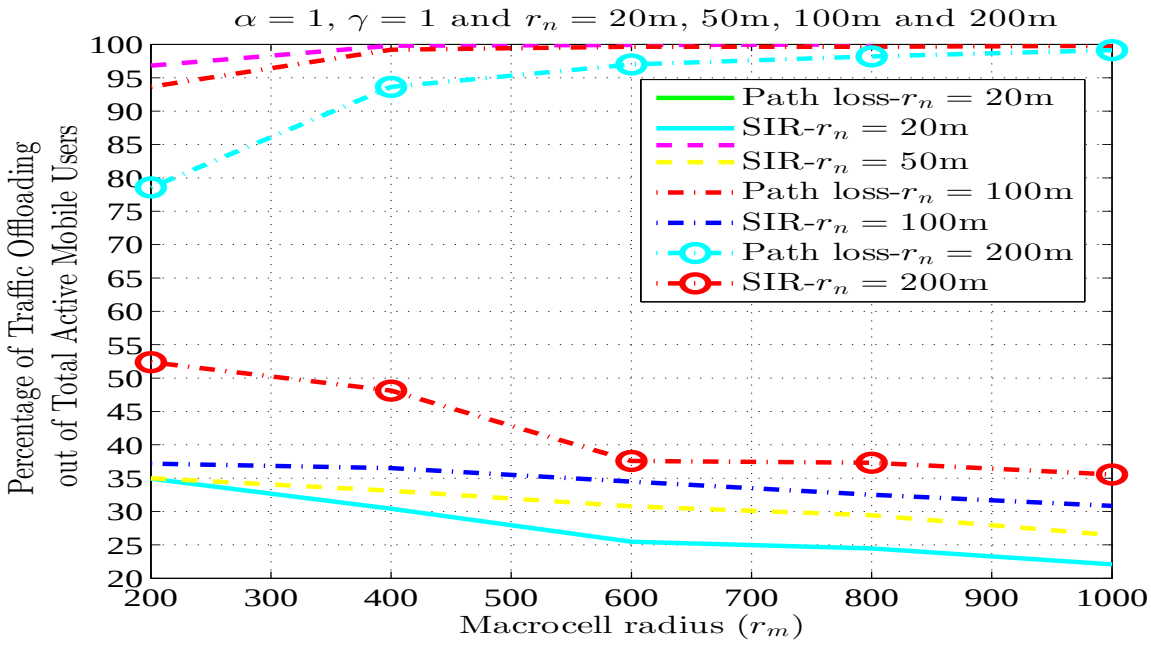

(a)

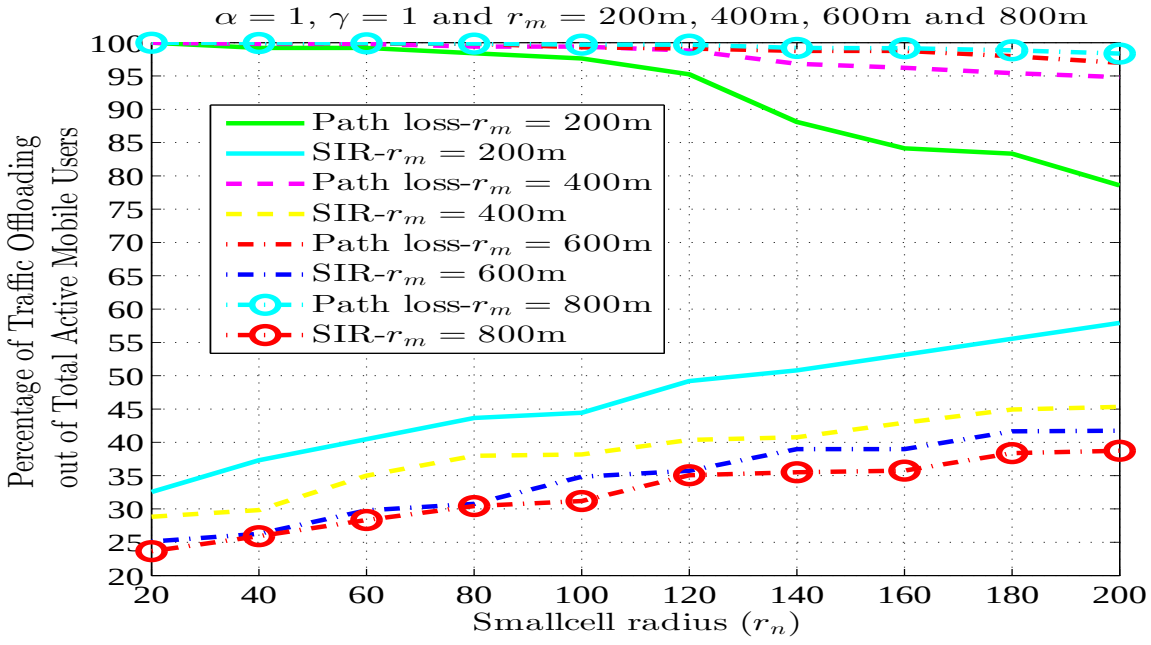

(b)

Figure 3.2: Percentage of an active mobile user only traffic offloadings (TOs) per macrocell as a function of active user density per m^2, radius of macrocell and radius of small cell.

3.6.2 Traffic–Type Dependent Offloading

Fig. 3.3 illustrates the percentage of TO onto SBS, WiFi APs or D2D enabled devices. It is assumed that γ and α are equal to 1, which means that the macrocell is fully loaded with active mobile users and all the small cells are open access. It is assumed that TO proportions from the total offloaded small cell traffic to SBSs, WiFi APs and D2D enabled links are given by $54\%, 38\%$ and 8%, respectively. For instance, if the total number of traffic offloaded to the small cells is 100 then 54 of them will go through SBS, 38 via WiFi APs and 8 to D2D. In order to provide a better understanding of the TO to SBS, WiFi APs and D2D, Fig. 3.3 depicts the percentage of the traffic distribution. Since the mobile data traffic is heterogeneous being composed of voice and text transmissions, multimedia applications, P2P connections, social networking applications, etc., it is assumed that voice and text will be associated with SBSs, multimedia and delay tolerant applications with WiFi APs and P2P connections with D2D connections [20]. Since voice and text services are of paramount importance for network operators, SBSs will provide uninterrupted QoS. On the other hand, compensation of the higher data requirements will be ensured by WiFi and D2D connections which will also diminish SBS backhaul volume.

3.6.3 Daily Traffic Profile and Small Cell Access Scheme Dependent Traffic Offloading

One of the fundamental reasons for small cell deployment is to reduce the traffic load when the data traffic usage is high and heterogeneous during a 24 hour period. Therefore, Fig. 3.4 depicts the impact of daily traffic profile and access scheme on TO. Fig. 3.4 illustrates the percentage of user offloading from MBS to small cell while considering both active and inactive mobile users. Fig. 3.4a demonstrates the effects of α for different γ values. As expected, the slope of the curve almost stays

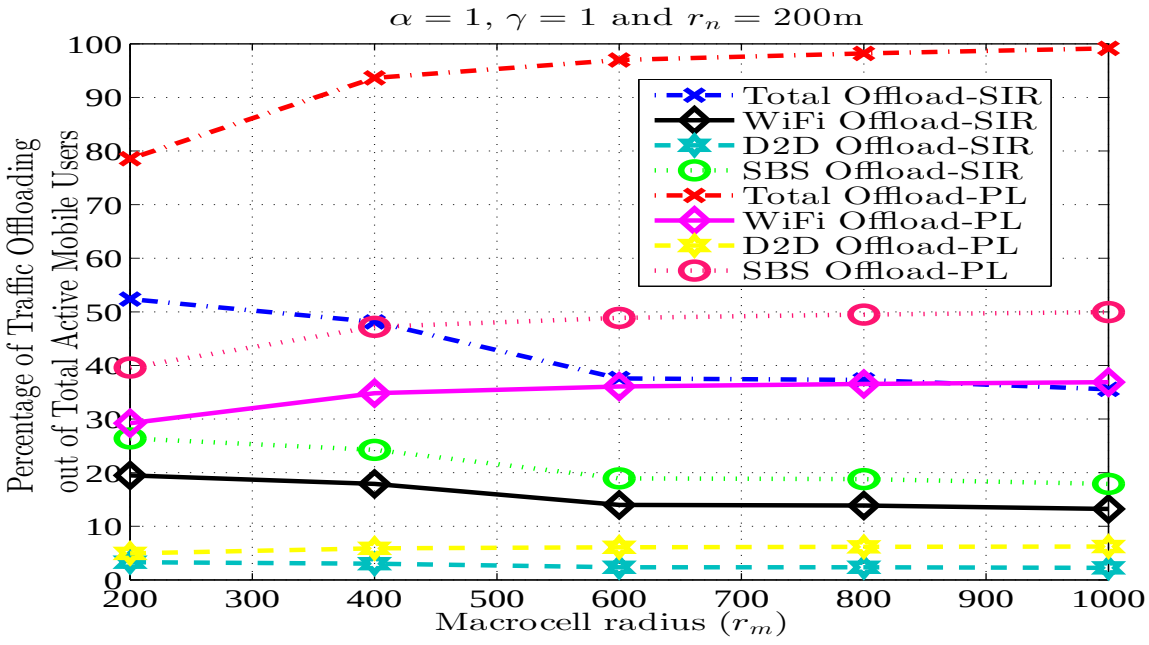

(a)

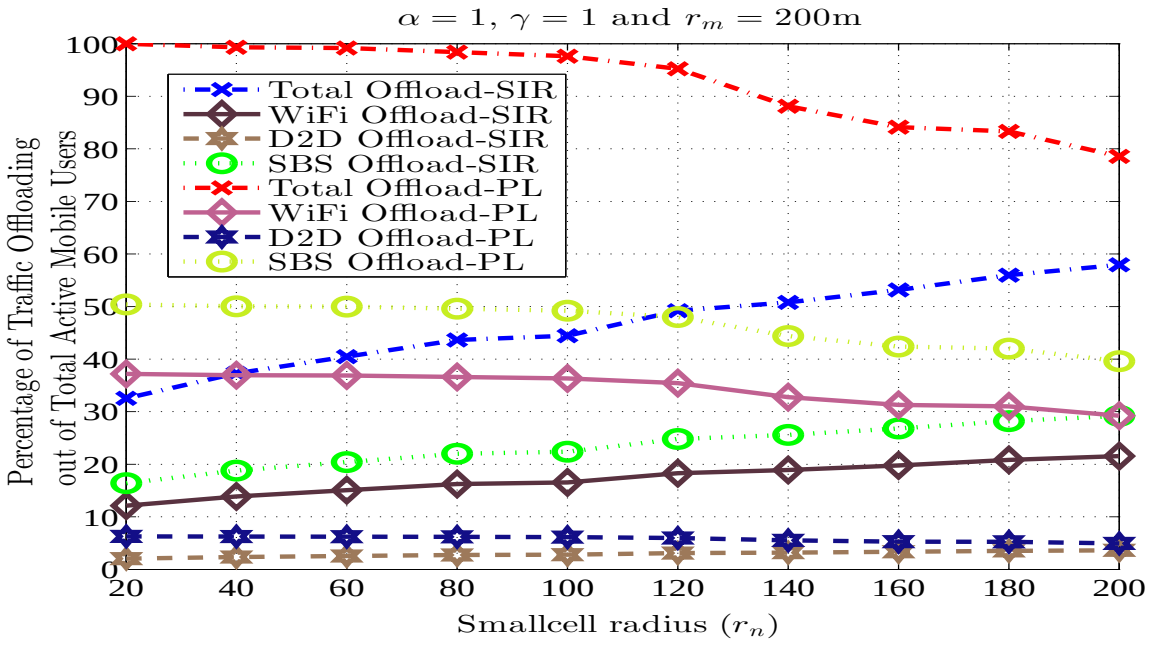

(b)

Figure 3.3: Percentage of an active mobile user only traffic offloadings (TOs) to small cells per macrocell as a function of traffic–type.

constant, which illustrates that γ is the main factor that alters the percentage of TO. For low traffic values, the percentage of TOs takes values in the interval (0%, 3%) when α is increasing from 0 to 1. In case of high traffic load, the percentage of offloadings ranges in the interval (0%, 30%). Fig. 3.4b depicts the impact of γ on the percentage for different α values. The curve of the offloading percentage changes drastically for different γ values. It is evident that the traffic load decreases when the percentage of the offloaded traffic reduces due to the diminishing number of active mobile users and small cells. As an example, low, medium and high traffic loads are chosen. The percentage of offloading takes values in the intervals (0%, 3%), (3%, 12%), and (12%, 21%), respectively.

3.7 Economics of Traffic Offloading

Network operators' exhibit special interest into TOs through proper placement of small cells since it is a necessity to reduce the total cost of ownership (TCO), CapEx which refers to the equipment and installation cost and OpEx which refers to the cost to keep the system running. Site lease and transportation generates the biggest chunk of the total cost in the network planning. In a traditional macrocell network, placement of a new cellular tower in a highly dense location i.e., downtown, can be impossible. Therefore, utilizing the already existing infrastructure and third party solutions such as WiFi, femtocells and D2D communications, are anticipated to reduce the total cost. Data offloading through WiFi and femtocells has a great value in different dimensions of a business such as hotspot operators, manufacturing devices and service providers. The greatest benefit in terms of cost savings is reducing the OpEx. First, operators only need to add little or no upgrades for the backhaul traffic due to the already existing backhaul infrastructures such as DSL lines, fiber, etc., for the TO which will relieve the congested traffic. Second, there is no need

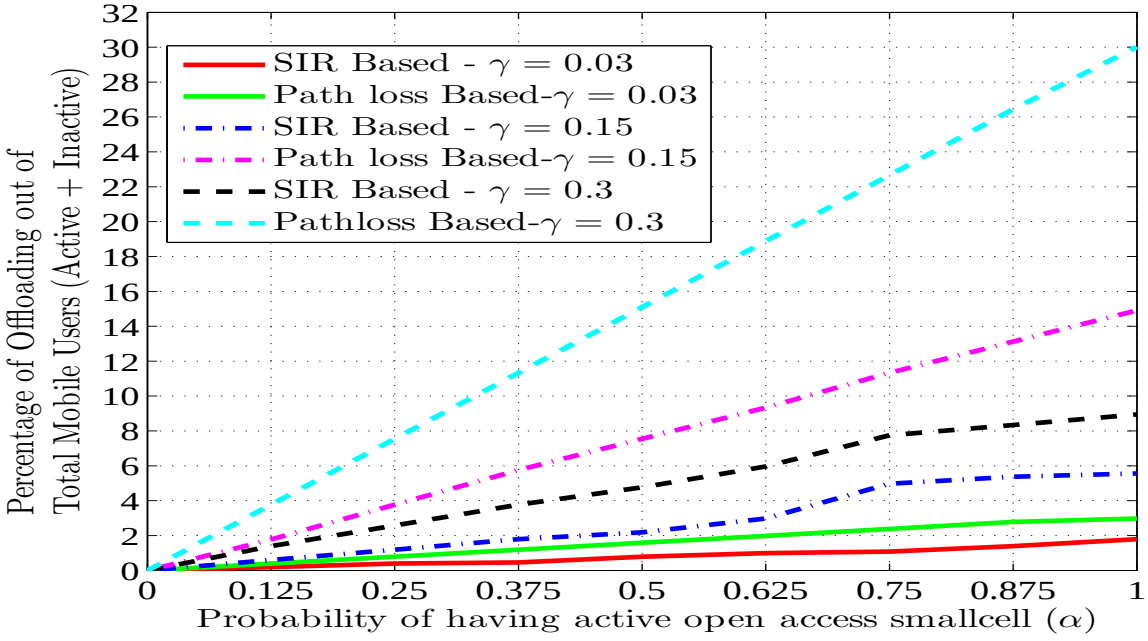

(a)

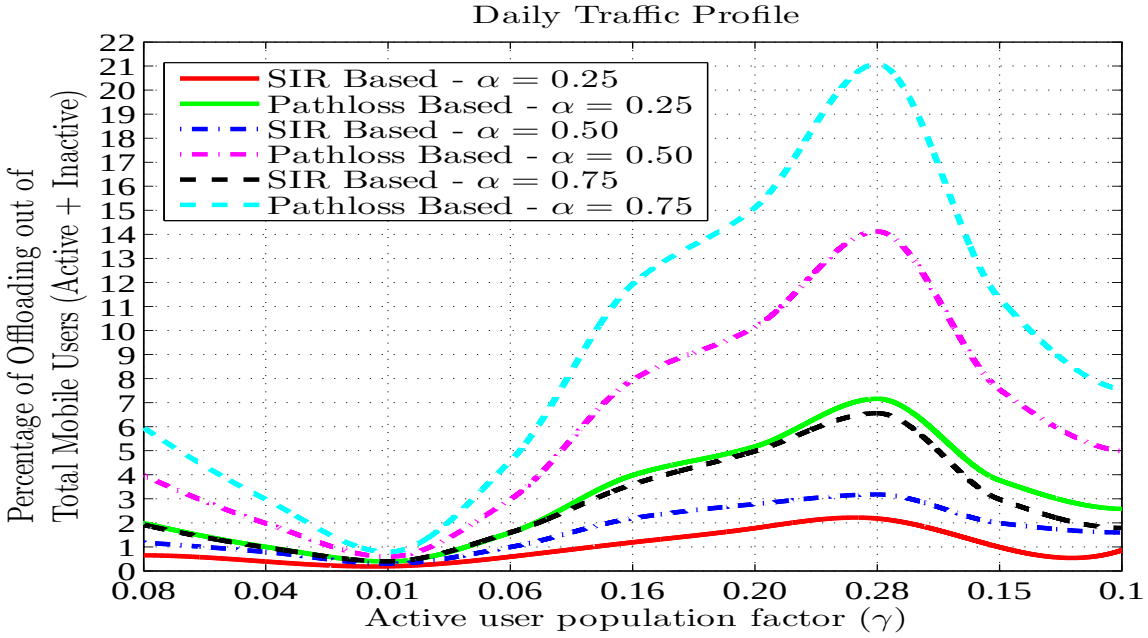

(b)

Figure 3.4: Percentage of total traffic offloading (TO) per macrocell as a function of active user population factor and the probability of having an open access small cell.

for drastic changes in the hardware and software for the radio access network. In a macrocell network, the cost per GB-RAN equals $21.80, while it is only $8.19 for the WiFi supported SBSs [65]. Therefore, both LTE SBSs and WiFi APs have shown significant CapEx and OpEx reductions opposed to LTE macrocells such as 85% decrease taking into account both CapEx and OpEx [54].

Reference [54] showed TCOs for scenarios where SBSs are cheaper for low density buildings. On the other hand, WiFi APs dominate the TCO with an increase in the density. SBSs are almost 31% cheaper for low density buildings while WiFi APs are 60% cheaper for higher density buildings. Hybrid and smart TO can be seen in Fig. 1.2b. If hybrid offloading takes place, it might further reduce TCO. Despite the fact that 60 GHz mmWave communications are still under maturation stage, they will bring a huge offloading relief for the indoor communications and backhaul traffic. Operators can easily build a mesh network with 60 GHz devices to eliminate the crowded usage of the wired backhaul connections. Another important aspect of the cost reduction is for the mobile subscribers. Since the current data plans for cellular 3G/4G networks are considerably high and limited per month, WiFi offloading in the residential areas diminishes the data usage and increase savings for each bill cycle. The mobile operator's business is to provide data services and they are supposed to generate revenues by offering such a service. One may wonder about the motivation for reducing the data load on a mobile operator's data network by offloading it to WiFi and small cells technologies which is equivalent to a scenario where a vendor willingly reduces the volume of the sale in a business. The motivation of an operator is evident based on the current revenue models. Users are keen to get data services and faster data rates but the cost that they are willing to pay is limited. This has resulted in several flat-charge models for the data services in mobile service contracts in Europe, America and many Asian countries. In this flat-charge model, the mobile

operator does not charge the customer for the "amount of the data", rather it charges the customers a fixed monthly rate for the "offering of the service", when and where needed. Hence, if these operators have a choice to seamlessly offload some of the users to other offloading technologies that are not managed by the operator, this will free up some user and data capacity in operator's system and will allow the operator to enroll more customers with a contract of "offering the service". These flat-charge models are one of the reasons for saturating average revenue per user (ARPU) for the operators. In short, in the presence of a flat-charge billing model the operator is not interested in serving a larger volume of data to each customer; rather the focus is on enrolling as many users as possible while ensuring that they have an experience of good service offering when they need the service in absence of any other alternative source.

Based on this information, the aforementioned strategies in this study can shrink the total costs. Therefore, adding low cost WiFi supported small cells will decrease the marginal cost for network operators and mobile subscribers, reduce the number of sites per network and expand the network coverage. Lastly, the reduction of the number of active cells per network will yield huge energy savings due to the fact that small cells are using very low power compared to the traditional macrocells. Even though, small cells are low cost solutions, a huge number of installed small cells can significantly increase the total cost. Therefore, the number of small cells is an issue that still needs to be carefully planned.

3.8 Summary

HetNets have gained significant attention due to their unique characteristics. Many studies are currently conducted to utilize this new concept more efficiently in 4G and 5G NGWNs. Due to the size and cost constraints on placing a new MBS in

the existing cellular networks, it is wise to use low cost and highly spectrally efficient WiFi and D2D enabled links supported small cells. One of the main objectives of HetNets is to help reduce the traffic load in the existing MBSs. Therefore, this study investigated the effect of daily heterogeneous traffic profile and exploited it in the PL based TO strategy where variously sized small cells are spread over the macrocell homogeneously. It is shown that changes in traffic load profiles and probability of having an active mobile user lead to changes in the number of active smallcells, as expected. It is also demonstrated that the heterogeneous nature of the traffic–type is also an important and useful parameter to spread the congested traffic over various types of technologies such as SBSs, WiFi APs and D2D enabled links. Delay tolerant applications can use WiFi APs and D2D enabled links where voice/text service can go through SBSs. This will not only reduce the over-the-air traffic but also truncate the wired backhaul bottleneck problem with the integration of WiFi and D2D communication technologies. In order to illustrate the improvements, the SIR based offloading is compared with the PL based method. It is shown that substantial offloading improvements can be achieved with the hybrid TO strategy, which allows for a reduction in the congested macrocell traffic. If the radius of the small cell is shorter than that of the macrocell, then PL based offloading will most likely provide higher offloading percentages than SIR based offloading in terms of transferring the congested traffic. This reduces the over-the-air signaling, operational and capital expenditures, and increases the spectral efficiency, data rates and coverage.

4. JOINT USER ASSIGNMENT AND BANDWIDTH ALLOCATION IN HETEROGENEOUS WIRELESS NETWORKS

4.1 Introduction

Besides considering traffic offloading and various traffic profiles, the bandwidth resource allocation should be investigated among the offloaded mobile users. In HetNets, researchers mainly assume that a MT connects to all existing networks in a multi-homing fashion. However, this vision overlooks the fact that the MT is equipped with only a limited number of radio interfaces for each network type, i.e., one cellular and one WiFi interface. Hence, the MT has to select one cellular BS and one WiFi AP from all the available ones to get its required bandwidth in a multi-homing fashion. In order to account for the limited number of interfaces for MTs, we formulate a joint user assignment and bandwidth allocation problem to support MTs with multi-homing capabilities.

The contributions of this study are summarized below:

- The multi-homing radio resource allocation problem is formulated as a non-convex MINLP [11, 34, 37, 48, 78, 83, 90] to jointly perform user network assignment and bandwidth allocation for a set of MTs with multi-homing capabilities within an overlapped coverage of WLAN APs and cellular BSs for best effort service.

- We show that the multi-homing radio resource allocation problem can be converted into a convex optimization problem after applying relaxation on the binary user assignment variable and reparameterization of bandwidth variable. A Lagrangian decomposition approach is proposed to solve the relaxed convex

optimization problem by dividing the problem into four-sub-problems.

- We derive a lower bound and an upper bound for the optimal value of the non-convex MINLP problem. A closed-form upper bound is derived using a modified Lagrange duality method. However, the relaxed convex optimization problem does not necessarily provide a binary solution and therefore, the relaxed convex problem cannot perform the user assignment. In order to ensure the binary assignment, we propose a heuristic method. We first assign the users and then allocate the bandwidth based on the selected user assignment. Using such an approach, a lower bound is derived. Furthermore, it is also illustrated that under certain conditions, the lower-bound coincides with the upper bound and thus it achieves the optimal value of the MINLP. In this way, the computational complexity is dramatically reduced.

- The General Algebraic Modeling System (GAMS)/Branch–And–Reduce Optimization Navigator (BARON) software is utilized to compare the results of the proposed heuristic algorithm [72]. The GAMS/BARON is a commercially available software and it incorporates the branch and bound method and exhibits global optimality while also utilizing the reduction tests. However, complexity and time consumption of GAMS/BARON increase dramatically when we consider a system with a large number of networks and MTs that compete on the available bandwidth of different networks.

4.1.1 Organization

The remainder of this chapter is structured as follows. The system model is presented in Section 4.2. The multi-homing radio resource allocation problem is formulated and solved in Section 4.3. Numerical results and discussions are given in Section 4.4. Finally, conclusions are drawn in Section 4.5.

4.2 System Model

We consider a HetNet where a combination of WLAN APs and cellular BSs present an overlapped coverage as depicted in Fig. 4.1. The network sets corresponding to WLAN APs and cellular BSs are denoted by $\mathcal{N}_1 = \{1, 2, \cdots, N_1\}$ and $\mathcal{N}_2 = \{N_1 + 1, \cdots, N_1 + N_2\}$, respectively. The total network set is denoted by $\mathcal{N} = \mathcal{N}_1 \cup \mathcal{N}_2$, where $\mathcal{N}_1 \cap \mathcal{N}_2 = \varnothing$. The set of MTs located within this HetNet is denoted by $\mathcal{M} = \{1, 2, \cdots, M\}$. Each MT is equipped with WiFi and cellular interfaces. The set of interfaces is denoted by $\mathcal{R} = \mathcal{R}_1 \cup \mathcal{R}_2$, where $\mathcal{R}_1$ and $\mathcal{R}_2$ represent the WiFi and cellular interfaces, respectively, and $\mathcal{R}_1 \cap \mathcal{R}_2 = \varnothing$. The allocated bandwidth from network $n \in \mathcal{N}$ to radio interface $r \in \mathcal{R}$ of $m \in \mathcal{M}$ MT is denoted by b_{nmr}. Even though some of smartphones with dual sim card present more than one cellular radio interface, these interfaces cannot be used simultaneously for two different calls. Therefore, we assume that the MT can have multiple interfaces of the same type, but the MT can only utilize one interface of the same type at a given moment of time. Hence, the MT can utilize one radio interface from $\mathcal{R}_1$ and one radio interface from $\mathcal{R}_2$ and aggregate the offered bandwidth from these two radio interfaces to support its ongoing call. The binary user assignment variable is defined by x_{nmr}.

4.3 Problem Formulation

In this section, the multi-homing resource allocation problem is formulated. We adopt a utility function perspective in order to account for the proportional fairness among users [46,74]. Let $u_{nmr}\,(b_{nmr})$ denote the utility function of network n allocating bandwidth b_{nmr} to $r \in \mathcal{R}$ of $m \in \mathcal{M}$. Then, the utility function can be defined as:

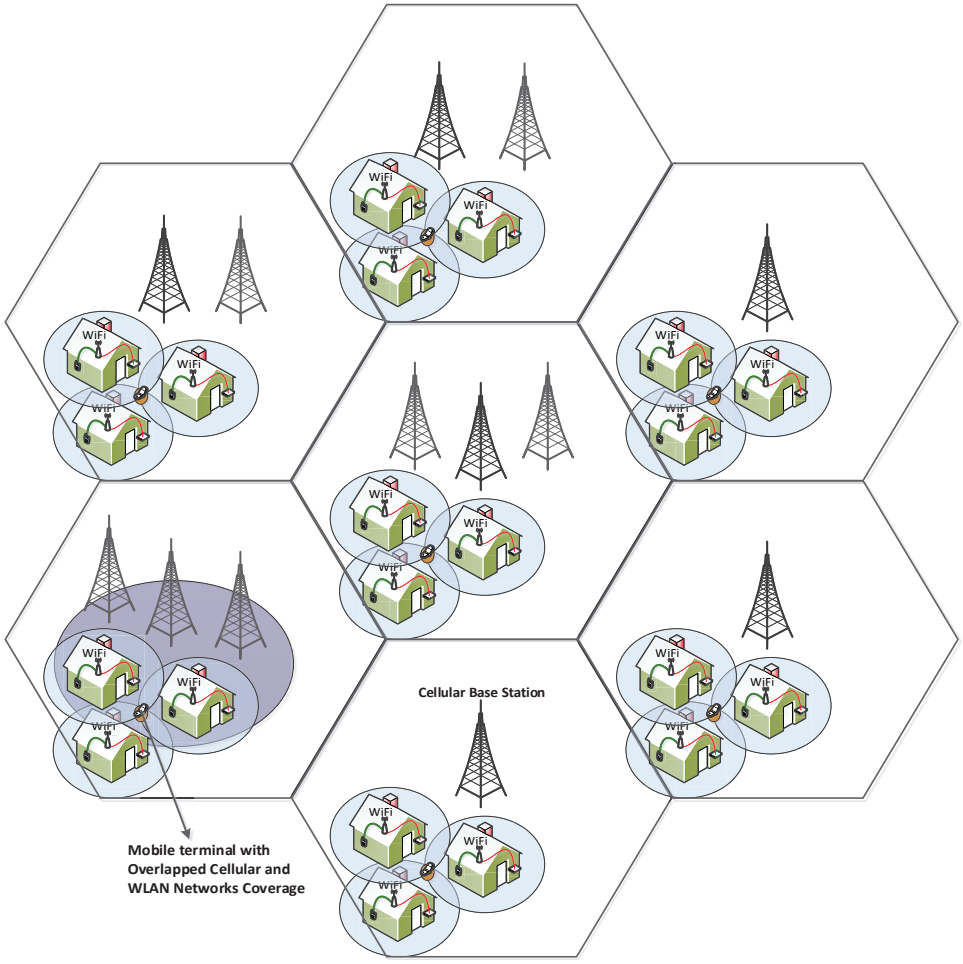

Figure 4.1: Cellular networks and WLAN APs overlapped coverage.

$$u_{nmr}\left(b_{nmr}\right) = x_{nmr} \ln\left(1 + \eta b_{nmr}\right), \tag{4.1}$$

where η is used for scalability of b_{nmr} and $x_{nmr} \in \{0, 1\}$ stands for the binary user assignment variable for interface $r \in \mathcal{R}$ of MT $m \in \mathcal{M}$ to network $n \in \mathcal{N}$.

The overall resource allocation objective of all the networks resumes to finding the optimum allocation $b_{nmr},\ \forall n \in \mathcal{N},\ \forall m \in \mathcal{M},\ \forall r \in \mathcal{R}$ that maximizes the total utility in the region, expressed as

$$U = \sum_{n\in\mathcal{N}} \sum_{m\in\mathcal{M}} \sum_{r\in\mathcal{R}} u_{nmr}\left(b_{nmr}\right). \tag{4.2}$$

For each network n, the allocated resources should be such that the total load in its coverage area is within the network capacity limitation Z_n, i.e.,

$$\sum_{m\in\mathcal{M}} \sum_{r\in\mathcal{R}} x_{nmr} b_{nmr} \leq Z_n, \quad \forall n \in \mathcal{N}. \tag{4.3}$$

The bandwidth resource allocation problem is formulated under the assumption of proportional fairness in the overlapped WLAN APs and cellular BSs. Using (4.1), (4.3) and binary assignment variable, x_{nmr}, the primary bandwidth resource allocation problem, (P_1), can be expressed in the form of the following non-convex MINLP

$$\max_{\mathbf{b},\mathbf{x}} \sum_{n\in\mathcal{N}} \sum_{m\in\mathcal{M}} \sum_{r\in\mathcal{R}} x_{nmr} \ln(1+\eta b_{nmr}) \tag{P_1}$$

$$\text{s.t.} \sum_{m\in\mathcal{M}} \sum_{r\in\mathcal{R}} x_{nmr} b_{nmr} \leq Z_n, \quad \forall n \in \mathcal{N} \tag{Cp_1}$$

$$\sum_{n\in\mathcal{N}_1} \sum_{r\in\mathcal{R}_1} x_{nmr} \leq 1, \quad m \in \mathcal{M} \tag{Cp_2}$$

$$\sum_{n\in\mathcal{N}_1} \sum_{r\in\mathcal{R}_2} x_{nmr} = 0, \quad m \in \mathcal{M} \tag{Cp_3}$$

$$\sum_{n\in\mathcal{N}_2} \sum_{r\in\mathcal{R}_2} x_{nmr} \leq 1, \quad m \in \mathcal{M} \tag{Cp_4}$$

$$\sum_{n\in\mathcal{N}_2} \sum_{r\in\mathcal{R}_1} x_{nmr} = 0, \quad m \in \mathcal{M} \tag{Cp_5}$$

$$b_{nmr} \geq 0, \quad m \in \mathcal{M}, n \in \mathcal{N}, r \in \mathcal{R} \tag{Cp_6}$$

$$x_{nmr} \in \{0,1\}, \ m \in \mathcal{M}, n \in \mathcal{N}, r \in \mathcal{R} \tag{Cp_7}$$

The objective function is given in (P_1), the constraint (Cp_1) ensures that the allocated

resource cannot exceed the capacity limit, the constraints (Cp_2) and (Cp_3) guarantee that a MT can only connect to WiFi networks using WiFi interfaces. Moreover, the constraints (Cp_4) and (Cp_5) assure that a MT can only establish a connection to the cellular BS using only its cellular interfaces. Furthermore, the constraint (Cp_6) secures that the allocated bandwidth is always a positive quantity, and (Cp_7) describes the binary nature of the assignment variable.

It can be seen that (P_1) is a non-convex MINLP problem which involves both binary variables, x_{nmr} and real–valued positive bandwidth variables, b_{nmr}. Due to the computational complexity and mathematical intractability, MINLP is a Non–deterministic Polynomial–time (NP)-hard problem [13, 56]. For instance, without considering the number of interfaces, i.e., $|\mathcal{N}| = 2$, $|\mathcal{M}| = 50$ and $|\mathcal{R}| = 1$, there will be a total of 2^{50} network and user assignments. In this study, a lower bound and an upper bound are derived for the value of objective function (P_1). Specifically, the binary variable is relaxed such that the MINLP problem resumes to a convex optimization formulation and a closed-form upper bound is derived using a modified Lagrange duality method. However, the relaxed convex optimization problem does not necessarily have a binary solution, and therefore, it might not be able to perform the user assignment. Motivated by the modified Lagrange duality method, a heuristic method is proposed to first assign the users and then allocate the bandwidth based on the selected user assignment. In this way, a lower bound is derived in a closed-form. Furthermore, it is also illustrated that under certain conditions, the lower-bound coincides with the upper bound and thus it achieves the optimality of the MINLP.

4.3.1 Upper-bound: A Convex Relaxation Approach

In order to convert the problem (P_1) into a convex optimization problem, we adopt the binary relaxation approach [37]. The binary constraint $x_{nmr} \in \{0, 1\}$ is modified

by allowing x_{nmr} to take any fractional value in the interval $[0, 1]$. In addition, a new variable $w_{nmr} = x_{nmr} b_{nmr}$ is introduced such that the relaxed optimization problem resumes to

$$\max_{\mathbf{w},\mathbf{x}} \sum_{n\in\mathcal{N}} \sum_{m\in\mathcal{M}} \sum_{r\in\mathcal{R}} x_{nmr} \ln(1 + \eta \frac{w_{nmr}}{x_{nmr}}) \tag{P_2}$$

$$\text{s.t.} \sum_{m\in\mathcal{M}} \sum_{r\in\mathcal{R}} w_{nmr} \leq Z_n, \quad \forall n \in \mathcal{N} \tag{Cr_1}$$

$$Cp_2 - Cp_5, \tag{Cr_2}$$

$$w_{nmr} \geq 0, \quad m \in \mathcal{M}, n \in \mathcal{N}, r \in \mathcal{R} \tag{Cr_3}$$

$$0 \leq x_{nmr} \leq 1, \quad m \in \mathcal{M}, n \in \mathcal{N}, r \in \mathcal{R} \tag{Cr_4}$$

It is illustrated in Appendix A that problem (P_2) is a convex optimization problem. In addition, it is easy to verify that there exists an interior point in the feasible region. Thus, the Slater's condition holds and the problem presents a zero duality gap [14]. In this way, the optimal solution of problem (P_2) can be derived using the Lagrange duality method. However, such an optimal solution is not necessarily binary, and it may not satisfy the binary constraint in problem (P_1).

In the following context, the optimal objective value for the relaxed problem (P_2), which is denoted as V_U^*, is derived in a closed-form using a modified Lagrange duality method. Consequently, if we denote the optimal objective value of (P_1) as v^*, v_U^* presents an upper-bound for v^*, i.e., $v^* \leq v_U^*$, since (P_2) is optimized over a larger constraint set.

The Lagrangian of problem (P_2) can be expressed as

$$L(\mathbf{w}, \mathbf{x}, \boldsymbol{\lambda}) = \sum_{n\in\mathcal{N}} \sum_{m\in\mathcal{M}} \sum_{r\in\mathcal{R}} x_{nmr} \ln\left(1 + \eta \frac{w_{nmr}}{x_{nmr}}\right) - \sum_{n\in\mathcal{N}} \lambda_n \left(\sum_{m\in\mathcal{M}} \sum_{r\in\mathcal{R}} w_{nmr} - Z_n\right), \tag{4.4}$$

where $\lambda_n \in \mathbb{R}^+$ stands for the Lagrange multiplier associated with the network bandwidth constraint, (Cr_1). The dual function is therefore

$$\begin{aligned} g(\boldsymbol{\lambda}) &= \max_{\mathbf{w}\in\mathcal{D}_1} L(\mathbf{w}, \mathbf{x}, \boldsymbol{\lambda}) \\ &\text{s.t.} \quad Cr_2 - Cr_4, \end{aligned} \tag{4.5}$$

where $\mathcal{D}_1$ denotes the feasible domain of constraint (Cr_1). Since the problem is convex with zero duality gap, the Karush–Kuhn–Tucker (KKT) condition holds [14]. Taking the derivative of $L(\mathbf{x}, \mathbf{w}, \boldsymbol{\lambda})$ over $\mathbf{w}$ yields

$$w_{nmr} = \left(\frac{1}{\lambda_n} - \frac{1}{\eta}\right)^+ x_{nmr}, \tag{4.6}$$

where it is assumed that $\lambda_n \neq 0$. If we assume $\frac{1}{\lambda_n} - \frac{1}{\eta} < 0$ $(\lambda_n > \eta)$ for any network $n \in \mathcal{N}$, then $w_{nmr} = 0, \forall m \in \mathcal{M}, r \in \mathcal{R}, n \in \mathcal{N}$, which does not meet the complementary slackness requirement

$$\lambda_n \left(\sum_{m\in\mathcal{M}} \sum_{r\in R} w_{nmr} - Z_n\right) = 0, \forall n \in \mathcal{N}. \tag{4.7}$$

Therefore, it can be seen that $0 < \lambda_n \leq \eta,\ \forall n \in \mathcal{N}$ and the relationship (4.6) between w_{nmr} and x_{nmr} can be simplified to

$$w_{nmr} = \left(\frac{1}{\lambda_n} - \frac{1}{\eta}\right) x_{nmr}. \tag{4.8}$$

Plugging (4.8) into (4.5) leads to

$$\begin{aligned} g(\boldsymbol{\lambda}) = & \max_{\mathbf{x}} \sum_{n\in\mathcal{N}} \sum_{m\in\mathcal{M}} \sum_{r\in\mathcal{R}} x_{nmr} A(\lambda_n) + \sum_{n\in\mathcal{N}} \lambda_n Z_n \\ & \text{s.t.} \quad Cr_2, Cr_4, \end{aligned} \tag{4.9}$$

where $A(\lambda_n) = \lambda_n/\eta - \ln\lambda_n + \ln\eta - 1$. It can be verified that $A(\lambda_n)$ is a monotonically decreasing function over $\lambda_n \in (0, \eta]$ with $\lim_{\lambda_n \to 0} A(\lambda_n) = \infty$ and $A(\eta) = 0$. Thus, $A(\lambda_n) \geq 0, \forall \lambda_n \in (0, \eta]$.

The problem above can be decomposed into four sub–problems*

$$\begin{aligned} \max_{x} \quad & \sum_{n\in\mathcal{N}_1} \sum_{m\in\mathcal{M}} \sum_{r\in\mathcal{R}_1} x_{nmr} A(\lambda_n) \\ \text{s.t.} \quad & \sum_{n\in\mathcal{N}_1} \sum_{r\in\mathcal{R}_1} x_{nmr} \leq 1, \quad m \in \mathcal{M} \\ & 0 \leq x_{nmr} \leq 1, \quad \forall n \in \mathcal{N}_1, m \in \mathcal{M}, r \in \mathcal{R}_1. \end{aligned} \tag{P_3}$$

$$\begin{aligned} \max_{x} \quad & \sum_{n\in\mathcal{N}_1} \sum_{m\in\mathcal{M}} \sum_{r\in\mathcal{R}_2} x_{nmr} A(\lambda_n) \\ \text{s.t.} \quad & \sum_{n\in\mathcal{N}_1} \sum_{r\in\mathcal{R}_2} x_{nmr} = 0, \quad m \in \mathcal{M} \\ & 0 \leq x_{nmr} \leq 1, \quad \forall n \in \mathcal{N}_1, m \in \mathcal{M}, r \in \mathcal{R}_2. \end{aligned} \tag{P_4}$$

* $\sum_{n\in\mathcal{N}} \lambda_n Z_n$ is neglected since it is optimized over $\mathbf{x}$

$$\begin{aligned}
\max_{x} \quad & \sum_{n\in\mathcal{N}_2}\sum_{m\in\mathcal{M}}\sum_{r\in\mathcal{R}_1} x_{nmr}A(\lambda_n) \\
\text{s.t.} \quad & \sum_{n\in\mathcal{N}_2}\sum_{r\in\mathcal{R}_1} x_{nmr} = 0, \quad m \in \mathcal{M} \\
& 0 \leq x_{nmr} \leq 1, \quad \forall n \in \mathcal{N}_2, m \in \mathcal{M}, r \in \mathcal{R}_1.
\end{aligned} \tag{P_5}$$

$$\begin{aligned}
\max_{x} \quad & \sum_{n\in\mathcal{N}_2}\sum_{m\in\mathcal{M}}\sum_{r\in\mathcal{R}_2} x_{nmr}A(\lambda_n) \\
\text{s.t.} \quad & \sum_{n\in\mathcal{N}_2}\sum_{r\in\mathcal{R}_2} x_{nmr} \leq 1, \quad m \in \mathcal{M} \\
& 0 \leq x_{nmr} \leq 1, \quad \forall n \in \mathcal{N}_2, m \in \mathcal{M}, r \in \mathcal{R}_2.
\end{aligned} \tag{P_6}$$

It is observed that the only feasible solution for problems (P_4) and (P_5) is all zeros. Therefore, only (P_3) and (P_6) need to be solved in this case.

Towards this end, we assume that N_1 WiFi networks and N_2 cellular networks are available. Moreover, for the sake of brevity, a new variable s_{nm} is defined as $s_{nm} = \sum_{r\in\mathcal{R}_1} x_{nmr}, n \in \mathcal{N}_1$. Thus, problem ($P_3$) resumes to

$$\max \sum_{n\in\mathcal{N}_1} A(\lambda_n)\left(\sum_{m\in\mathcal{M}} s_{nm}\right) \tag{4.10}$$

$$\text{s.t.} \sum_{n\in\mathcal{N}_1} s_{nm} \leq 1, \quad m \in \mathcal{M} \tag{4.11}$$

$$0 \leq s_{nm} \leq 1, \quad \forall n \in \mathcal{N}_1, m \in \mathcal{M}$$

In order to obtain a better understanding of this optimization problem, matrix $\mathbf{S} = [s_{nm}]$ is introduced as follows:

$$\mathbf{S} = \begin{bmatrix} s_{11} & s_{12} & \cdots & s_{1M} \\ s_{21} & s_{22} & \cdots & s_{2M} \\ \vdots & \vdots & \ddots & \vdots \\ s_{N_1 1} & s_{N_1 2} & \cdots & s_{N_1 M} \end{bmatrix}. \tag{4.12}$$

In this way, the constraint (4.11) can be interpreted as: the summation of all elements in each column is less than 1. Also, the term associated with $A(\lambda_n)$ in (4.10), i.e., $\sum_{m=1}^{M} s_{nm}$, can be interpreted as the summation of all elements in nth row. It is observed that the maximum of the objective function (4.10) depends on the value of λ_n. However, it is proved in Appendix B that all λ_n are equal, i.e.,

$$\lambda_1 = \cdots = \lambda_{N_1}. \tag{4.13}$$

Based on (4.13), the objective function (4.10) is reduced to:

$$\sum_{n\in\mathcal{N}_1} A(\lambda_n) \left(\sum_{m\in\mathcal{M}} s_{nm} \right) = A(\lambda_1) \sum_{m\in\mathcal{M}} \left(\sum_{n\in\mathcal{N}_1} s_{nm} \right).$$

It turns out that it is maximized when

$$\sum_{n\in\mathcal{N}_1} s_{nm} = 1, \quad m \in \mathcal{M}, \tag{4.14}$$

and it admits the optimal value $MA(\lambda_1)$.

Defining $h_{nm} = \sum_{r\in\mathcal{R}_2} x_{nmr}, n \in \mathcal{N}_2$ and following similar steps yield the optimality condition for problem (P_6):

$$\sum_{n\in\mathcal{N}_2} h_{nm} = 1, \quad m \in \mathcal{M}. \tag{4.15}$$

Similarly, the optimal value is expressed as $MA(\lambda_{N_1+1})$, where

$$\lambda_{N_1+1} = \cdots = \lambda_{N_1+N_2}. \tag{4.16}$$

Combining these results, the dual function $g(\boldsymbol{\lambda})$ is expressed as:

$$g(\boldsymbol{\lambda}) = MA(\lambda_1) + MA(\lambda_{N_1+1}) + \lambda_1 Z_{\mathrm{w}} + \lambda_{N_1+1} Z_{\mathrm{c}},$$

where

$$Z_{\mathrm{w}} = \sum_{i=1}^{N_1} Z_i \tag{4.17}$$

$$Z_{\mathrm{c}} = \sum_{j=N_1+1}^{N_1+N_2} Z_j. \tag{4.18}$$

Equations (4.17) and (4.18) express the total bandwidth assigned by the WiFi and cellular networks, respectively. It is also assumed that the same type of networks have the same bandwidth capacity $Z_1 = Z_2 = \cdots = Z_{N_1}$ and $Z_{N_1+1} = Z_{N_1+2} = \cdots = Z_{N_1+N_2}$, e.g., the situation where each WiFi network assumes 11 Mbps and each cellular network admits 2 Mbps [43]. The dual problem resumes to minimize $g(\boldsymbol{\lambda})$ with respect to $\boldsymbol{\lambda}$

$$\begin{aligned} \min_{\boldsymbol{\lambda}} \quad & MA(\lambda_1) + MA(\lambda_{N_1+1}) + \lambda_1 Z_{\mathrm{w}} + \lambda_{N_1+1} Z_{\mathrm{c}} \\ \text{s.t.} \quad & 0 < \lambda_1 \leq \eta,\ 0 < \lambda_{N_1+1} \leq \eta. \end{aligned} \tag{4.19}$$

The dual problem (4.19) is a convex optimization problem and achieves the closed-form solution:

$$\begin{aligned}\lambda_1^* = \cdots = \lambda_{N_1}^* &= \frac{M\eta}{M + \eta Z_{\mathrm{w}}}, \\ \lambda_{N_1+1}^* = \cdots = \lambda_{N_1+N_2}^* &= \frac{M\eta}{M + \eta Z_{\mathrm{c}}}.\end{aligned} \tag{4.20}$$

In this case, since problem (P_2) presents a zero duality gap, it follows that

$$v_U^* = MA(\lambda_1^*) + MA(\lambda_{N_1+1}^*) + \lambda_1^* Z_w + \lambda_{N_1+1}^* Z_c, \tag{4.21}$$

where λ_1^* and $\lambda_{N_1+1}^*$ are given in (4.20). Moreover, v_U^* represents an upper-bound for the original MINLP problem, i.e., $v^* \leq v_U^*$.

The optimal primal points $\mathbf{x}^*$ are chosen such that conditions (4.14) and (4.15) are met. In terms of $\mathbf{x}$, they are expressed as

$$\begin{aligned}\sum_{n\in\mathcal{N}_1}\sum_{r\in\mathcal{R}_1} x_{nmr}^* = 1, \quad m \in \mathcal{M}, \\ \sum_{n\in\mathcal{N}_2}\sum_{r\in\mathcal{R}_2} x_{nmr}^* = 1, \quad m \in \mathcal{M}.\end{aligned} \tag{4.22}$$

In the meantime, all the variables associated with (P_4) and (P_5) are zeros. Moreover, since $\mathbf{w}$ is expressed in terms of $\mathbf{x}$ in (4.6), the constraint associated with variable $\mathbf{w}$, (Cr_1), also needs to be checked

$$\sum_{m\in\mathcal{M}}\sum_{r\in\mathcal{R}} w_{nmr} = Z_n, \quad \forall n \in \mathcal{N}, \tag{4.23}$$

where the equality is achieved due to the complementary slackness in (4.7). Specifically, the optimal points $\mathbf{w}^*$ can be expressed as

$$w^*_{nmr} = \left(\frac{1}{\lambda^*_n} - \frac{1}{\eta}\right) x^*_{nmr} = \begin{cases} Z_{\mathrm{w}} x^*_{nmr}/M, & n \in \mathcal{N}_1 \\ Z_{\mathrm{c}} x^*_{nmr}/M, & n \in \mathcal{N}_2 \end{cases} \tag{4.24}$$

and (4.23) resumes to

$$\begin{aligned} \sum_{m\in\mathcal{M}} \sum_{r\in\mathcal{R}_1} x^*_{nmr} &= \frac{MZ_n}{Z_{\mathrm{w}}} = \frac{M}{N_1}, \quad n \in \mathcal{N}_1 \\ \sum_{m\in\mathcal{M}} \sum_{r\in\mathcal{R}_2} x^*_{nmr} &= \frac{MZ_n}{Z_{\mathrm{c}}} = \frac{M}{N_2}, \quad n \in \mathcal{N}_2. \end{aligned} \tag{4.25}$$

In a more compact form, (4.22) and (4.25) can be considered in terms of s^*_{nm} and h^*_{nm} such that the optimality conditions for problem (P_2) can be depicted in a two-dimensional space as follows

$$\sum_{n\in\mathcal{N}_1} s^*_{nm} = 1, \quad m \in \mathcal{M} \tag{4.26}$$

$$\sum_{n\in\mathcal{N}_2} h^*_{nm} = 1, \quad m \in \mathcal{M} \tag{4.27}$$

$$\sum_{m\in\mathcal{M}} s^*_{nm} = \frac{MZ_n}{Z_{\mathrm{w}}} = \frac{M}{N_1}, \quad n \in \mathcal{N}_1, \tag{4.28}$$

$$\sum_{m\in\mathcal{M}} h^*_{nm} = \frac{MZ_n}{Z_{\mathrm{c}}} = \frac{M}{N_2}, \quad n \in \mathcal{N}_2, \tag{4.29}$$

where $0 \leq s_{nm} \leq 1$ and $0 \leq h_{nm} \leq 1$.

4.3.2 Lower-bound: A Heuristic Method

If a binary s_{nm} and h_{nm} satisfying the above constraints can be found, then any x_{nmr} with $s_{nm} = \sum_{r\in R_1} x_{nmr},\ n \in N_1$ and $h_{nm} = \sum_{r\in R_2} x_{nmr},\ n \in N_2$ (the rest $\mathbf{x}$ are all zeros) is an optimal solution for the original MINLP problem (P_1). This argument can be proved in two steps: first, such an $\mathbf{x}$ satisfies the optimality conditions (4.26)

- (4.29) for problem (P_2) and thus achieves a larger objective value than v^*; second, such an $\mathbf{x}$ is a feasible solution for problem (P_1) and consequently achieves a lower objective value than v^*. In this way, the argument is proved and the corresponding optimal w is given by (4.24).

Combining (4.26) with (4.28) and (4.27) with (4.29), the problem whether a binary optimal solution exists can be interpreted as two matrix assignment problems: (1) If a $N_1 \times M$ matrix $\mathbf{S}^*$ with binary elements can be found such that the summation of all elements in each column is 1 and the summation of all elements in each row is $\frac{M}{N_1}$. (2) If a $N_2 \times M$ matrix $\mathbf{H}^*$ with binary elements can be found such that the summation of all elements in each column is 1 and the summation of all elements in each row is $\frac{M}{N_2}$. However, it can be seen that generally such two matrices do not exist and only fractional optimal solutions can be obtained from problem (P_2). Therefore, in this section, a heuristic method is proposed based on the optimality conditions (4.26) - (4.29). Specifically, the proposed heuristic method first assigns users and then optimizes the bandwidth based on the selected user assignments.

It can be seen that optimality conditions (4.26) and (4.27) are based on constraints (Cp_2) and (Cp_4), respectively, which states that every MT has to connect to a WiFi/celluar network to maximize the total utility. In addition, conditions (4.28) and (4.29) are derived from the bandwidth constraint (Cp_1), which claims that the bandwidth for each network has to be fully utilized to achieve a maximum utility function. Motivated by this fact, we round the RHS of (4.28) and (4.29) to the

largest integers not greater than them and relax (4.26) and (4.27) as follows

$$\sum_{n\in\mathcal{N}_1} s^*_{nm} \leq 1, \quad m \in \mathcal{M} \tag{4.30}$$

$$\sum_{n\in\mathcal{N}_2} h^*_{nm} \leq 1, \quad m \in \mathcal{M} \tag{4.31}$$

$$\sum_{m\in\mathcal{M}} s^*_{nm} = \left\lfloor \frac{MZ_n}{Z_{\mathrm{w}}} \right\rfloor = \left\lfloor \frac{M}{N_1} \right\rfloor, \quad n \in \mathcal{N}_1, \tag{4.32}$$

$$\sum_{m\in\mathcal{M}} h^*_{nm} = \left\lfloor \frac{MZ_n}{Z_{\mathrm{c}}} \right\rfloor = \left\lfloor \frac{M}{N_2} \right\rfloor, \quad n \in \mathcal{N}_2, . \tag{4.33}$$

Then, any binary s_{nm} and h_{nm} satisfying (4.30), (4.31), (4.32) and (4.33) is a feasible solution for problem (P_1). Equivalently, the binary s_{nm} and h_{nm} are obtained by alternatively finding two matrices $\mathbf{S}^*$ and $\mathbf{H}^*$ such that for each matrix, the summation of all elements in each column is less than 1 and the summation of all elements in each row is $\left\lfloor \frac{M}{N_1} \right\rfloor$ and $\left\lfloor \frac{M}{N_2} \right\rfloor$, respectively. It is easy to verify that such two binary matrices always exist. Specifically, we select $\mathbf{S}^*$ and $\mathbf{H}^*$ as follows:

$$S^* = \underbrace{\left[\begin{array}{cccc} \underbrace{1\cdots1}_{L_1} & \underbrace{0\cdots0}_{L_1} & \cdots & \underbrace{0\cdots0}_{L_1}\ \underbrace{0\cdots0}_{K_1} \\ \underbrace{0\cdots0}_{L_1} & \underbrace{1\cdots1}_{L_1} & \cdots & \underbrace{0\cdots0}_{L_1}\ \underbrace{0\cdots0}_{K_1} \\ \vdots & \vdots & \ddots & \vdots \quad\ \vdots \\ \underbrace{0\cdots0}_{L_1} & \underbrace{0\cdots0}_{L_1} & \cdots & \underbrace{1\cdots1}_{L_1}\ \underbrace{0\cdots0}_{K_1} \end{array}\right]}_{M} \Bigg\} N_1, \tag{4.34}$$

$$H^* = \underbrace{\left[\begin{array}{cccc} \underbrace{0\cdots0}_{K_2} & \underbrace{0\cdots0}_{L_2} & \cdots & \underbrace{0\cdots0}_{L_2} \quad \underbrace{1\cdots1}_{L_2} \\ \underbrace{0\cdots0}_{K_2} & \underbrace{0\cdots0}_{L_2} & \cdots & \underbrace{1\cdots1}_{L_2} \quad \underbrace{0\cdots0}_{L_2} \\ \vdots & \vdots & \ddots & \vdots \quad \vdots \\ \underbrace{0\cdots0}_{K_2} & \underbrace{1\cdots1}_{L_2} & \cdots & \underbrace{0\cdots0}_{L_2} \quad \underbrace{0\cdots0}_{L_2} \end{array}\right]}_{M} \Bigg\} N_2 \tag{4.35}$$

where $L_1 = \left\lfloor \frac{M}{N_1} \right\rfloor$, $L_2 = \left\lfloor \frac{M}{N_2} \right\rfloor$, and K_1, K_2 are the remainders of $\frac{M}{N_1}$ and $\frac{M}{N_2}$, respectively. In this selection, even though the last K_1 users are not assigned any WiFi bandwidth, they are compensated with the cellular bandwidth. Similarly, the first K_2 users are not assigned any cellular bandwidth, they are compensated with the WiFi bandwidth. Thus, the user assignment is made with respect to s_{nm} and h_{nm}. Then, the specific interface can be randomly picked such that $s^*_{nm} = \sum_{r \in R_1} x^*_{nmr}, n \in N_1$ and $h^*_{nm} = \sum_{r \in R_2} x^*_{nmr}, n \in N_2$.

To this end, what remains is to allocate bandwidth based on the selected user assignments. It can be obtained by solving the following convex optimization problem:

$$\begin{aligned} \max_{\mathbf{w}} \quad & \sum_{n \in N} \sum_{m \in M} \sum_{r \in R} x^*_{nmr} \ln(1 + \eta \frac{w_{nmr}}{x^*_{nmr}}) \\ \text{s.t.} \quad & \sum_{m \in M} \sum_{r \in R} w_{nmr} \leq Z_n, \quad n \in N \\ & w_{nmr} \geq 0 \\ & x^*_{nmr} = 1 \end{aligned}$$

where x^*_{nmr} stands for the user assignments based on (4.34) and (4.35). It is easy to verify that the above optimization problem is maximized when the bandwidth of each

network is equally allocated for the assigned users. In a matrix form, it is represented in (4.36) and (4.37) where W_1^* and W_2^* stand for the bandwidth allocation for WiFi and cellular networks, respectively.

$$W_1^* = \underbrace{\left[\begin{array}{cccc} \underbrace{\frac{Z_1}{L_1}\cdots\frac{Z_1}{L_1}}_{L_1} & \underbrace{0\cdots0}_{L_1} & \cdots & \underbrace{0\cdots0}_{L_1} \quad \underbrace{0\cdots0}_{K_1} \\ \underbrace{0\cdots0}_{L_1} & \underbrace{\frac{Z_1}{L_1}\cdots\frac{Z_1}{L_1}}_{L_1} & \cdots & \underbrace{0\cdots0}_{L_1} \quad \underbrace{0\cdots0}_{K_1} \\ \vdots & \vdots & \ddots & \vdots \quad \vdots \\ \underbrace{0\cdots0}_{L_1} & \underbrace{0\cdots0}_{L_1} & \cdots & \underbrace{\frac{Z_1}{L_1}\cdots\frac{Z_1}{L_1}}_{L_1} \quad \underbrace{0\cdots0}_{K_1} \end{array}\right]}_{M} \Bigg\} N_1, \tag{4.36}$$

$$W_2^* = \underbrace{\left[\begin{array}{cccc} \underbrace{0\cdots0}_{K_2} & \underbrace{0\cdots0}_{L_2} & \cdots & \underbrace{0\cdots0}_{L_2} \quad \underbrace{\frac{Z_{N_1+1}}{L_2}\cdots\frac{Z_{N_1+1}}{L_2}}_{L_2} \\ \underbrace{0\cdots0}_{K_2} & \underbrace{0\cdots0}_{L_2} & \cdots & \underbrace{\frac{Z_{N_1+1}}{L_2}\cdots\frac{Z_{N_1+1}}{L_2}}_{L_2} \quad \underbrace{0\cdots0}_{L_2} \\ \vdots & \vdots & \iddots & \vdots \quad \vdots \\ \underbrace{0\cdots0}_{K_2} & \underbrace{\frac{Z_{N_1+1}}{L_2}\cdots\frac{Z_{N_1+1}}{L_2}}_{L_2} & \cdots & \underbrace{0\cdots0}_{L_2} \quad \underbrace{0\cdots0}_{L_2} \end{array}\right]}_{M} \Bigg\} N_2 \tag{4.37}$$

Therefore, using this heuristic method, the user is assigned based on the matrices (4.34) and (4.35). In the mean time, the bandwidth is allocated according to

the matrices (4.36) and (4.37). Additionally, a closed-form utility function value is derived as a lower bound of the MINLP and it can be expressed as

$$v_L^* = N_1 L_1 \ln\left(1 + \frac{\eta Z_w}{L_1}\right) + N_2 L_2 \ln\left(1 + \frac{\eta Z_c}{L_2}\right). \tag{4.38}$$

The difference between the original MINLP and the heuristic method is bounded by

$$v^* - v_L^* \leq v_U^* - v_L^*. \tag{4.39}$$

In this way, even though we are not able to get the difference between our heuristic method and the MINLP analytically since v^* is generally not tractable, an upper-bound is obtained to measure how our heuristic method works.

As discussed earlier, if two matrices $\mathbf{S}^*$ and $\mathbf{H}^*$ can be found such that conditions (4.26) - (4.29) are met, then the optimality of problem (P_1) is achieved. This occurs in our heuristic method when $K_1 = 0$ and $K_2 = 0$, or equivalently, the remainders of M/N_1 and M/N_2 are zeros. In this case, our heuristic method is optimal based on the user assignments (4.34), (4.35) and bandwidth allocations (4.36), (4.37). Furthermore, v_L^* in (4.38) coincides with v_U^* in (4.21) and thus achieves v^* in a closed-form.

4.4 Numerical Results

In this section, our proposed method is validated via numerical simulations. In particular, the heuristic solution is compared with the optimal solution yielded by GAMS/BARON. The transmission capacity for each cellular BSs and WiFi APs are 2 Mbps and 11 Mbps, respectively [43, 53]. The number of MTs with multi–homing capability has range between $[10, 50]$ and η is chosen to be 1.

Fig. 4.2 shows the comparison of upper bound, (4.21), our proposed heuristic method, (4.38) and global optimal solutions obtained by GAMS/BARON. It can be

seen that the numerical results coincide very well with GAMS/BARON and provide near optimal results. As discussed earlier, the upper bound is obtained by optimizing over a larger feasible domain, which results in a slightly greater objective function values over GAMS/BARON as shown in Fig. 4.2. On the other hand, the heuristic method takes values less than GAMS/BARON since it is calculated by a feasible solution of (P_1).

It can be observed that when the number of each network type is a common denominator for the number of MTs, the solution in (4.38) yields the optimal result. This observation also coincides with our analytical result in Section 4.3. The main reason behind this is that (4.34), (4.35), (4.36) and (4.37) assure that each user gets connected to both cellular and WiFi network and enjoys the multi-homing capability. Thus, it maximizes the objective function. Due to the nature of logarithmic function, if the amount of already existing resources increase then this will increase the total worth. Therefore, the objective function assumes larger values when the number of MTs increases.

One interesting observation in Fig. 4.2a is that if we consider the two-network case where $\mathcal{N}_1 = 1$ and $\mathcal{N}_2 = 1$. In this case, since both $\mathbf{S}^*$ and $\mathbf{H}^*$ have only one row, all the elements of $\mathbf{S}^*$ and $\mathbf{H}^*$ are ones to ensure the condition that the summation of all elements in each column is 1. Following this particular structure, for both matrices, the requirements (4.28) and (4.29) for the summation of all elements in each row is always met. Therefore, the validation of this special case is also confirmed in the matrix interpretation. Basically, the remainders are always zero when $N_1 = N_2 = 1$. Hence, by applying the modified Lagrange duality method, the relaxed problem (P_2) is ensured to have a binary optimal solution with the proposed heuristic method, which is also globally optimal for the non-convex MINLP problem (P_1).

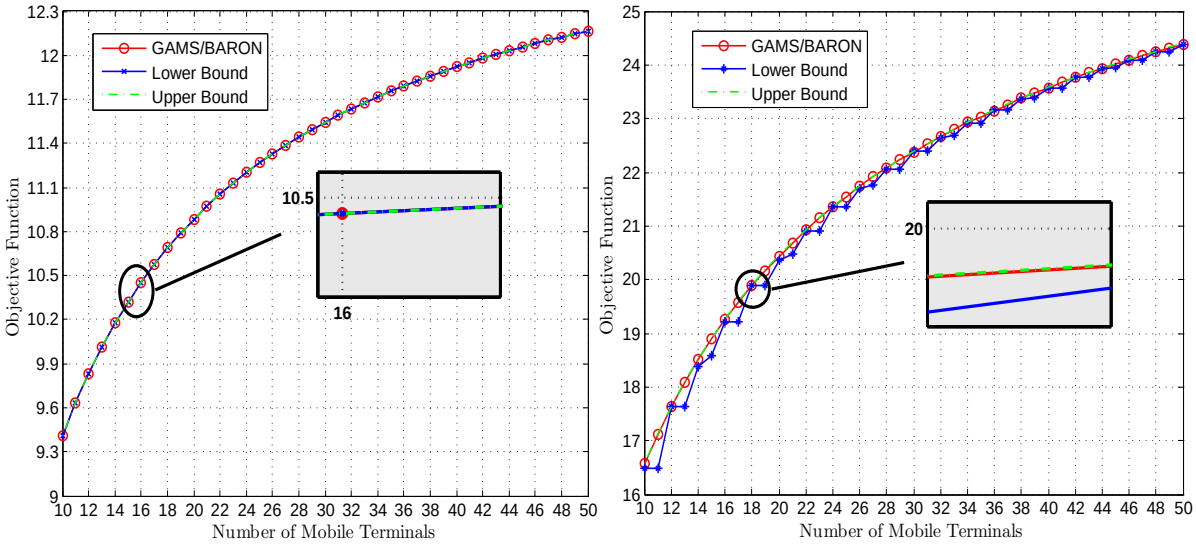

(a) $|\mathcal{N}_1| = 1$ and $|\mathcal{N}_2| = 1$.

(b) $|\mathcal{N}_1| = 2$ and $|\mathcal{N}_2| = 3$.

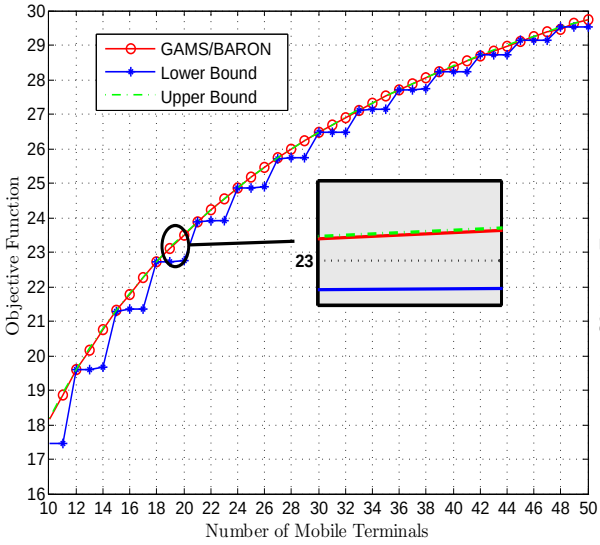

(c) $|\mathcal{N}_1| = 3$ and $|\mathcal{N}_2| = 2$.

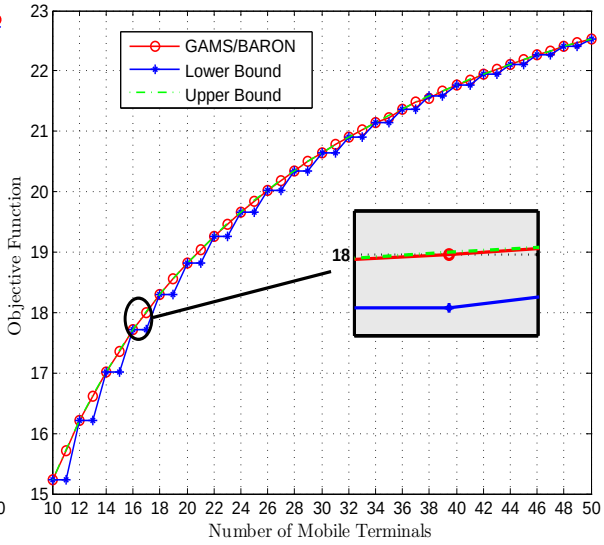

(d) $|\mathcal{N}_1| = 2$ and $|\mathcal{N}_2| = 2$.

Figure 4.2: Bounds on objective function compared with the optimal solution of GAMS/BARON.

4.5 Summary

In this chapter, the joint user assignment and optimal bandwidth allocation problem for HetNets is investigated under the set-up where the MTs present multi–

homing capability. In particular, the problem of maximizing the overall network bandwidth capacity is considered. First, we formulate the primal problem as a non-convex MINLP (P_1) and transform it into a convex optimization problem (P_2) using a change of variables and the binary variable relaxation approach. Then, the modified Lagrange duality method is adopted and the problem is decomposed into four-subcomponents. It is shown that the optimal solutions of the relaxed convex optimization problem yields to the upper bound for the original non-convex MINLP and the proposed heuristic method further provides a lower bound which also performs near optimal solution of the original non-convex MINLP. In addition, the difference between the original non-convex MINLP and the heuristic method is determined analytically. The validity of the proposed method is confirmed by numerical results.

5. LLOYD'S ALGORITHM APPROXIMATION FOR COVERAGE PROBABILITY IN HETEROGENEOUS CELLULAR NETWORKS

5.1 Introduction

The previous chapters provided insight into the random and heterogeneous nature of NGWNs which brings to attention the importance of coverage probability for each mobile user. Due to the highly dynamic nature of HetNets, BSs are deployed neither totally random nor totally deterministic. Therefore, in this chapter, we investigate the coverage probability for traditional hexagonal BS deployments and random BS deployments. The main contributions of this chapter are summarized as follows.

- We propose a semi-analytical strategy by adopting the Lloyd's algorithm to account for the scenarios that lie between the pessimistic random PPP-based deployment and the optimistic structural BS deployment.
- We derive the link distance distribution for each iteration of Lloyd's algorithm by using the EM algorithm. It is shown that the link distance can be approximated well by a mixture of Weibull distributions.
- By integrating the link distance distribution into the PPP analysis, we provide a coverage probability analysis.

5.1.1 Organization

The rest of the chapter is organized as follows. The Lloyd's algorithm is described in Section 5.2. The analysis of link distance distribution is given in Section 5.3. Section 5.4 presents the coverage probability study. The numerical results are presented in Section 5.5. The concluding remarks are provided in Section 5.6.

5.2 Lloyd's Algorithm Approach

A two–dimensional (2D) Voronoi diagram is a tessellation in which each polygon depicts the set of points nearest to a central generator point. Voronoi diagrams present diverse applications in many fields such as wireless communications, astronomy, archaeology, physics, mathematics, and coding [64, 85]. Lloyd's algorithm incrementally moves the generator of each polygon to the centroid of that polygon and maximizes the distance between adjacent generators [52]. The maximization procedure creates repulsion between adjacent generators until the generators establish a fixed state such as centroidal Voronoi tessellation (CVT). The resultant Voronoi diagram gives a structural geometry asymptotically, depending on how many iteration steps are used [59]. In this study, we initialize the tessellation of BSs based on a PPP. While the initial geometry captures the randomness of BS deployment, the asymptotic Voronoi diagram with Lloyd's algorithm yields a structural BS deployment. Each iteration of the Lloyd's algorithm represents an intermediate deployment scenario between the random and structural BS deployments, which motivates us to adopt Lloyd's algorithm for modeling BS deployment. A demonstration of iteration steps {0, 9, 490} is illustrated in Fig. 5.1. In order to exploit Lloyd's algorithm for modeling BS deployment, the analytical expression of link distance distribution at each iteration of Lloyd's algorithm is required. To the best of our knowledge, the link distance distribution is not available in the literature, and an approximate distribution is derived in the next section by exploiting the EM algorithm.

5.3 Link Distance Distribution Analysis

Consider a snapshot of a wireless network that covers an area A. The users are distributed uniformly in the area. Each user is associated with the closest BS, i.e., the users in a polygon generated with Voronoi tesselation are connected to the

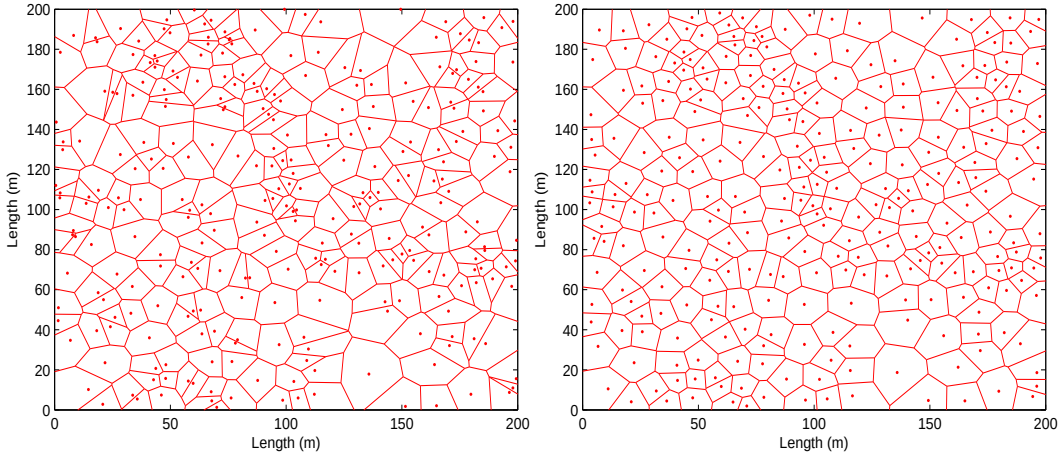

(a) Iteration 0.

(b) Iteration 9.

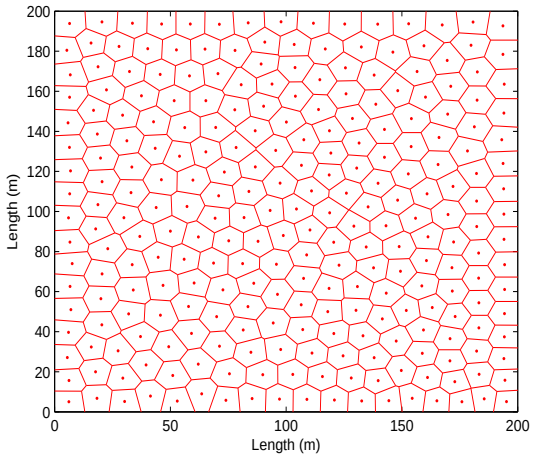

(c) Iteration 490.

Figure 5.1: Illustration of transition from random BS deployment to structural BS deployment with the Lloyd's algorithm.

corresponding generator of that polygon. The link distance between a user and its associated BS is denoted by r. As an initial stage of the Lloyd's algorithm, we consider a random BS deployment where BSs are spatially distributed in the area as a realization of a homogeneous 2D PPP Φ with intensity λ. The probability density function (PDF) of link distance is equivalent to the null probability for the PPP [2]

and is given by

$$\begin{aligned} f_r(r) &= \frac{\mathrm{d}F_r(r)}{\mathrm{d}r} = \frac{\mathrm{d}}{\mathrm{d}r}\left(1 - \mathbb{P}\left[r > R\right]\right) \\ &= e^{-\lambda\pi r^2} 2\lambda\pi r, \end{aligned} \tag{5.1}$$

which corresponds to a Rayleigh distribution with variance $1/2\lambda\pi$. On the other hand, considering the case of hexagonal tessellation, the PDF of link distance is given by [7]

$$f_r(r) = \begin{cases} \frac{\pi r}{\sqrt{3}R^2}, & 0 \leq r \leq R. \\ \frac{2\sqrt{3}r}{R^2}\left[\frac{\pi}{6} - \cos^{-1}\left(\frac{R}{r}\right)\right], & R \leq r \leq \frac{2R\sqrt{3}}{3}. \\ 0, & r \geq \frac{2R\sqrt{3}}{3}. \end{cases} \tag{5.2}$$

The transition from (5.1) to (5.2) via Lloyd's algorithm can be approximated as a mixture of Weibull distributions by employing the EM algorithm. A mixture of Weibull distributions can be expressed as

$$f_r(r) = \sum_{j=1}^{l} \phi_j \left(\frac{\varphi_j}{\delta_j} \left(\frac{r}{\delta_j} \right)^{\varphi_j - 1} e^{\left(-\frac{r}{\delta_j}\right)^{\varphi_j}} \right) , \tag{5.3}$$

where ϕ_j is the weight of jth component and $\sum_{j=1}^{l} \phi_j = 1$, δ_j and φ_j are the scale parameter and the shape parameter, respectively, and l is the number of Weibull distributions. In order to consider various BS intensities, we define δ_j to be $\psi_j \sqrt{\lambda_0/\lambda}$, where λ_0 is a constant and ψ_j is the scale parameter when $\lambda = \lambda_0$. The main reasons for using a mixture of Weibull distributions are: (i) Rayleigh distribution is a special case of a Weibull distribution if the Weibull parameters are properly selected, (ii) The support of Weibull distribution is $[0, \infty]$, and (iii) Weibull distribution can provide negative and positive skewness, a feature required in the transitions from (5.1) to (5.2). Next, we discuss the calculations of parameters ϕ_j, δ_j and φ_j with the EM

algorithm.

5.3.1 EM Algorithm for Link Distance Distribution

We have a training set $r = \{r^{(1)}, r^{(2)}, \cdots, r^{(m)}\}$ consisting of m independent observations generated by considering each iteration step of Lloyd's algorithm. Our goal is to fit the Weibull parameters to the link distance distribution by utilizing the EM algorithm. The EM algorithm consists of two steps, namely, the expectation (E)-step and the maximization (M)-step. The reader is referred to [22] for more detailed explanations about the EM algorithm.

The complete log-likelihood is defined as

$$\mathcal{L}(w_j, \theta) = \sum_{i=1}^{m} \sum_{j=1}^{l} w_j^{(i)} \log \left[\frac{\varphi_j}{\delta_j} \left(\frac{r_i}{\delta_j} \right)^{\varphi_j - 1} \exp(-\frac{r_i^{\varphi_j}}{\delta_j^{\varphi_j}}) \phi_j \right], \tag{5.4}$$

where $\theta = \{\varphi_j, \delta_j, \phi_j\}$ and $w_j^{(i)} = p(z^{(i)} = j | r^{(i)}; \theta)$ denotes the posterior probabilities associated with the hidden label information $z^{(i)}$. The steps of the EM algorithm are:

- E-step: Choose w_j to maximize $\mathcal{L}(w_j, \theta)$

$$w_j^t = \arg\max_{w_j} \mathcal{L}(w_j, \theta^t).$$

- M-step: Choose θ to maximize $\mathcal{L}(w_j, \theta)$

$$\theta^{t+1} = \arg\max_{\theta} \mathcal{L}(w_j^t, \theta).$$

Maximizing (5.4) with respect to the parameters φ_j and δ_j, we obtain (5.5) and (5.6), respectively

$$\nabla_{\varphi} \mathcal{L}(w_j, \theta) = \sum_{i=1}^{m} \sum_{j=1}^{l} w_j^{(i)} \left(\frac{1}{\varphi_j} + \left(1 - \left(\frac{r_i}{\delta_j} \right)^{\varphi_j} \right) \log(\frac{r_i}{\delta_j}) \right), \tag{5.5}$$

Table 5.1: Numerical Values of ϕ_j, φ_j and δ_j as outputs of EM algorithm.

Iteration	ϕ_j			φ_j			δ_j			Iteration	ϕ_j			φ_j			δ_j		
	ϕ_1	ϕ_2	ϕ_3	φ_1	φ_2	φ_3	δ_1	δ_2	δ_3		ϕ_1	ϕ_2	ϕ_3	φ_1	φ_2	φ_3	δ_1	δ_2	δ_3
0	0.3333	0.3333	0.3333	2.0063	2.0164	2.0265	0.5622	0.5616	0.5609	**15**	0.3244	0.3309	0.3448	1.8793	2.5936	3.0010	0.4128	0.5018	0.4942
1	0.3332	0.3333	0.3334	2.0301	2.0401	2.0501	0.5512	0.5501	0.5489	**16**	0.3225	0.3312	0.3463	1.8688	2.6446	3.0642	0.4041	0.5046	0.4919
2	0.3331	0.3333	0.3336	2.0523	2.0648	2.0774	0.5412	0.5396	0.5381	**17**	0.3202	0.3317	0.3481	1.8568	2.7016	3.1238	0.3958	0.5074	0.4896
3	0.3330	0.3333	0.3337	2.0724	2.0912	2.1100	0.5323	0.5303	0.5284	**18**	0.3167	0.3329	0.3504	1.8400	2.7655	3.1746	0.3878	0.5101	0.4870
4	0.3328	0.3333	0.3339	2.0968	2.1222	2.1476	0.5248	0.5221	0.5196	**19**	0.3123	0.3347	0.3531	1.8281	2.8267	3.2104	0.3806	0.5123	0.4842
5	0.3325	0.3333	0.3342	2.1132	2.1503	2.1868	0.5180	0.5147	0.5115	**20**	0.3090	0.3361	0.3549	1.8359	2.8762	3.2334	0.3746	0.5141	0.4820
6	0.3322	0.3332	0.3346	2.1240	2.1786	2.2318	0.5116	0.5079	0.5045	**21**	0.3066	0.3371	0.3562	1.8423	2.9249	3.2567	0.3692	0.5154	0.4804
7	0.3318	0.3332	0.3350	2.1284	2.2078	2.2846	0.5053	0.5020	0.4987	**22**	0.3042	0.3381	0.3577	1.8420	2.9746	3.2803	0.3643	0.5159	0.4790
8	0.3313	0.3331	0.3356	2.1226	2.2378	2.3463	0.4983	0.4970	0.4946	**23**	0.3028	0.3385	0.3586	1.8523	3.0160	3.3000	0.3602	0.5161	0.4782
9	0.3308	0.3329	0.3363	2.1057	2.2693	2.4201	0.4898	0.4930	0.4926	**24**	0.3028	0.3383	0.3589	1.8660	3.0553	3.3212	0.3566	0.5160	0.4779
10	0.3305	0.3324	0.3371	2.0603	2.3067	2.5223	0.4781	0.4904	0.4933	**25**	0.3034	0.3377	0.3589	1.8766	3.0959	3.3469	0.3534	0.5156	0.4780
11	0.3301	0.3316	0.3383	1.9929	2.3615	2.6521	0.4627	0.4904	0.4962	**26**	0.3042	0.3370	0.3588	1.8829	3.1359	3.3732	0.3505	0.5150	0.4782
12	0.3292	0.3307	0.3401	1.9248	2.4367	2.7822	0.4458	0.4929	0.4986	**27**	0.3048	0.3363	0.3589	1.8848	3.1749	3.3987	0.3481	0.5142	0.4785
13	0.3277	0.3305	0.3418	1.8934	2.5004	2.8724	0.4323	0.4962	0.4984	**28**	0.3051	0.3357	0.3591	1.8850	3.2120	3.4205	0.3460	0.5132	0.4786
14	0.3260	0.3306	0.3434	1.8822	2.5503	2.9402	0.4217	0.4991	0.4964	**29**	0.3054	0.3352	0.3594	1.8872	3.2478	3.4406	0.3442	0.5122	0.4788

$$\nabla_\delta \mathcal{L}(w_j, \theta) = \sum_{i=1}^{m} \sum_{j=1}^{l} w_j^{(i)} \left(-\frac{\varphi_j}{\delta_j} + \frac{\varphi_j}{\delta_j} \left(\frac{r_i}{\delta_j} \right)^{\varphi_j} \right). \tag{5.6}$$

In order to maximize (5.4) with respect to ϕ_j when $\sum_{j=1}^{l} \phi_j = 1$, the Lagrangian function is constructed as

$$\Lambda(\phi_j) = \sum_{i=1}^{m} \sum_{j=1}^{l} w_j^{(i)} \log \phi_j + \lambda \left(\sum_{j=1}^{l} \phi_j - 1 \right), \tag{5.7}$$

where λ stands for a Lagrange multiplier. After taking the derivative of (5.7) with respect to ϕ_j and equating it to zero, we obtain:

$$\phi_j = \frac{1}{m} \sum_{i=1}^{m} w_j^{(i)}. \tag{5.8}$$

An iterative method such as Limited Broyden-Fletcher-Goldfarb-Shanno (L-BGFS) can be applied to obtain φ_j and δ_j [63] due to the fact that φ_j and δ_j in (5.5) and (5.6) do not have explicit forms.

5.4 Coverage Probability

Probability of coverage is the ratio of the network area where signal-to-interference-noise ratio (SINR) is greater than a certain threshold T to the total area. It can be defined as

$$p_c\left(T,\lambda,\gamma\right) \triangleq \mathbb{P}\left[\text{SINR} > T\right] = \mathbb{P}\left[\frac{hr^{-\gamma}}{\sigma^2 + I_r} > T\right], \tag{5.9}$$

where $\gamma \geq 2$ is the path loss exponent, h denotes the channel gain between tagged BS and its user, and σ^2 is the noise power. Variable I_r stands for the total interference power received from the neighboring BSs and is given by

$$I_r = \sum_{n \in \Phi / b_o} g_n R_n^{-\gamma}, \tag{5.10}$$

where b_o is the tagged BS, g_n and R_n are the channel gain and the distance between the nth interfering BS and the tagged user, respectively. Assuming that the channel gains are characterized with i.i.d. exponential distributions where $\mathbb{E}[h] = \mathbb{E}[g_n] = \mu$, (5.9) is expressed as

$$\begin{aligned} p_c\left(T,\lambda,\gamma\right) &= \mathbb{E}_r\left[\mathbb{P}\left[\text{SINR} > T|r\right]\right] \\ &= \int_{r>0} \mathbb{P}\left[\frac{hr^{-\gamma}}{\sigma^2 + I_r} > T|r\right] f_r(r)dr \\ &= \int_{r>0} e^{-\mu T r^{\gamma}\sigma^2} \mathscr{L}_{I_r}\left(\mu T r^{\gamma}\right) f_r(r)dr, \end{aligned} \tag{5.11}$$

where $\mathscr{L}_{I_r}\left(\cdot\right)$ is the Laplace transform of I_r and is given by

$$\begin{aligned} \mathscr{L}_{I_r}\left(\mu T r^{\gamma}\right) &= \mathbb{E}_{I_r}\left[e^{-\mu T r^{\gamma} I_r}\right] \\ &= \mathbb{E}_{\Phi, g_n}\left[e^{-\mu T r^{\gamma} \sum_{n \in \Phi \setminus b_0} g_n R_n^{-\gamma}}\right]. \end{aligned} \tag{5.12}$$

Due to the independence of fading coefficients, (5.12) can be re-written as

$$\mathscr{L}_{I_r}\left(\mu T r^{\gamma}\right)=\mathbb{E}_{\Phi}\left[\prod_{n\in\Phi\setminus b_0}\mathbb{E}_g[\exp\left(-\mu T r^{\gamma} g R_n^{-\gamma}\right)]\right]. \tag{5.13}$$

By considering the properties of probability generating functional (PGFL) [2,17, ch.4, p.126], (5.13) can be expressed as

$$\begin{aligned}\mathscr{L}_{I_r}(s)&=\exp\left(-2\pi\lambda\left(\int_r^{\infty}\left(1-\mathbb{E}_g[\exp(-sgk^{-\gamma})]\right)kdk\right)\right),\\&=\exp\left(-2\pi\lambda\int_0^{\infty}\left(\int_r^{\infty}\left(1-e^{-sk^{-\gamma}g}\right)kdk\right)f(g)d(g)\right).\end{aligned} \tag{5.14}$$

Plugging (5.3) and (5.14) into (5.11), and using the substitution $r^{\varphi}=u$, the coverage probability is expressed as

$$\begin{aligned}&p_c(T,\lambda,\gamma)\\&=\sum_{j=1}^{l}\left(\frac{\phi_j}{\varphi_j}\int_0^{\infty}e^{\lambda\pi u_j^{\frac{\varphi_j}{2}}(1-\beta(T,\gamma))-\mu T u_j^{\frac{\varphi_j}{\gamma}}-\frac{u_j}{\delta_j^{\varphi_j}}}du_j\right),\end{aligned} \tag{5.15}$$

where

$$\beta(T,\gamma)=\frac{2(\mu T)^{\frac{2}{\gamma}}}{\gamma}\mathbb{E}\left(g^{\frac{2}{\gamma}}\Gamma\left(-\frac{2}{\alpha},g\mu T\right)-\Gamma\left(-\frac{2}{\alpha},0\right)\right)$$

and $\Gamma(c,b)$ stands for the incomplete Gamma function.

5.5 Numerical Results

In this section, we evaluate Lloyd's algorithm approximation for coverage probability with computer simulations. BSs are arranged according to a homogeneous PPP in a 300×300 square meter area where $\lambda=1$ unless other stated. We consider

a 75×75 square meter in the middle of the total coverage area to eliminate the boundary effect [2]. We consider a Rayleigh fading channel and set γ to be 4. The parameters φ_j, δ_j, and ϕ_j are provided in TABLE 5.1 by using the EM algorithm when $l = 3$, $m = 10^4$, and $\lambda_0 = \lambda = 1$. It is worth emphasizing that a mixture of three Weibull distributions is sufficient to characterize the link distance distribution. The values in the TABLE 5.1 are employed in the calculation of coverage probability.

In Fig. 5.2, the link distance distribution is investigated when $\lambda = 1$ and $\lambda = 0.25$. The mixture of Weibull distributions obtained via the EM algorithm agrees with the results of Lloyd's algorithm. Lloyd's algorithm performs like a bridge between (5.1) and (5.2). The radius of each Voronoi cell becomes evenly distributed as a result of increase in the iteration values, therefore, $f_r(r)$ converges to (5.2). This is mainly due the fact that the shape of Voronoi tessellation becomes more consistent as in the case of hexagonal-like tessellations. In Fig. 5.3, the impact of Lloyd's algorithm on coverage probability is investigated. As seen in Fig. 5.3, Lloyd's algorithm represents the intermediate deployment scenarios between the pessimistic, i.e., random, and the optimistic, i.e., structural, BS deployments. In Fig. 5.4, we compare the coverage probability of the random PPP BS model, hexagonal BS model, and Lloyd's approximation. The tightness of the proposed method for coverage probability is illustrated for different iterations of Lloyd's algorithm, i.e., $\{0, 2, 9, 29\}$. If the iteration value increases then the coverage probability for the proposed method tends to approach the hexagonal BS tessellation. It is important to note that the analytical approximations lose the tractability of Lloyd's algorithm at larger iteration values such as after iteration number 9. The analytical approximation suffers from the fact that PGFL assumption begins to fail. Nevertheless, the proposed approximation holds for low SIRs.

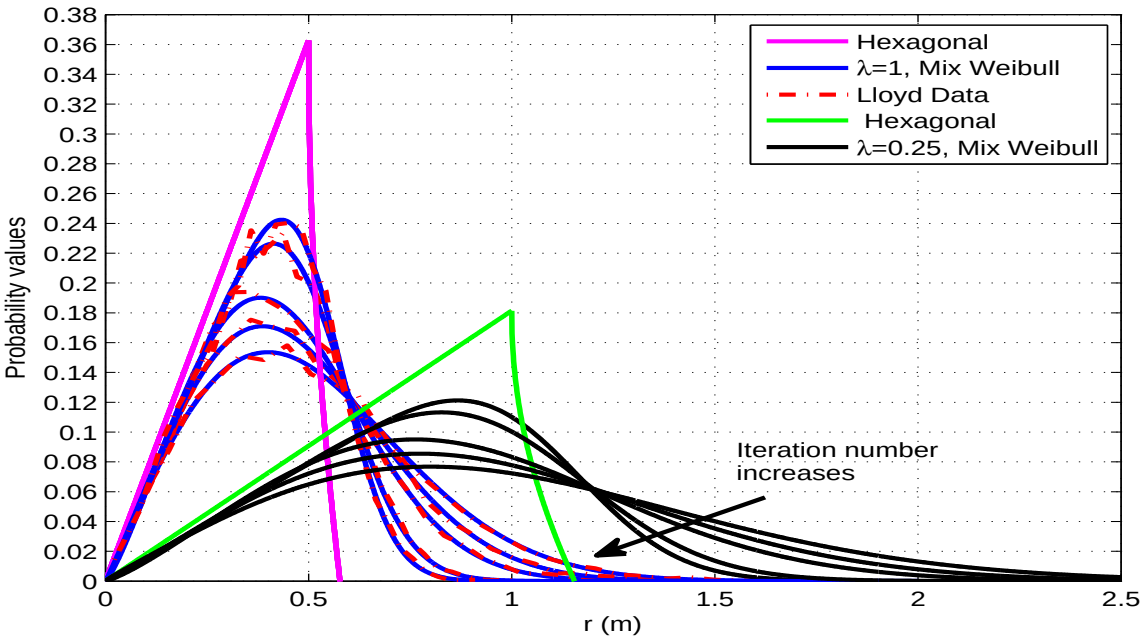

Figure 5.2: The transition from Rayleigh distribution to hexagonal distribution.

5.6 Summary

In this study, the impact of Lloyd's algorithm on the coverage probability of wireless networks is investigated. The link distance distribution is modeled as a mixture of Weibull distributions. Its parameters are derived based on the EM method at each iteration of Lloyd's algorithm. The numerical results show that if the Lloyd's algorithm is employed, the transitions between pessimistic PPP to optimistic hexagonal deployment can be approximately modeled.

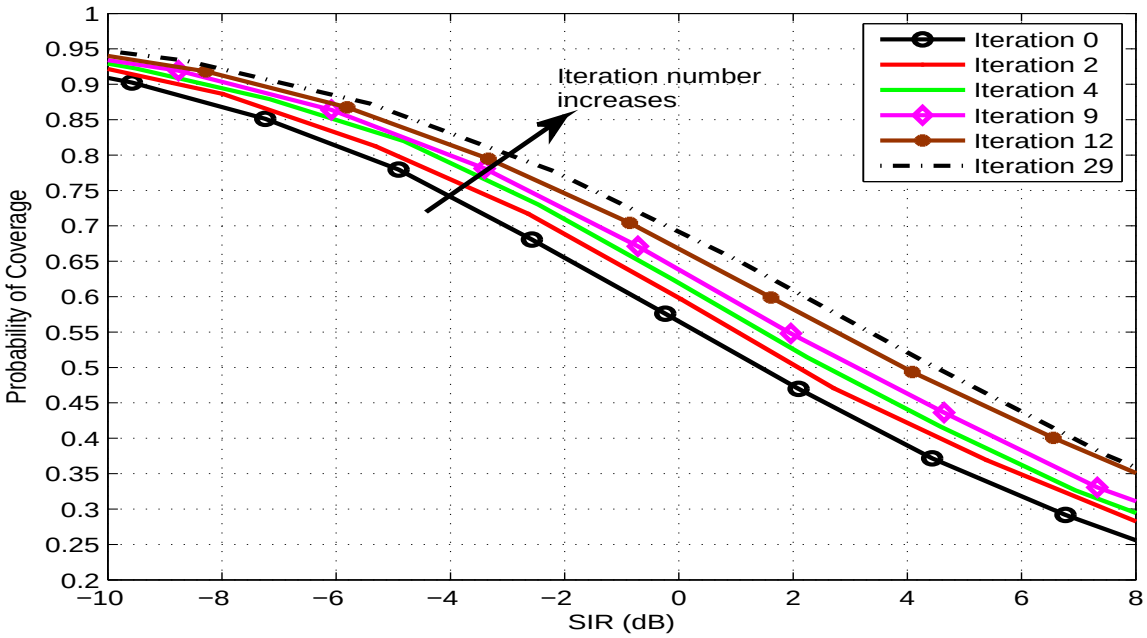

Figure 5.3: The variation of the coverage probability for a given number of iterations of Lloyd's algorithm.

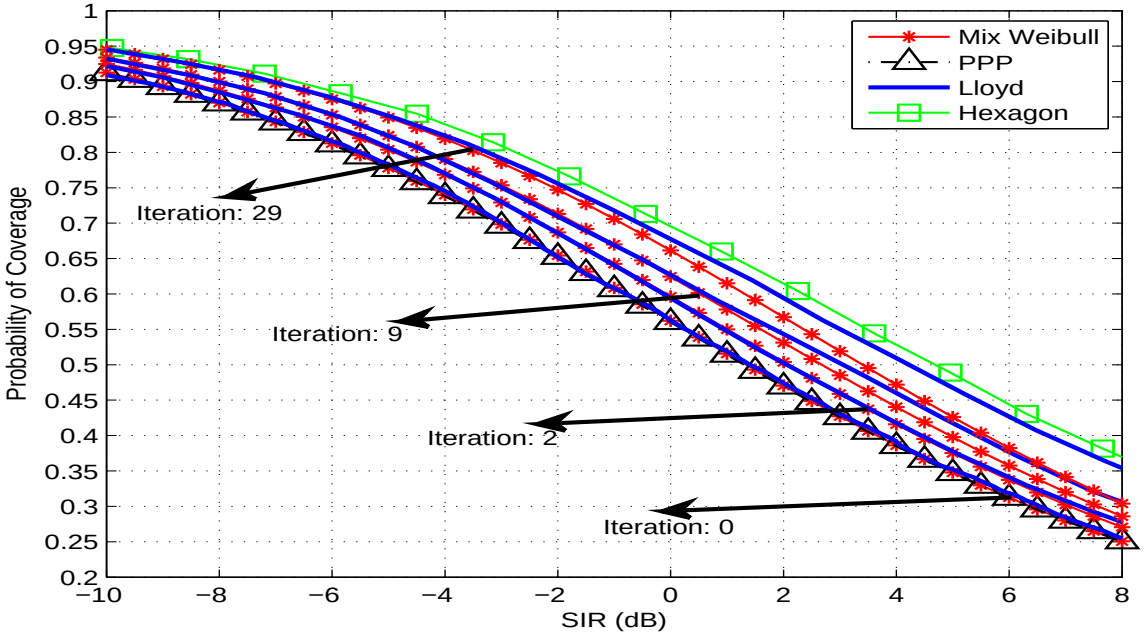

Figure 5.4: The coverage probability for PPP and hexagonal BS deployments and Lloyd's algorithm approximation.

6. CONCLUSIONS AND FUTURE DIRECTIONS

HetNets are a key solution to meet the increasing capacity demand from cellular networks. This had led to a new paradigm shift from MBS based networks to combinations of MBS and low powered nodes such as femtocells, picocells, DAS and D2D links. An expected effect of the increasing heterogeneity in NGWNs brought many research areas into the picture such as user/cell association, traffic offloading, radio resource allocation and coverage analysis. Some of these research problems were addressed in this dissertation. Next, we summarize all the contributions in this work as follows.

In Chapter 2, the number of active small cells is calculated based on different probabilistic distribution models. This number if then used to evaluate the downlink power consumption of HetNets.

In Chapter 3, the traffic offloading for a combination of MBS, SBS, WiFi and D2D links is investigated. It is shown that the shorter transmission can lead to greater traffic offloading with path loss based strategy. Different cellular networks sizes and access schemes are incorporated into this analysis.

In Chapter 4, HetNets create many great opportunities that can improve the QoS of the mobile users. Therefore, it is a must to develop new radio resource allocation mechanisms. Therefore, the joint user/network assignment and bandwidth allocation problem is formulated as a MINLP to account for the MT's limited number of radio interfaces and the abundant wireless network options. MINLP problems are intractable and computationally inefficient, thus, we transform the problem into a convex optimization problem via a binary variable relaxation approach. The proposed solution achieves a near optimal user assignment and bandwidth allocation at

reduced computational complexity.

In Chapter 5, we proposed a baseline model to model the transition from traditional hexagonal models to randomly located HetNets. The BSs locations of each tier are sampled from an independent homogeneous PPPs to account for randomness. In order to provide a tractable mathematical analysis, the EM algorithm is employed to model the link distance distribution. Furthermore, it is shown that Lloyd's algorithm may approximately model each step of the transition.

Some of the potential future research directions that require further investigation are:

- **Power Consumption:** Investigation of the deployment of hybrid backhaul technologies, CO_2 emission analysis and the mobility behavior of active mobile users and total mobile users where both categories of users adopt heterogeneous mobility patterns. Another interesting research challenge related to this study is the analysis of evolution in downlink power consumption and the number of active SBSs from the perspective of multiple or K–tier HetNets.

- **Resource Allocation:** One research area that needs to be well investigated is the context of green communications. This is motivated by the increasing BS energy consumption which also affects the CO_2 emissions.

  - Investigation of the impact of energy efficiency of each MT and wireless network. For instance, if MT utilizes both of the available interfaces at the same time, then battery consumption might increase. Since the battery consumption is one of the biggest concerns in the design of smart phones, a practical resource allocation approach could be addressed in this set-up by minimization of energy consumption while still maximizing the allocated bandwidth.

- Due to the increasing volume in the CO_2 emissions in the information and communication technology (ICT) industry, on/off strategy can be used to minimize the power consumption. An on/off strategy can be modeled via binary variables. This analysis could be carried out by minimizing $Blog(1+\frac{P}{B})$ while at the same time maximizing the multi–homing capacity. This might also be combined with a cross layer optimization approach.

- **Coverage Analysis:** The advantage of the Lloyd's algorithm approximation compared to the Gibbs point process should be further investigated. The Gibbs point process could be used to model the hard-core point process and the cluster point process. The tractability of the Lloyd's algorithm approximation should be clarified. Mean interference-to-signal ratio (MISR) can also be incorporated along with the SIR analyis [36, 50]. Another interesting research application for the Lloyd's algorithm may be in the aftermath of disaster areas. As a futuristic approach, BSs can be placed on drones, i.e., autonomous planes. BSs can yield coverage to areas such as disaster/public safety regions, rural areas and downtown areas. We can also utilize such a strategy for the self organized networks (SON) networks to decide the best coverage options for a given area. All these applications can be part of the 5G and NGWN.

REFERENCES

[1] Jeffrey Andrews. Seven ways that HetNets are a cellular paradigm shift. *IEEE Commun. Mag.*, 51(3):136–144, 2013.

[2] Jeffrey Andrews, Francois Baccelli, and Radha Krishna Ganti. A tractable approach to coverage and rate in cellular networks. *IEEE Trans. Commun.*, 59(11):3122–3134, Nov. 2011.

[3] Jeffrey Andrews, Sarabjot Singh, Qiaoyang Ye, Xingqin Lin, and Harpreet Dhillon. An overview of load balancing in HetNets: Old myths and open problems. *Wireless Communications, IEEE*, 21(2):18–25, 2014.

[4] Malik Wahaj Arshad, Anders Vastberg, and Tomas Edler. Energy efficiency gains through traffic offloading and traffic expansion in joint macro pico deployment. In *Proc. IEEE Wireless Commun. and Networking Conf. (WCNC'12)*, pages 2203–2208, Paris.

[5] Gunther Auer, Vito Giannini, Claude Desset, Istvan Godor, Per Skillermark, Magnus Olsson, Muhammad Ali Imran, Dario Sabella, Manuel Gonzalez, Oliver Blume, and Albrecht Fehske. How much energy is needed to run a wireless network? *IEEE Wireless Communs. Magazine*, 18(5):40–49, 2011.

[6] Gunther Auer, Vito Giannini, István Gódor, Per Skillermark, Magnus Olsson, Muhammad Ali Imran, Dario Sabella, Manual Gonzalez, Claude Desset, and Oliver Blume. Cellular energy efficiency evaluation framework. In *Proc. IEEE 73rd. Vehicular Tech. Conf. (VTC–Spring'11)*, pages 1–6, Budapest.

[7] Konstantinos Baltzis. Analytical and closed-form expressions for the distribution of path loss in hexagonal cellular networks. *Wireless Personal Commun.*, 60(4):599–610, 2011.

[8] Mike Beasley. iOS 7 becomes first commercial software to support multipath TCP, allowing simultaneous WiFi and cell network connections. `http://9to5mac.com/2013/09/19/ios-7-becomes-first-commercial-software-to-support-multipath-tcp-allowing-simultaneous-wi-fi-and-cell-network-connections/`, 2013.

[9] Mehdi Bennis, Meryem Simsek, Andreas Czylwik, Walid Saad, Stefan Valentin, and Merouane Debbah. When cellular meets WiFi in wireless small cell networks. *IEEE Commun. Mag.*, 51(6):44–50, 2013.

[10] Micha Benoliel, Stanislav Shalunov, and Greg Hazel. Open garden-You are the internet. `https://opengarden.com/home`, 2014.

[11] Dimitri Bertsekas, Gregory Lauer, Nils Sandell, and Thomas Posbergh. Optimal short-term scheduling of large-scale power systems. *Automatic Control, IEEE Transactions on*, 28(1):1–11, Jan 1983.

[12] Ingmar Blau, Gerhard Wunder, Ingo Karla, and Rolf Sigle. Decentralized utility maximization in heterogeneous multicell scenarios with interference limited and orthogonal air interfaces. *EURASIP Journal on Wireless Communications and Networking*, 2009:2, 2009.

[13] Pierre Bonami, Mustafa Kilinc, and Jeff Linderoth. Algorithms and software for convex mixed integer nonlinear programs. In *Mixed integer nonlinear programming*, pages 1–39. Springer, 2012.

[14] Stephen Boyd and Lieven Vandenberghe. *Convex optimization*. Cambridge University Press, 2004.

[15] Kameswari Chebrolu and Ramesh Rao. Bandwidth aggregation for real-time applications in heterogeneous wireless networks. *Mobile Computing, IEEE Transactions on*, 5(4):388–403, 2006.

[16] Woon Hau Chin, Zhong Fan, and Russell Haines. Emerging technologies and research challenges for 5G wireless networks. *Wireless Communications, IEEE*, 21(2):106–112, 2014.

[17] Sung Nok Chiu, Dietrich Stoyan, , Wilfrid Kendall, and Joseph Mecke. *Stochastic geometry and its applications*. Wiley, United Kingdom, Sep. 2013.

[18] Xiaoli Chu, David Lopez Perez, Yang Yang, and Fredrik Gunnarsson. *Heterogeneous cellular networks: Theory, simulation and deployment*. Cambridge University Press, 2013.

[19] CISCO. Cisco visual networking index: Global mobile data traffic forecast update, 2013–2018. `http://www.cisco.com/en/US/solutions/collateral/ns341/ns525/ns537/ns705/ns827/white_paper_c11-520862.pdf`, 2014.

[20] COMSCORE. How tablets, smartphones and connected devices are changing U.S. digital media consumption habits. `http://www.ipmark.com/pdf/Omnivoros.pdf`, 2011.

[21] Guillaume de la Roche, Alvaro Valcarce, David Lopez Perez, and Jie Zhang. Access control mechanisms for femtocells. *IEEE Commun. Mag.*, 48(1):33–39, January 2010.

[22] Arthur Dempster, Nan Laird, and Donald Rubin. Maximum likelihood from incomplete data via the EM algorithm. *Royal Statistical Society*, 39(1):1–38, 1977.

[23] Na Deng, Wuyang Zhou, and Martin Haenggi. The Ginibre point process as a model for wireless networks with repulsion. *IEEE Trans. Wireless Commun.*, 14(1):107–121, Jan. 2015.

[24] EARTH. Energy aware radio and network technologies. `https://bscw.ict-earth.eu/pub/bscw.cgi/d38532/EARTH_WP2_D2.1_v2.pdf`, Apr. 2011.

[25] Ali Riza Ekti, Erchin Serpedin, and Khalid Qaraqe. Lloyd's algorithm approximation for coverage probability in heterogeneous cellular networks. *to be submitted*, 2015.

[26] Ali Riza Ekti, Erchin Serpedin, and Khalid Qaraqe. Resource allocation algorithms for heterogeneous wireless networks: An overview. *Algorithms*, June 2015, to be submitted.

[27] Ali Riza Ekti, Muhammad Zeeshan Shakir, Khalid Qaraqe, Erchin Serpedin, and Muhammad Imran. On the traffic offloading in WiFi supported heterogeneous wireless networks. *Springer Journal of Signal Processing Systems, under review*, 2015.

[28] Ali Riza Ekti, Muhammad Zeeshan Shakir, Erchin Serpedin, and Khalid Qaraqe. Downlink power consumption of HetNets based on the probabilistic traffic model of mobile users. In *Personal Indoor and Mobile Radio Communications (PIMRC), 2013 IEEE 24th International Symposium on*, pages 2797–2802, Sept 2013.

[29] Ali Riza Ekti, Muhammad Zeeshan Shakir, Erchin Serpedin, and Khalid Qaraqe. End-to-end downlink power consumption of heterogeneous small-cell networks based on the probabilistic traffic model. In *Wireless Communications and Networking Conference (WCNC), 2014 IEEE*, pages 1138–1142, April 2014.

[30] Ali Riza Ekti, Xu Wang, Muhammad Ismail, Erchin Serpedin, and Khalid Qaraqe. Joint user assignment and bandwidth allocation in heterogeneous wireless networks. *IEEE Transactions on Vehicular Technology, under review*, 2015.

[31] Daquan Feng, Chenzi Jiang, Gubong Lim, Leonard Cimini, Gang Feng, and Geoffrey Ye Li. A survey of energy–efficient wireless communications. *IEEE Communs. Surveys & Tutorials*, 15(1):167–178, 2013.

[32] Gerhard Fettweis and Ernesto Zimmermann. ICT energy consumption–trends and challenges. In *Proc. of the 11th Intl. Symp. on Wireless Personal Multimedia Communs. (WPMC'08)*, Lapland, Finland, Sep. 2008.

[33] Amitabha Ghosh, Nitin Mangalvedhe, Rapeepat Ratasuk, Bishwarup Mondal, Mark Cudak, Eugene Visotsky, Timothy Thomas, Jeffrey Andrews, Ping Xia, Han Shin Jo, Harpreet Dhillon, and Thomas Novlan. Heterogeneous cellular networks: From theory to practice. *IEEE Commun. Mag.*, 50(6):54–64, 2012.

[34] Georgios Giannakis, Vassilis Kekatos, Nikolaos Gatsis, Seung Jun Kim, Hao Zhu, and Bruce Wollenberg. Monitoring and optimization for power grids: A signal processing perspective. *Signal Processing Magazine, IEEE*, 30(5):107–128, 2013.

[35] Anjin Guo and Martin Haenggi. Spatial stochastic models and metrics for the structure of base stations in cellular networks. *IEEE Trans. Wireless Commun.*, 12(11):5800–5812, Nov. 2013.

[36] Martin Haenggi. The mean interference-to-signal ratio and its key role in cellular and amorphous networks. *Wireless Communications Letters, IEEE*, 3(6):597–600, Dec 2014.

[37] Mahdi Hajiaghayi, Min Dong, and Ben Liang. Jointly optimal channel and power assignment for dual-hop multi-channel multi-user relaying. *Selected Areas in Communications, IEEE Journal on*, 30(9):1806–1814, 2012.

[38] Ziaul Hasan, Hamidreza Boostanimehr, and Vijay Bhargava. Green cellular networks: A survey, some research issues and challenges. *IEEE Communs. Surveys & Tutorials*, 13(4):524–540, 2011.

[39] Robert William Heath, Marios Kountouris, and Tianyang Bai. Modeling heterogeneous network interference using Poisson point processes. *IEEE Trans. Signal Process*, 61(16):4114–4126, 2013.

[40] IEEE. IEEE, Std 802.11–2012: Wireless LAN medium access control and physical layer specifications, 2012.

[41] Muhammad Ismail, Atef Abdrabou, and Weihua Zhuang. Cooperative decentralized resource allocation in heterogeneous wireless access medium. *IEEE Trans. Wireless Commun.*, 12(2):714–724, 2013.

[42] Muhammad Ismail and Weihua Zhuang. Decentralized radio resource allocation for single–network and multi–homing services in cooperative heterogeneous wireless access medium. *IEEE Trans. Wireless Commun.*, 11(11):4085–4095, 2012.

[43] Muhammad Ismail and Weihua Zhuang. A distributed multi–service resource allocation algorithm in heterogeneous wireless access medium. *IEEE J. Sel. Areas Commun.*, 30(2):425–432, 2012.

[44] Muhammad Ismail, Weihua Zhuang, Erchin Serpedin, and Khalid Qaraqe. A survey on green mobile networking: From the perspectives of network operators and mobile users. *Communications Surveys Tutorials, IEEE*, PP(99):1–1, 2015.

[45] Jingon Joung, Chin Keong Ho, and Sumei Sun. Spectral efficiency and energy efficiency of OFDM systems: Impact of power amplifiers and countermeasures. *IEEE J. Sel. Areas Commun.*, 32(12):1–13, 2014.

[46] Frank Kelly. Charging and rate control for elastic traffic. *European transactions on Telecommunications*, 8(1):33–37, 1997.

[47] Manzoor Ahmed Khan, Cuong Truong, Thomas Geithner, Fikret Sivrikaya, and Sahin Albayrak. Network level cooperation for resource allocation in future wireless networks. In *Wireless Days, 2008. WD '08. 1st IFIP*, pages 1–5, Nov 2008.

[48] Seung Jun Kim and Georgios Giannakis. Scalable and robust demand response with mixed-integer constraints. *Smart Grid, IEEE Transactions on*, 4(4):2089–2099, 2013.

[49] Lei Lei, Zhangdui Zhong, Kan Zheng, Jiadi Chen, and Hanlin Meng. Challenges on wireless heterogeneous networks for mobile cloud computing. *Wireless Communications, IEEE*, 20(3):34–44, 2013.

[50] Yingzhe Li, Francois Baccelli, Harpreet Dhillon, and Jeffrey Andrews. Statistical modeling and probabilistic analysis of cellular networks with determinantal point processes. *arXiv preprint arXiv:1412.2087*, 2015.

[51] Dantong Liu, Yue Chen, Kok Keong Chai, Tiankui Zhang, and Maged Elkashlan. Opportunistic user association for multi-service HetNets using Nash bargaining solution. *Communications Letters, IEEE*, 18(3):463–466, March 2014.

[52] Stuart Patrick Lloyd. Least squares quantization in pcm. *IEEE Trans. Inf. Theory*, 28(2):129–137, Mar. 1982.

[53] Changqing Luo, Hong Ji, and Yi Li. Utility-based multi-service bandwidth allocation in the 4G heterogeneous wireless access networks. In *Wireless Communications and Networking Conference, 2009. WCNC 2009. IEEE*, pages 1–5, April 2009.

[54] Joe Madden. Economic case studies of small cells and WiFi. `http://www.fiercewireless.com/tech/story/madden-economic-case-studies-small-cells-and-wi-fi/2013-06-28`, 2013.

[55] Marco Ajmone Marsan, Luca Chiaraviglio, Delia Ciullo, and Michela Meo. Optimal energy savings in cellular access networks. In *Proc. IEEE Intl. Conf. on Commun. Workshops (ICC'09)*, pages 1–5, Dresden.

[56] Garey Michael and Johnson David. Computers and intractability: A guide to the theory of NP-completeness. *WH Freeman & Co., San Francisco*, 1979.

[57] Paolo Monti, Sibel Tombaz, Lena Wosinska, and Jens Zander. Mobile backhaul in heterogeneous network deployments: Technology options and power

consumption. In *Proc. IEEE 14th. Intl. Conf. on Transparent Optical Networks (ICTON'12)*, pages 1–7, Coventry.

[58] Itaru Nakata and Naoto Miyoshi. Spatial stochastic models for analysis of heterogeneous cellular networks with repulsively deployed base stations. *Elsevier Performance Evaluation*, 78:7–17, Aug. 2014.

[59] Donald Joseph Newman. The hexagon theorem. *IEEE Trans. Inf. Theory*, 28(2):137–139, Mar. 1982.

[60] Dusit Niyato and Ekram Hossain. Bandwidth allocation in 4G heterogeneous wireless access networks: A noncooperative game theoretical approach. In *Global Telecommunications Conference, 2006. GLOBECOM '06. IEEE*, pages 1–5, Nov 2006.

[61] Dusit Niyato and Ekram Hossain. A cooperative game framework for bandwidth allocation in 4G heterogeneous wireless networks. In *Communications, 2006. ICC '06. IEEE International Conference on*, volume 9, pages 4357–4362, June 2006.

[62] Dusit Niyato and Ekram Hossain. A noncooperative game-theoretic framework for radio resource management in 4G heterogeneous wireless access networks. *Mobile Computing, IEEE Transactions on*, 7(3):332–345, March 2008.

[63] Jorge Nocedal. Updating quasi-newton matrices with limited storage. *Mathematics of Computation*, 35(151):773–782, Jul. 1980.

[64] Atsuyuki Okabe, Barry Boots, Kokichi Sugihara, and Sung Nok Chiu. *Spatial tessellations: Concepts and applications of Voronoi diagrams*. Wiley, United Kingdom, Jul. 2000.

[65] Monica Paolini. Cost savings and revenue benefits from next generation hotspot WiFi. http://www.wballiance.com/wba/wp-content/uploads/downloads/2013/09/Cost-savings-and-revenue-benefits-from-NGH.pdf, 2013.

[66] Xuebing Pei, Tao Jiang, Daiming Qu, Guangxi Zhu, and Jian Liu. Radio-resource management and access-control mechanism based on a novel economic model in heterogeneous wireless networks. *Vehicular Technology, IEEE Transactions on*, 59(6):3047–3056, 2010.

[67] Philip Harley. Short distance attenuation measurements at 900 mhz and 1.8 ghz using low antenna heights for microcells. *in IEEE J. Sel. Areas Commun.*, 7(1):5–11, Jan. 1989.

[68] Sundeep Rangan, Theodore Scott Rappaport, and Elza Erkip. Millimeter-wave cellular wireless networks: Potentials and challenges. *Proceedings of the IEEE*, 102(3):366–385, March 2014.

[69] Theodore Scott Rappaport, Wonil Roh, and Kyungwhoon Cheun. Mobile's millimeter-wave makeover. *Spectrum, IEEE*, 51(9):34–58, Sept. 2014.

[70] Fred Richter, Albrecht Fehske, and Gerhard Fettweis. Energy efficiency aspects of base station deployment strategies for cellular networks. In *Proc. IEEE 70th. Vehicular Tech. Conf. (VTC–Fall'09)*, pages 1–5, Anchorage.

[71] Ignacio Rodriguez, Huan Cong Nguyen, Niels Jorgensen, Troels Bundgaard Sorensen, Jan Elling, Morten Brok Gentsch, and Preben Mogensen. Path loss validation for urban micro cell scenarios at 3.5 ghz compared to 1.9 ghz. In *Proc. of the IEEE Global Commun. Conf. (GLOBECOM'13)*, Atlanta.

[72] Nick Sahinidis. Gams: BARON MINLP solver. `http://www.gams.com/dd/docs/solvers/baron/index.html`, 2014.

[73] Muhammad Zeeshan Shakir and Mohamed Slim Alouini. On the area spectral efficiency improvement of heterogeneous network by exploiting the integration of macro-femto cellular networks. In *Proc. IEEE Intl. Conf. on Commun. Workshops (ICC'12)*, pages 5695–5700, Ottawa.

[74] Hongxia Shen and Tamer Basar. Differentiated internet pricing using a hierarchical network game model. In *American Control Conference, 2004. Proceedings of the 2004*, volume 3, pages 2322–2327. IEEE, 2004.

[75] Wei Shen and Qing An Zeng. Resource management schemes for multiple traffic in integrated heterogeneous wireless and mobile networks. In *Computer Communications and Networks, 2008. ICCCN'08. Proceedings of 17th International Conference on*, pages 1–6. IEEE, 2008.

[76] Simon Saunders, and Alejandro Zavala. *Antenna and propagation for wireless communication systems, 2nd ed.* John Wiley & Sons Ltd., Chicester, UK, Mar. 2007.

[77] Sarabjot Singh, Harpreet Dhillon, and Jeffrey Andrews. Offloading in heterogeneous networks: Modeling, analysis, and design insights. *IEEE Trans. Wireless Commun.*, 12(5):2484–2497, 2013.

[78] Hamza Soury, Faouzi Bader, Musbah Shaat, and Mohamed Slim Alouini. Joint sub-carrier pairing and resource allocation for cognitive networks with adaptive relaying. *EURASIP Journal on Wireless Communications and Networking*, 2013(1):1–15, 2013.

[79] Hina Tabassum, Muhammad Zeeshan Shakir, and Mohamed Slim Alouini. Area green efficiency of two tier heterogeneous cellular networks. In *Proc. IEEE Conf. Global Commun. Workshops (GC'12)*, pages 529–534, Anaheim.

[80] Abd Elhamid Taha, Hossam Hassanein, and Hussein Mouftah. On robust allocation policies in wireless heterogeneous networks. In *Quality of Service in Heterogeneous Wired/Wireless Networks, 2004. QSHINE 2004. First International Conference on*, pages 198–205, Oct 2004.

[81] Orawan Tipmongkolsilp, Said Zaghloul, and Admela Jukan. The evolution of cellular backhaul technologies: Current issues and future trends. *IEEE Commun. Surveys & Tuts.*, 13(1):97–113, 2011.

[82] Sibel Tombaz, Paolo Monti, Kun Wang, Anders Vastberg, Marco Forzati, and Jens Zander. Impact of backhauling power consumption on the deployment of heterogeneous mobile networks. In *Proc. IEEE Conf. Global Communs. Workshops (GC'11)*, pages 1–5, Houston.

[83] Mohammad Faisal Uddin, Chadi Assi, and Ali Ghrayeb. Joint optimal af relay assignment and power allocation in wireless cooperative networks. *Computer Networks*, 58:58–69, 2014.

[84] Xiaofei Wang, Athanasios Vasilakos, Min Chen, Yunhao Liu, and Ted Taekyoung Kwon. A survey of green mobile networks: Opportunities and challenges. *Springer Jour. Mobile Networks and Applications*, 17(1):4–20, 2012.

[85] Ziyang Wang, Rainer Schoenen, Halim Yanikomeroglu, and Marc StHilaire. The impact of user spatial heterogeneity in heterogeneous cellular networks. In *Proc. IEEE Global Commun. Conf. (GLOBECOM)*, Austin.

[86] Jingjin Wu, Yujing Zhang, Moshe Zukerman, and Edward Kai Ning Yung. Energy-efficient base-stations sleep-mode techniques in green cellular networks: A survey. *Communications Surveys Tutorials, IEEE*, 17(2):803–826, Secondquarter 2015.

[87] Liang Wu, Yi Zhong, and Wenyi Zhang. Spatial statistical modeling for heterogeneous cellular networks - an empirical study. In *Proc. IEEE Veh. Technol. Conf. (VTC)*, Seoul, Korea, May 2014.

[88] Lin Xiang, Francesco Pantisano, Roberto Verdone, Xiaohu Ge, and Min Chen. Adaptive traffic load–balancing for green cellular networks. In *Proc. IEEE 22nd Intl. Symp. on Personal Indoor and Mobile Radio Commun. (PIMRC'11)*, pages 41–45, Toronto.

[89] Kok Kiong Yap, Te Yuan Huang, Masayoshi Kobayashi, Yiannis Yiakoumis, Nick McKeown, Sachin Katti, and Guru Parulkar. Making use of all the networks around us: A case study in Android. In *Proceedings of the 2012 ACM SIGCOMM workshop on Cellular networks: operations, challenges, and future design*, pages 19–24. ACM, 2012.

[90] Wei Yu and Raymond Lui. Dual methods for nonconvex spectrum optimization of multicarrier systems. *Communications, IEEE Transactions on*, 54(7):1310–1322, 2006.

[91] Weihua Zhuang and Muhammad Ismail. Cooperation in wireless communication networks. *Wireless Communications, IEEE*, 19(2):10–20, April 2012.

APPENDIX A

In this appendix, it is proved that problem (P_2) is a convex optimization problem. The Hessian matrix of the function $x_{nmr}\ln(1+\eta\frac{w_{nmr}}{x_{nmr}})$ is first calculated as follows

$$H = \begin{bmatrix} -\frac{w_{nmr}^2}{\left(\frac{w_{nmr}}{x_{nmr}}+1\right)^2 x_{nmr}^3} & \frac{w_{nmr}}{\left(\frac{w_{nmr}}{x_{nmr}}+1\right)^2 x_{nmr}^2} \\ \frac{w_{nmr}}{\left(\frac{w_{nmr}}{x_{nmr}}+1\right)^2 x_{nmr}^2} & -\frac{1}{\left(\frac{w_{nmr}}{x_{nmr}}+1\right)^2 x_{nmr}} \end{bmatrix} \tag{A.1}$$

It is observed that the Hessian matrix (A.1) is positive semi-definite, which leads to the fact that the function $x_{nmr}\ln(1+\eta\frac{w_{nmr}}{x_{nmr}})$ is a concave function. Furthermore, the objective function in (P_2) is concave since the summation of concave functions is also concave. Therefore, problem (P_2) is a convex optimization problem due to the fact that all the constraints are affine [14].

APPENDIX B

In this appendix, it is proved that $\lambda_1 = \cdots = \lambda_n$. Assume not all $\lambda_n, n = 1, \cdots, N_1$ are equal to each other, then there exists a λ_k in this sequence such that $\lambda_k > \lambda_{\min}$, where $\lambda_{\min} = \min_{n=1,\cdots,N_1} \lambda_n$. Since $A(\lambda_n)$ is a monotonically decreasing function, it follows that $A(\lambda_k) < A(\lambda_{\min})$. Therefore, in order to maximize (4.10), the kth row of $\mathbf{S}$ is assigned to be all zeros. In other words, if any positive value is assigned to the row corresponding to $A(\lambda_k)$, then that value can be added to the row corresponding to $A(\lambda_{\min})$ which will yield a larger objective value. Consequently, it follows that

$$s_{km} = 0,\ m \in \mathcal{M},$$

and moreover

$$x_{kmr} = 0,\ m \in \mathcal{M},\ r \in \mathcal{R}_1.$$

Due to (4.6),

$$w_{kmr} = 0,\ m \in \mathcal{M},\ r \in \mathcal{R}_1. \tag{B.1}$$

It remains that

$$\begin{aligned} \sum_{m\in\mathcal{M}} \sum_{r\in\mathcal{R}} w_{kmr} - Z_k &= \sum_{m\in\mathcal{M}} \sum_{r\in\mathcal{R}_1} w_{kmr} \\ &+ \sum_{m\in\mathcal{M}} \sum_{r\in\mathcal{R}_2} w_{kmr} - Z_k = -Z_k, \end{aligned} \tag{B.2}$$

where the last equality follows from (B.1) and the fact that $k \in \mathcal{N}_1$ (the cellular interface cannot connect to the WiFi network). Based on (4.7), $\lambda_k = 0$. Then, the assumption that $\lambda_k > \lambda_{\min}$ leads to $\lambda_{\min} < 0$, which is contradictory to the nonnegativity property of the Lagrange multiplier $\boldsymbol{\lambda}$. In addition, the argument that $\lambda_k = 0$ also voids the assumption $\lambda_n \neq 0$ when deriving (4.6). This completes the proof.